Dissertation
submitted to the
Combined Faculties for the Natural Sciences
and for Mathematics
of the Ruperto-Carola University of Heidelberg, Germany
for the degree of
Doctor of Natural Sciences

presented by
Diplom-Physiker Holger Braun
born in Nordhorn
Oral examination: 26.04.2006

**A new hypothesis for the
1470-year cycle of
abrupt warming events
in the last ice-age**

Referees:

**Prof. Dr. Kurt Roth
Prof. Dr. Augusto Mangini**

In this thesis, a new hypothesis is presented for the glacial 1470-year climate cycle, which manifests itself in abrupt warming events (the so-called Dansgaard-Oeschger events, or DO events). According to the hypothesis, two century-scale solar cycles could explain the regularity in the timing of the DO events, since the periods of these two cycles are close to integer factors of 1470 years. This hypothesis is tested with a coupled climate model of intermediate complexity. It is shown that abrupt warming events, which reproduce many features of the DO events (in particular their time scale of 1470 years), can occur in the climate model in response to two centennial-scale freshwater cycles, with periods close to those of the two known solar cycles. The plausibility of these model results is tested with a very simple conceptual model, in which DO events represent abrupt switches between two modes of the thermohaline ocean circulation. It is shown that the millennial-scale response of the climate model to the century-scale forcing is a plausible consequence of the high degree of non-linearity and the large characteristic time scale of the thermohaline circulation. As a result, the glacial 1470-year climate cycle might indeed be caused by the Sun, despite the lack of a corresponding solar frequency.

In dieser Arbeit wird eine neue Hypothese zur Erklärung des 1470-Jahres Klimazyklus abrupter Erwärmungen in der letzten Eiszeit vorgestellt, der sogenannten Dansgaard-Oeschger (DO) Ereignisse. Gemäß dieser Hypothese könnten zwei kürzere Sonnenzyklen die Regelmäßigkeit im zeitlichen Auftreten der DO Ereignisse erklären, da ihre Perioden im Bereich von ganzzahligen Teilern von 1470 Jahren liegen. Diese Hypothese wird mittels eines gekoppelten Klimamodells mittlerer Komplexität getestet. Es wird gezeigt, dass sich durch zwei Süßwasserzyklen, mit Perioden im Bereich der zwei bekannten Sonnenzyklen, abrupte Erwärmungen im Klimamodell auslösen lassen, die große Ähnlichkeiten mit den DO Ereignissen aufweisen (und insbesondere eine Zeitskala von 1470 Jahren haben). Die Plausibilität dieser Modellergebnisse wird mittels eines sehr einfachen konzeptionellen Modells getestet. DO Ereignisse stellen in diesem Modell abrupte Wechsel zwischen zwei Moden der thermohalinen Ozeanzirkulation dar. Es wird gezeigt, dass die langsame Antwort des Klimamodells auf die schnelleren Antriebszyklen eine plausible Folge der extremen Nichtlinearität und der langen Zeitskala der thermohalinen Zirkulation ist. Folglich kann der eiszeitliche 1470-Jahres Klimazyklus in der Tat durch die Sonne verursacht sein, obwohl die Sonne keinen Zyklus der entsprechenden Frequenz aufweist.

Contents

1 Introduction

In 1871, Sir Joseph Norman Lockyer, a British astronomer who launched the journal Nature and edited it for the first 50 years, argued that *in meteorology, as in astronomy, the thing to hunt down is a cycle.* In climatology, cycles indeed play an outstanding role: Since the leading stimulus for the climate of the Earth originates from the movement of the Earth on its orbit around the Sun, many climatologic variables exhibit cyclic components. The most obvious of these cycles, the one-year cycle due to the annual revolution of the Earth around the Sun, and the 24-hour cycle owing to the diurnal rotation of the Earth on its axis, are so outstanding that our calendar is based upon them. Longer (i.e. multi-millennial scale) variations of the orbital parameters (*obliquity, precession, eccentricity*) also evolve in cycles, with many sinusoidal components of which only a few are dominant. The effects of these changes is, not surprisingly, less obvious. According to the so-called Milankovic-theory[1], the succession of the ice-ages results from these variations of the Earth's orbital parameters.

While the climatological effect of changes in the Earth's orbital parameters is primarily due to variations in the regional and seasonal distribution of the solar radiation received by the Earth and its atmosphere, changes in solar activity - in luminosity, for instance - also act as a stimulus for the climate of the Earth. Since 1843, when the German amateur astronomer Samuel Heinrich Schwabe discovered that the average number of sun-spots increases and decreases with a quasi-period of roughly 10-11 years (the so-called *Schwabe* cycle), solar activity is know to exhibit pronounced cycles. Meanwhile, longer (i.e. century-scale) cycles have been detected, above all the *Gleissberg* (period: about 87 years) and the *Suess/DeVries* (period: about 210 years) cycle. However, since up to now satellites have been monitoring variations of the "solar constant" over only 20 years, the magnitude of solar luminosity variations over the century-scale cycles is still very speculative.

The signature of the orbital and solar forcing cycles in terrestrial climate archives is often difficult to detect, since the signals are small and since the Earth's climate is very complex: It often responds in a nonlinear way to the astronomical drivers and exhibits considerable internal variability on all time scales. As a consequence, climatic time series are typically composed of a continuous range of spectral components and are therefore at best quasi-periodic, despite the existence of pronounced forcing cycles. Many climatic time series from the last ice-age, however, show a somewhat different pattern: As will be discussed in chapter 2, a very pronounced spectral component corresponding to a period of 1470 years is present in a large number of climatic time series from that time. This cycle is manifested in abrupt warming events, the so-called Dansgaard-Oeschger (DO) events, which are most pronounced in the North Atlantic region. The origin of the 1470-year cycle is still controversial, since no external forcing with a corresponding frequency is known.

In this thesis, a new hypothesis for the glacial 1470-year climate cycle is presented and tested with a climate model (the model CLIMBER-2 from the Potsdam Institute for Climate Impact Research, see chapter 3): According to this hypothesis, the combined effect of the solar Gleissberg and Suess/DeVries cycles, which are very pronounced spectral components in records of solar activity (as discussed in chapter 4), could explain the glacial 1470-year climate cycle. The reason why the glacial climate response to the century-scale solar cycles can be on the millennial-scale is the high degree of non-linearity of the DO events: Model simulations suggest that the events represent switches between two different modes of the ocean circulation, and that these switches evolve as highly non-linear threshold processes. But the response of a non-linear system does not necessarily exhibit the same spectral components as the forcing (as illustrated in chapter 5).

This potential difference in the spectral properties of the forcing and its response is the basis for the new hypothesis to explain the 1470-year climate cycle (chapter 6): A superposition of two century-scale forcing cycles, with periods close to the known solar cycles, can show a period of 1470 years, which is not manifested as a corresponding spectral component. But if the system that is forced by this superposition is highly nonlinear, it can be most sensitive to the 1470-year period of the forcing. In chapter 7, a test of this hypothesis is performed with the climate model. It is shown that DO-like warming events, with a characteristic time scale of 1470 years, can indeed be triggered by the combined effect two forcing cycles, with periods close to the known solar cycles.

In chapter 8, the stability of the simulated 1470-year climate cycle with respect to variations of the forcing is demonstrated with the climate model. The plausibility of the results is illustrated with a simple conceptual model (chapter 9), which is designed to mimic the response of the far more complex climate model. In chapter 10, the implications of the new hypothesis are discussed. It is shown that the hypothesis can resolve a couple of open questions, for which previous hypotheses on the glacial 1470-year climate cycle have not yet given a satisfactory answer.

2 Dansgaard-Oeschger events

Until a few decades ago, ice-ages were generally regarded as stable epochs, in which the climatic conditions were generally much colder than during warm ages. By the beginning of the 1990s, however, when the GRIP and GISP2 ice-cores had been drilled in Greenland, convincing evidence existed that dramatic climate changes repeatedly occurred during the last ice-age: In these two ice-cores, as well as in previous ones, massive millennial-scale warming events were recorded (figure 2.1), which were also confirmed in other climate archives[2]. More than twenty of these pronounced climatic shifts happened in the last ice-age. Named after their discoverers, the Danish glaciologist Willy Dansgaard and his Swiss colleague Hans Oeschger, these warming events are today referred to as Dansgaard-Oeschger (DO) events.

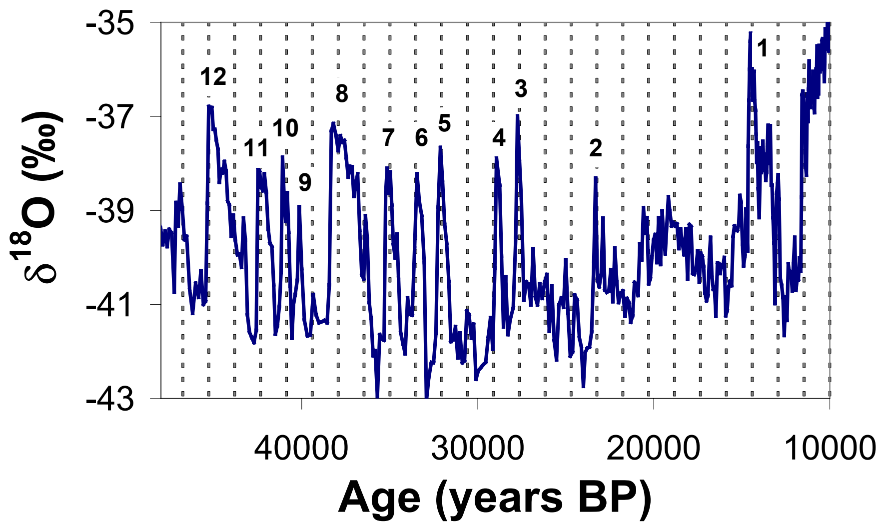

Figure 2.1: DO events in the GISP2 ice-core from Greenland[2].
Shown is the δ^{18}O-signal (i.e. the ratio between the stable isotopes ^{18}O and ^{16}O relative to a standard) in the layer-counted part of the GISP2 ice-core from Greenland. In this part of the ice-core, twelve DO events (1-12) stand out as sudden increases in δ^{18}O, i.e. as warming events. The spacing between the onset of successive events is often close to 1470 years or integer multiples thereof, as indicated by the dashed lines (which are spaced by 1470 years).

2.1 Abrupt climate change in the last ice-age

2.1.1 DO events in Greenland

DO events show a very characteristic temperature evolution in Greenland (figure 2.2). This can be inferred from the isotopic ratio of stable isotopes in the ice-cores[3, 4, 5] (oxygen, deuterium, nitrogen and argon, for example)[1]: With the start of a DO event, regional temperatures in Greenland rapidly increase over a few decades. According to the present state of knowledge, this initial temperature rise is of the order of 10-15 Kelvin[4, 5]. This warming is followed by a gradual cooling trend with variable duration of centuries to millenia. At the end of the events, Greenland temperature typically drops back to pre-event values over a couple of decades.

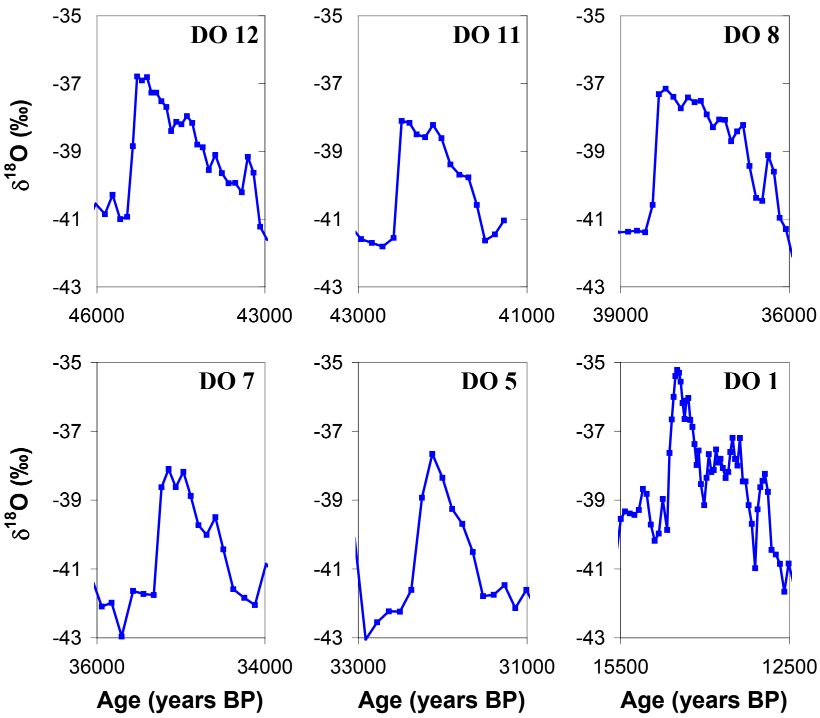

Figure 2.2: Temporal evolution of DO events.
The figure shows the DO events 12, 11, 8, 7, 5 and 1 as observed in the δ^{18}O-signal of the GISP2 ice-core. DO events have a characteristic temporal evolution with a very rapid initial warming, followed by a gradual cooling trend and a more rapid temperature drop at the end of the events.

[1]Stable isotopes can be used as a *paleothermometer* since fractionation processes produce a correspondence between local temperature and the isotopic ratios, for example the O^{18}/O^{16}-ratio.

2.1.2 An interhemispheric see-saw

It is now well established that the DO events in the Greenland isotopic data represent real climatic changes, since their effects are also documented in other areas[6], for example in the North Atlantic region[7] and in western Europe[8]. In the northern hemisphere, regional temperature anomalies during DO events are often in phase, i.e. large parts of the northern hemisphere warm synchronously with Greenland. In the southern hemisphere, temperature variations are often in anti-phase to Greenland: Antarctica, for example, warms when Greenland is cold[9].

To explain this apparent bipolarity, changes of the interhemispheric heat transport were suggested to occur during DO events: According to that hypothesis, most of the Northern hemisphere is expected to warm during warm intervals in Greenland, while the South cools. A physical mechanism by which such a *see-saw* between the hemispheres could be realised is a change in the thermohaline circulation[2] of the Atlantic ocean[11]: The Atlantic ocean circulation transports a huge amount of heat from the southern hemisphere to the North (roughly 10^{15} W)[12]. Consequently, an increase in the thermohaline circulation (THC) is expected to warm the North Atlantic region, at the expense of the South. Increases in the thermohaline circulation during DO events could thus provide a possible explanation for the phase relation between the two hemispheres during the events.

2.1.3 Discrete climate states

The characteristic temporal pattern of DO events, as seen for example in the Greenland ice-cores, suggests that these events represent shifts between metastable states of the climate system. Such shifts might occur between different modes of the THC: Models indicate that the thermohaline circulation exhibits more than one stable state of operation[13, 14]. This notion is also supported by paleoclimatic data[15]. Model simulations further suggest that transitions between these states can be very rapid: A shift of the glacial THC mode could occur within roughly a decade[16]. The abruptness of the warming in Greenland with the onset of the DO events is therefore also consistent with the idea that ocean circulation changes provide the mechanism which is inherent in the events.

[2] The thermohaline circulation is the part of the global ocean circulation that is driven by density differences. The expression *thermohaline* is due to the fact that the density of ocean water depends on temperature and salinity. The thermohaline circulation provides a major contribution to the heat budget of the North Atlantic region, warming annual-mean surface temperatures locally by up to 10 Kelvin[10].

2.1.4 Timescale of DO events

Spectral analysis of the oxygen isotope time series from the GISP2 ice-core, which was layer-counted down to about 50000 years before present and therefore has an independent timescale, reveals a prominent peak at a period of 1470 years[2] (figure 2.3). A spectral peak at a similar frequency was also reported to be present in the GRIP ice-core[17], in the Camp Century ice-core, and in a number of sediment-cores (see discussion in [2]).

The value of 1470 years is not very far from the characteristic timescale of the thermohaline circulation, which is of the order of 1000 years. But the value is much larger than the timescale of atmospheric processes, for example. The timescale of the events is therefore another argument for an involvement of the thermohaline circulation in the DO oscillations. Since changes in the THC could consequently explain many characteristics of the DO event, it is not surprising that most hypotheses for the events somehow involve changes in the thermohaline circulation.

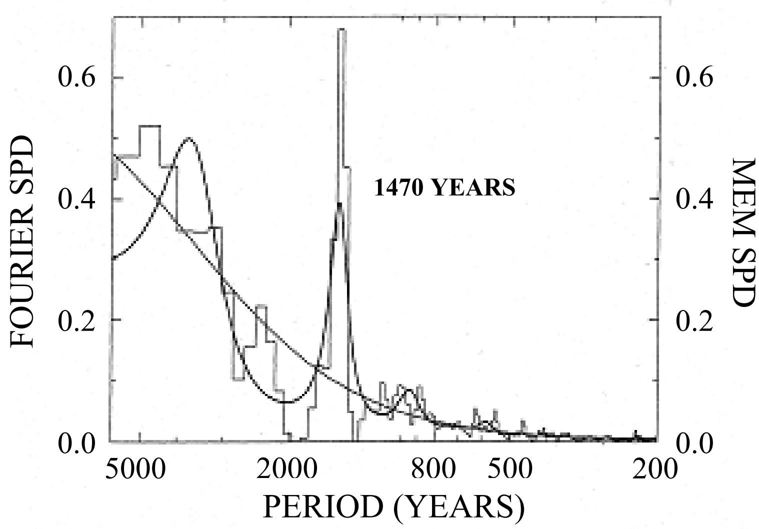

Figure 2.3: Frequency-spectrum of $\delta^{18}O$ in the GISP2 ice-core.
Spectral power density (SPD) as obtained from the layer-counted time-interval from 12000 to 50000 years before present. The heavy solid line is derived by the maximum entropy method (MEM), the light solid line is obtained by Fourier analysis. Red noise is depicted by the monotonically decreasing third curve. The figure is taken from[2].

2.2 Unknown trigger of Dansgaard-Oeschger events

While a certain consensus has already been reached on the role of ocean circulation changes as the mechanism that is most likely inherent in DO events, the trigger of these events remains very speculative. In principle, they could be caused by purely internal processes (i.e. they could represent a self-sustained oscillation of the climate system[18, 19, 20]) or, at least to some degree, by external drivers (orbital or solar forcing[21, 22, 23, 24, 25, 26]). Each of these hypothesis can explain certain aspects of the DO-events, but so-far none of them is convincing.

2.2.1 Self-sustained oscillations of the climate system

Internal oscillations were regarded as the most likely explanation for the events as long as model simulations suggested that a large perturbation (a complete shutdown of the thermohaline circulation, for instance) was required to cause DO oscillations. Such a shutdown cannot easily be excited and therefore requires a big trigger, which could only be provided by internal processes, for example by large-scale ice-sheet instabilities. Model simulations[16], however, indicate that a complete shutdown of the thermohaline circulation is not required to terminate DO events. A small trigger might thus be sufficient to explain the occurrence of DO oscillations. These results agree with reconstructions of the Atlantic ocean circulation in the last glacial, which suggest that North Atlantic deep water formation remained active after the end of DO events[14, 15] (it was probably interrupted only during the so-called Heinrich events[14]).

Moreover, models suggest that self-sustained, millennial-scale oscillations of the atmosphere-ocean system are unlikely[11] (such oscillations mainly occur in highly idealised models and under particular circumstances, for example for specific boundary conditions). Internal oscillations thus still require a trigger from another compartment of the climate system, for example from the cryosphere[3]. Meltwater pulses from the continental ice-sheets might in principle deliver this trigger. Ice-sheets, however, are more likely to exhibit longer-term (i.e. multi-millennial) oscillations[27]. Therefore, it is difficult to come up with a credible explanation of the glacial 1470-year climate cycle by internal processes only.

2.2.2 External forcing

A purely external trigger might more easily account for the excitation of a millennial-scale oscillation in the Atlantic ocean and could thus, at least in principle, explain the DO-events. The main problem of this idea is that an external 1470-year forcing cycle is not known. Furthermore, if the glacial 1470-year climate cycle was

[3] *cryosphere* means *ice-sphere* (from the Greek word *kryos* = ice, chill)

caused by an external trigger, some signature of the trigger should also be present in climatic time series from the Holocene[4]. The prominent 1470-year climate cycle, however, is restricted to the last glacial and is not present in the Holocene part of the oxygen isotope data of the Greenland ice-cores[2][5].

2.2.3 Stochastic resonance

Another hypothesis postulates that DO events were caused by a combination of both a weak external trigger and a noisy signal, arising from internal climate variability[23, 30]. This hypothesis was suggested in order to explain the characteristic spacing between successive DO events, as documented in the GISP2 ice-core: In the layer-counted part of this ice-core, the spacing of DO events is often close to integer multiples of 1470 years[31, 32] (for example 1470 years, 2940 years, 4410 years, etc.; compare figure 2.1). To some degree, this pattern can be explained by the principle of stochastic resonance[24, 33].

Because of the dynamics of the thermohaline circulation, stochastic resonance is an appealing concept to explain DO events: As discussed above, models suggest that the ocean circulation exhibits fundamentally different modes of operation, and that transitions between these modes can be excited if a certain forcing crosses a threshold. When a periodic forcing acts, which itself is too weak to cross this threshold, additional noise can raise the forcing above the threshold. Noise, arising from internal processes (weather, for example) could thus amplify a periodic external signal such that switches in the ocean circulation are caused which result in DO events. A stochastic trigger therefore requires a weaker periodic forcing component than a periodic external trigger. Apart from this, however, the concept of stochastic resonance suffers from similar deficiencies as the hypothesis of a purely external trigger: Most of all, a 1470-year forcing cycle of uncertain existence is still required in order to synchronise the timing of the DO events.

2.2.4 Erroneous regularity of the events?

Since none of the aforementioned hypotheses gives a satisfactory explanation for the apparent 1470-year time scale of the DO events, the reliability of the spectral peak in the oxygen isotope data of the GISP2 ice-core might be questioned. Paleoclimatic data indeed often exhibit deficiencies (uncertainties in the chronology, low

[4] The Holocene is the present warm age.

[5] It should be mentioned that a multi-centennial drift-ice cycle in the North Atlantic[28] has often been considered as the Holocene counterpart of the glacial 1470-year climate cycle. But this drift-ice cycle does not correlate with a millennial-scale forcing cycle; it rather coincides with "rapid (100- to 200-year) conspicuously large-amplitude variations" in proxies of solar variability[28]. Moreover, higher resolution data suggest that the drift-ice oscillations occur mainly on the time scale of 300-500 years, but not on the millennial scale[29].

time-resolution, etc.) which could possibly produce spurious peaks in the spectral composition of the time series. Therefore, it cannot be ruled out that the DO events are in fact less regular than suggested by the GISP2 ice-core. But because spectral peaks of similar periods are also present in a number of other climate records with different chronologies and different sampling rates, it is not likely that the glacial 1470-year climate cycle is purely erroneous (for example the result of aliasing, as suggested in the publication given in [34]).

Errors in the chronology of climate archives are likely to diminish and to broaden sharp peaks in the spectrum of the time series, or to shift the peak in the frequency domain. It is less likely that a nonsignificant spectral peak in an arbitrarily chosen time series is lifted beyond the significance level due to uncertainties in the chronology of the time series. This indicates that the regularity of the glacial 1470-year climate cycle is real, and it might even be higher than indicated by the GISP2 ice-core. An additional argument for the authenticity of the regular 1470-year glacial climate cycle is that the GISP2 ice-core, unlike most other climate archives, was layer-counted in the relevant time-interval. The chronology of this ice-core might therefore be considered as more trustworthy than the ones of other climate records.

To conclude this chapter, the DO events indeed appear to be part of a fairly regular 1470-year glacial climate cycle. During the Holocene, however, a similar cycle seems to be absent in almost all climatic time series. Various hypotheses were already proposed in order to explain the occurrence of the DO events, but a plausible explanation for their 1470-year time scale is still missing.

3 DO events in the model CLIMBER

Most of the studies which are presented in this thesis were performed with the coupled climate system model CLIMBER[1]-2 of the Potsdam-Institute for Climate Impact Research (PIK). In the first part of this chapter, a short description of the model is given; a detailed description has already been published[35]. In the second part of this chapter, earlier simulations of the DO events with CLIMBER-2 are reviewed.

3.1 Description of CLIMBER-2

3.1.1 Basic overview

CLIMBER-2 is a so-called *Earth system model of intermediate complexity* (EMIC), designed for long term simulations (up to the multi-millennial scale) of large-scale patterns (of the order of a few thousand kilometre) of the Earth system[36]. The model version that was used for the analyses as presented here contains sub-models (so-called modules) of the atmosphere, of the oceans (including sea-ice) and of the land (including vegetation). These modules interact through exchange of momentum, energy and matter (water, for example). Modules of the continental ice-sheets and of the carbon cycle are presently being developed and were therefore not yet included in the applied model version. This means that the continental ice-sheets, the sea-level and the atmospheric CO_2 concentration in the model are fixed either at Last Glacial Maximum (LGM) or modern pre-industrial (MOD) values. This corresponds to an atmospheric CO_2 concentration of 200 ppm and 280 ppm, respectively, and to a global sea-level for the LGM which is 120 metre lower than today. LGM continental ice-sheets are based on a published reconstruction[37].

3.1.2 Model resolution

In order to enable simulations over tens of thousands of years, the model resolution is coarse, and the description of the relevant processes (physical, biological, geochemical) is often simplified. CLIMBER-2 only resolves the large-scale, time-averaged climatic variables (i.e. the mean climate conditions in each grid cell of the model), but not the effects of weather or inter-annual variability (i.e. the

[1]CLIMBER is an acronym for **CLIM**ate-**B**iosph**ER**e model.

short-term variance of the climate conditions in each grid cell). The time step in CLIMBER-2 is one day, with a longer time step in some modules or sub-modules (for example in the radiative scheme of the atmosphere, in the ocean module and in the vegetation module). The spatial resolution is low and resolves only individual continents/sub-continents and ocean basins. The model grid for the atmospheric and terrestrial modules is illustrated in figure 3.1. The latitudinal resolution is 10°

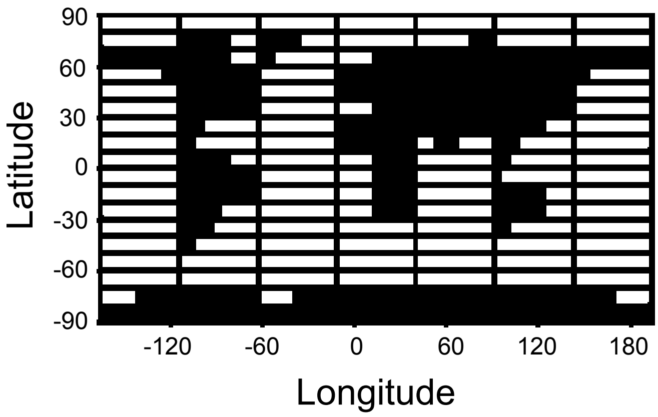

Figure 3.1: Atmospheric and terrestrial grid of CLIMBER-2.
Representation of the atmosphere and land surface in the model (present-day boundary conditions). Note that the resolution of the ocean module is different (as discussed in the text). The figure is taken from [35].

for the atmosphere and land surface, and 2.5° for the oceans. Note that the resolution of the ocean model in the applied model version is higher than shown in figure 3.1 and also higher than described in [35]. In longitude, the Earth's surface and the atmosphere is divided into seven equal sectors (of about 51°), while the ocean module resolves only the three main ocean basins (Atlantic, Indian Ocean, Pacific). Each oceanic grid box is in contact with one, two or three atmospheric grid boxes, depending on the width of the ocean basin. Vertically, the ocean module resolves 20 unevenly spaced levels. In the atmosphere, a universal vertical structure for the temperature and humidity fields is assumed. Ten vertical levels are considered for the calculation of wind velocities and the transport of energy and water. For the computation of the radiative fluxes, sixteen vertical levels exist.

The atmospheric long-wave radiative scheme of CLIMBER-2 accounts for water vapour, carbon dioxide and ozone. Clouds are treated as black-body radiators. The short-wave radiation scheme accounts for water vapour, clouds, aerosols and ozone. Two types of clouds are considered: large-scale stratiform and cumuli. The model resolves six surface types: open water, sea-ice, forest, grassland, bare soil and continental ice. Different types can coexist in each grid cell. Vegetation cover changes dynamically with the climatic conditions, and these changes directly affect the climate system, for example through variations in albedo and transpiration.

3.1.3 Applicability for paleoclimate simulations

Any type of *flux adjustment* was avoided in CLIMBER-2. This means that no unphysical “correction” in the fluxes of momentum, energy and matter were used in order to simulate present-day climate conditions successfully. Flux adjustment is problematic for the simulation of climate states with very different boundary conditions[35]. Since CLIMBER-2 does not contain flux adjustment terms, the model is applicable for the simulation of climates fundamentally different from the present one. Owing to the low computing time of the model, CLIMBER-2 can easily be run to equilibrium, and a large number of studies with different model set-ups can be performed. Earlier studies showed that despite of its simplicity and low resolution, the model is able to reproduce the main characteristics of the present climate fairly realistically[35]. Moreover, many aspects of past climates, for example of the last glacial maximum (21000 years before present) and of the mid-Holocene (6000 years before present), were also reproduced by CLIMBER-2[38, 39].

3.2 Simulation of DO events with CLIMBER-2

3.2.1 Glacial modes of the Atlantic THC

In a couple of studies with the model, Dansgaard-Oeschger events were already simulated[16, 24, 40, 41]. In the first of these publications[16], it was shown that CLIMBER-2 exhibits more than one possible state of operation for the glacial North Atlantic thermohaline circulation. Three modes were discussed: A so-called *stadial* mode (which is the only stable mode for LGM conditions), an *interstadial* mode (this mode is metastable and can be excited by a small perturbation), and a third mode that is not relevant for this thesis (this mode is unstable and can only be excited by a large perturbation).

The main difference between the stadial and the interstadial mode is the location of NADW[2] formation (see figure 3.2). In the interstadial mode, warm and salty surface water from lower latitudes reaches the Nordic Seas before its density is high enough[3] to cause an instability in the vertical stratification. This instability eventually leads to deep water formation, which in the interstadial mode takes place near 65° N, similar to the present situation. In the stadial mode, however, NADW formation is shifted to about 50° N, i.e. to south of Iceland. Warm surface water from the subtropics thus does not reach the Nordic Seas anymore, and extensive

[2]NADW = North Atlantic deep water

[3]due to cooling at higher latitudes (in particular at the sea-ice margin)

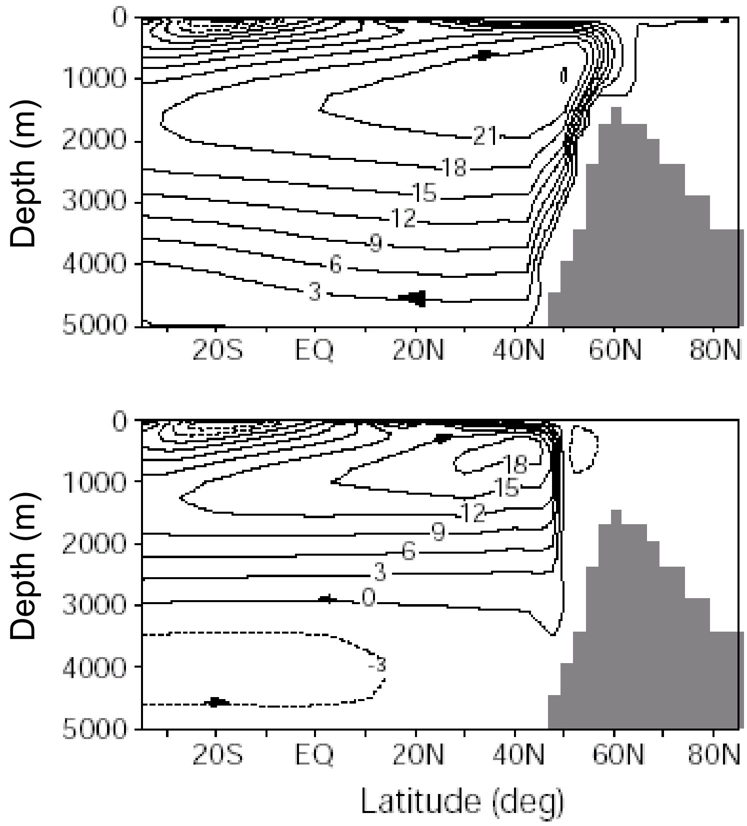

Figure 3.2: Glacial THC in CLIMBER-2.
Shown is the stream function (in Sverdrup [Sv], 1 Sv = 10^6 m^3/s) for the Atlantic. Upper panel: Interstadial mode. Lower panel: stadial mode. The shaded area represents the ridge between Greenland and Scotland. The figure is taken from[16].

sea-ice cover can form in that area. Since sea-ice efficiently insulates the atmosphere from the ocean, and also substantially increases the albedo of the ocean surface, a large temperature gradient between the ocean water and the surface air can be sustained here. Very low temperatures can thus occur above the ice. This means that in the stadial mode of the model, annual mean temperatures in the North Atlantic region (in particular in Greenland) are several Kelvin lower than in the interstadial mode (figure 3.3), with a much larger cooling in winter than in summer.

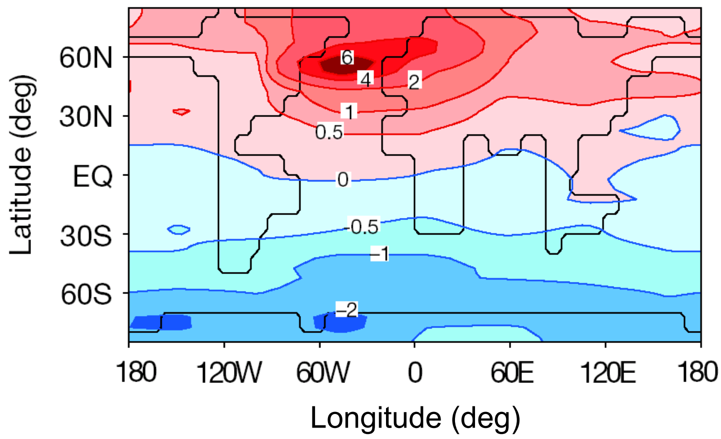

Figure 3.3: Global temperature anomalies in the interstadial mode. The figure shows the simulated differences in annual mean surface air temperature in Kelvin (interstadial mode minus stadial mode). In the interstadial mode, the North Atlantic region is up to 6°C warmer than in the stadial mode. The figure is taken from[16]. Note that the set-up of the continents corresponds to LGM boundary conditions and is therefore slightly different than shown in figure 3.1.

3.2.2 DO events as abrupt switches in the ocean circulation

In the same study, the interstadial mode of the glacial thermohaline circulation was suggested to correspond to warm intervals in Greenland (i.e. to warm phases during DO events), and the stadial mode to cold intervals[16]. Abrupt shifts between the two modes were proposed as the mechanism that is inherent in the observed DO oscillations: To trigger switches between the modes, a small periodic perturbation in the freshwater flux to the North Atlantic (which was intuitively linked with an external forcing) was prescribed. Since the density of the ocean water depends on salinity (but also on temperature), the forcing caused periodic variations of the Atlantic surface density field. Transitions from the stadial mode into the interstadial mode of the model were excited by a reduction of the freshwater fluxes (i.e. by an increase in the surface salinity and thus in surface density). Similarly, transitions back into the stadial mode were triggered by an increase of the freshwater flux (and thus by a decrease in surface density). Most important, the transitions between both modes were abrupt processes - they evolved very rapidly, as a threshold process: As long as the freshwater perturbation was below a certain threshold, transitions of the THC did not occur. But when the forcing was strong enough to cross the relevant threshold, the ocean circulation switched its mode within approximately a decade.

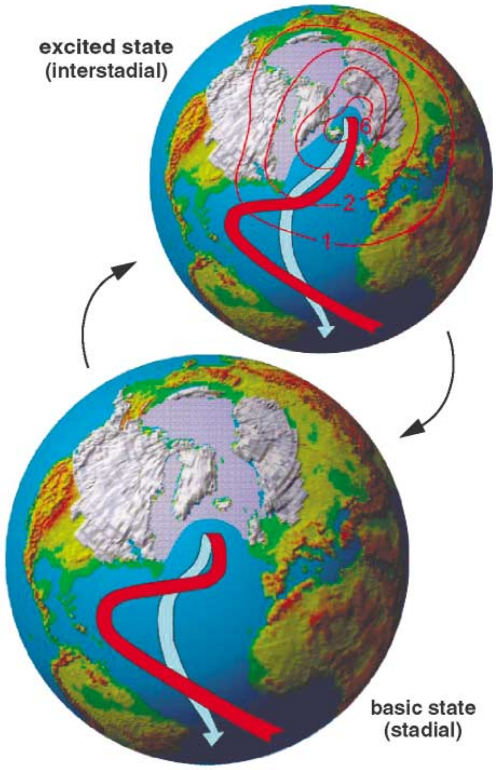

Figure 3.4: Schematic illustration of the two glacial climate states.
Upper part: Interstadial ("warm") state. Lower part: Stadial ("cold") state. The contour lines in the upper part illustrate the annual mean surface air temperature difference between the interstadial and the stadial state, compare figure 3.3. The arrows schematically show the ocean circulation (red: surface currents, light blue: deep currents). North Atlantic sea-ice cover is substantially reduced in the interstadial mode. The figure is taken from[24].

Switches from the stadial mode into the interstadial one resulted in abrupt warming events in the North Atlantic region, with a temperature increase of more than 5 Kelvin in Greenland (compare figure 3.4) over only a few years. This warming lasted for a few centuries, until the forcing crossed a second threshold and a transition back into the stadial mode was triggered. The simulated warming events had many similarities with the DO events as observed in various climate archives: Several important patterns of the DO events were reproduced, in particular the time evolution of Greenland temperature (including the abruptness of the initial warming), the global pattern of the events and the phase relation of the Antarctic response. The characteristic time scale of 1470 years of the Dansgaard-Oeschger events, however, remained unexplained: In the simulations with CLIMBER-2, a sinusoidal forcing cycle with a period of about 1500 years was prescribed to obtain a spacing of 1500 years between successive warming events. But the origin of this forcing cycle remained very speculative.

3.2.3 Stochastic resonance

In a subsequent study, it was shown that in order to trigger DO events, noise[4] can provide an efficient amplifier for a small periodic forcing signal[24]. This amplifier mechanism is due to the threshold process which is inherent in the switches between the two ocean circulation modes: If the periodic signal itself is too small to cross the threshold, some additional variations (noise, for example) can push the forcing beyond the threshold. This mechanism is called *stochastic resonance* (compare section 2.2.3). In the case when noise is also present, the periodic component in the forcing can be substantially smaller than in the case without noise. Despite the presence of noise, the simulated DO events can still be rather regular for many choices of the signal-to-noise ratio.

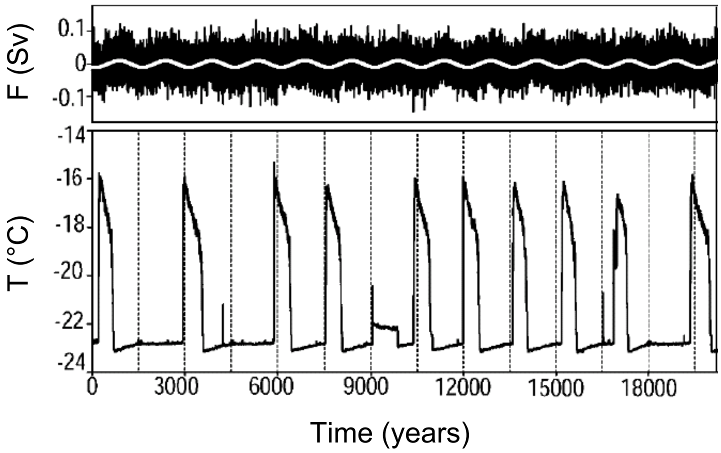

Figure 3.5: DO events as obtained by stochastic resonance.
Top panel: Forcing in the model simulations. The forcing represents a freshwater perturbation (in Sverdrup, 1 Sv = 10^6 m^3/s) that is added to the North Atlantic. It consists of two components: white noise with a standard deviation of 0.035 Sverdrup (black curve), and a sinusoidal signal with an amplitude of 0.01 Sverdrup and a period of 1500 years (white line). Bottom panel: model response (temperature over the Northern Atlantic, in °C). Dotted lines indicate the minima of the sinusoidal forcing signal. The figure is taken from[24].

[4]Noise can mimic natural short-term climate variability (weather, for example), which is not explicitly resolved in the model.

In addition to this amplifier mechanism, the principle of stochastic resonance can also give a possible explanation why the observed DO events are often spaced by integer multiples of 1470 years (compare section 2.2.3): In the context of stochastic resonance, DO events are not triggered by a purely periodic signal, but also by an additional random component. This means that some of the peaks of the 1470-year sinusoidal forcing cycle encounter a stochastic component which is "in phase". As a consequence, constructive interference occurs: the stochastic component pushes the periodic cycle beyond the threshold. In other cases, the stochastic component is "out of phase". As a result, constructive interference does not occur and the threshold is not crossed. This means that not all of the peaks of the periodic forcing component actually trigger DO events. Instead, sometimes a peak is missed. Assuming a 1470 year forcing cycle, stochastic resonance can thus explain the occurrence of waiting times near integer multiples of 1470 years.

For this reason, stochastic resonance provides an appealing concept to explain the timing of DO events. But this concept still requires the existence of a 1470-year forcing cycle. Such a cycle has not been found. Moreover, were the DO events triggered by an external 1470-year cycle, this cycle would also be expected to operate in the Holocene. Some signature of the forcing cycle should thus also be present in climate archives from the Holocene. Though indications for a roughly 1500-year quasi-period in drift-ice from the North Atlantic were presented a couple of years ago[28], this cycle is not a signature of a 1500-year sinusoidal forcing cycle: The drift-ice cycle was rather reported to coincide with "rapid (100- to 200-year), conspicuously large-amplitude variations"[28] in proxies of solar activity. In line with these findings, those proxies do not show a spectral component of about 1470 years, but they show very pronounced components in the century range (see chapter 4). The existence of a 1470-year forcing cycle is therefore very questionable. Consequently, the apparent lack of this forcing cycle is the most important limitation of earlier studies with CLIMBER-2, in which DO events were already simulated.

4 Solar variability and climate

The role of solar variability in climate change is poorly understood. On the one hand, many paleoclimatic archives convincingly show a signature of the known century-scale solar activity cycles. This suggest that variations of the Sun contributed substantially to reconstructed temperature changes in the past. On the other hand, it is not known which mechanisms could explain the magnitude of the solar signal in the climate records. Therefore, the influence of solar variability on the Earth's climate is still very uncertain.

4.1 Schwabe cycle

Thanks to direct satellite observations it is now well-known that the luminosity of the Sun has not been constant over the last two 11-year solar cycles[42, 43]. In the satellite data, the total solar irradiance[1] varied by about 0.1 percent in the course of the last two solar cycles, i.e. by roughly 1 W/m^2. These data thus proved that the "solar constant" is in fact not constant over the 11-year cycle (the so-called *Schwabe cycle*, named after the German amateur astronomer Samuel Heinrich Schwabe). Those variations, however, are not sufficiently slow to allow the Earth's climate to reach full equilibrium (this is due to the large heat capacity of the oceans, for example). Moreover, they are small compared with fluctuations in the Earth's radiation balance (due to changes in cloudiness, for example, which play a very important role for the radiation budget[44]). It is therefore not surprising that variations in the solar constant were not detected until the satellite era. Because of their small magnitude, the observed solar changes are generally considered to be too small to have an important direct influence on climate. But it should be mentioned that solar irradiance variations are not uniform over all wavelengths: The relative variations in the ultra-violet range, for example, are much higher (up to an order of a few percent over the 11-year cycle) than the variations in total solar irradiance[45].

[1] The total solar irradiance (TSI) is the solar flux at the Earth integrated over all wavelengths, ironically also called "solar constant".

4.2 Gleissberg cycle

It is also known that the 11-year cycle is not the only solar cycle. The sunspot-number record, for example, which is the longest record of direct observations of solar activity, exhibits an additional cyclic component with a period close to 90 years. This cycle manifests itself as an amplitude modulation of the 11-year cycle (figure 4.1) and was first discovered by the German astronomer Wolfgang Gleissberg[46]. Since a cycle with a similar period is present in many solar and solar-terrestrial phenomena[47] (for example in auroral records and in records of the cosmogenic isotope ^{14}C[48, 49]), the existence of a solar activity cycle with a period somewhere in the range of 80-90 years, called *Gleissberg cycle*, is now generally accepted .

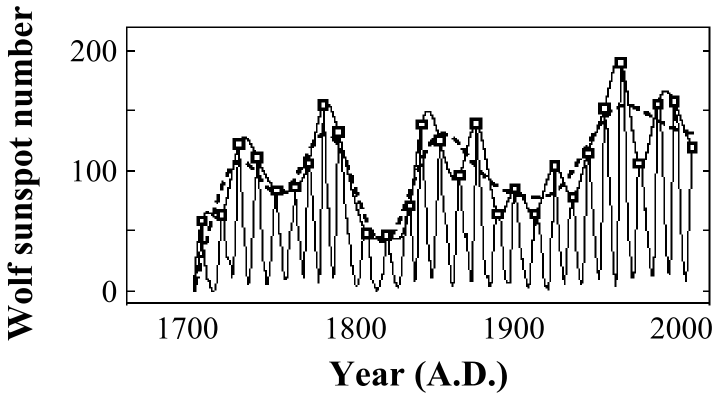

Figure 4.1: Relative sunspot-number record.
The solid line (exhibiting decadal-scale oscillations) shows variations of the so-called Wolf sunspot number over the last three centuries. The Wolf number is a measure for solar magnetic activity and increases with a higher number of individual sun-spots and with a higher number of sunspot groups on the Sun's surface. The white boxes define the envelope of the Wolf sunspot number curve. The dashed line shows the envelope smoothed by a low-pass filter. The figure is taken from[49].

4.3 de Vries / Suess cycle

A general consensus now exists that, in addition to the Schwabe cycle and the Gleissberg cycle, solar activity exhibits a third cycle with a period of slightly more than 200 years. Because of its length, this cycle is difficult to observe in the comparably short sunspot record. But records of cosmogenic radionuclides (for example

^{14}C and ^{10}Be), as more indirect indicators for solar activity, can be used to identify this cycle: Cosmogenic radionuclides are produced by the interaction of cosmic rays with atoms in the Earth's atmosphere. Since their production rate varies with the solar magnetic field (but also with the Earth's geomagnetic field), the concentration of ^{14}C and ^{10}Be in climate archives (for example ^{14}C in tree-rings, ^{10}Be in ice-cores) can be used to study solar variability in the past[50, 51]. Because of the long half-lives of the radionuclides (^{14}C: 5730 years, ^{10}Be: about 1.5 million years), this method is applicable to study changes in solar activity far back in time.

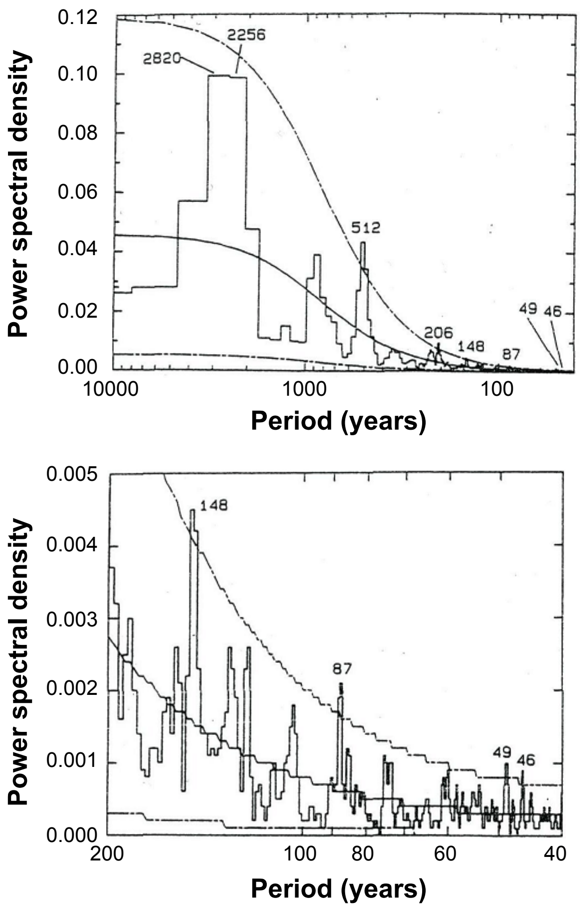

Figure 4.2: Fourier spectrum of past $\Delta^{14}C$-variations.
Power spectral density as calculated from an about 11000-year long record of past ^{14}C-variations in the atmosphere, obtained from tree rings. The 2σ significance level is given by the upper curve. Periods exceeding the 2σ level are: 512 years, 206 years, 148 years, 87 years and 46-49 years. The figure is taken from[48]. For more information, see that publication.

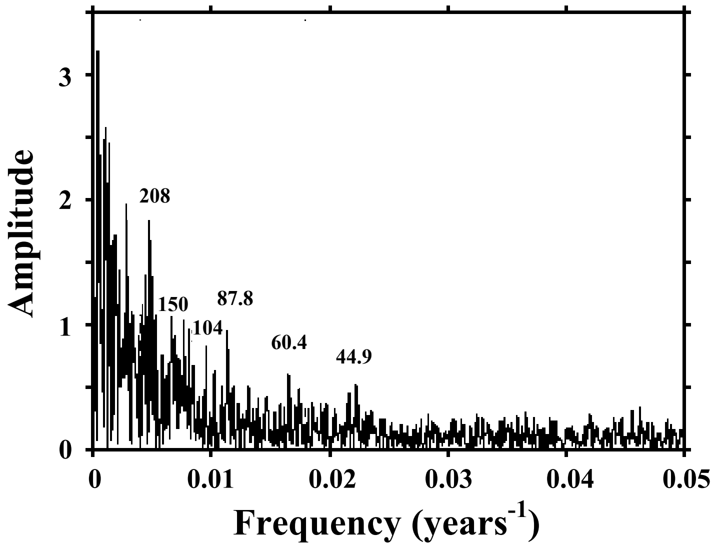

Figure 4.3: Fourier spectrum of ^{14}C-variations in the INTCAL98 record. The INTCAL98 record represents an about 12000-year long record of past ^{14}C-variations, obtained mainly from annual tree rings. The periods of prominent spectral components as given in the figure can be explained by an amplitude-modulation of a 88-year cycle by a 208-year cycle. The values of 44.9 years and 104 years correspond to the second harmonics. Periods of 150 years and 60.4 years correspond to combination tones. The figure is taken from [49]. For more information, see that publication.

Records of cosmogenic radionuclides reveal the existence of the third solar cycle, with a period of about 210 years[48, 52], compare figures 4.2 and 4.3. Such a pattern was first observed by the Dutch physicist Hessel de Vries and later elaborated by Hans Eduard Suess, an Austrian-American geochemist[53, 54]. Named after these, the 210-year cycle is today generally referred to as *de Vries cycle* or *Suess cycle*, respectively. For a number of reasons, it is very plausible that this cycle is of solar origin: A roughly 210-year cycle is present in the ^{14}C-data [48] as well as in the ^{10}Be-data [52] (which would indeed be expected for a solar cycle), and the cycle is amplitude-modulated by the geomagnetic field[52]. This would also be expected for a solar cycle. Moreover, pronounced solar minima (the so-called Maunder minimum, the Spörer minimum and the Wolf minimum, at about 1700, 1500 and 1300 years A.D.) are spaced by roughly 200 years. This suggests that the de Vries-cycle is also reflected in the sunspot data. Evidence from various climate archives suggests that the de Vries-cycle, and possibly also the Gleissberg cycle, is also manifested as a climate cycle[2, 55, 56].

4.4 Other cycles

Apart from the Schwabe cycle (about 11 years), the Gleissberg cycle (about 87 years) and the de Vries/Suess cycle (about 210 years, in the following referred to as *DeVries-cycle*), other periodicities are often discussed in the context of solar variability: the well-known Hale cycle, and much more hypothetic cycles with periods in the range of centuries to millennia. The *Hale cycle*, named after the American astronomer George Ellery Hale, is a 22-year cycle during which the polarity of sunspot pairs reverses. Since this cycle is mainly a magnetic cycle, it is less likely to have a noteworthy effect on the Earth's climate. In line with that, satellite data of total solar irradiance variations over the last two decades mainly show the 11-year Schwabe cycle, shorter term fluctuations, and possibly an additional long-term trend, but apparently no 22-year cycle[42, 43] .

The presence of further spectral peaks in time series of solar variability proxies could indicate the possible existence of additional solar cycles on the centennial and millennial time scale: For example, a millennial-scale solar cycle with a period of roughly 2300 years, named *Hallstatt cycle*, was suggested to exist[50]. This cycle, however, is far more speculative since it is not possible to detect such a long cycle in any record of direct observations of solar activity. Moreover, additional peaks in the ^{14}C-record could also result from a number of other effects, for example from an amplitude-modulation of the known solar cycles[49] (which would produce additional combination tones and harmonics in the spectrum), from purely climatic effects (for example from changes in the ocean circulation, which affect the ^{14}C-record since the uptake of carbon by the ocean varies when the ocean circulation changes[57]) or from variations in the geomagnetic field of the Earth (these affect the ^{14}C-record since the production rate of ^{14}C also varies with the geomagnetic dipole moment).

4.5 Channels for solar influence on climate

While the time scale of the known solar cycles (about 11, 87 and 210 years) is fairly accepted, little evidence exists on the mechanisms by which observed solar signatures in various climate archives[2, 28, 55, 56, 58, 59] could be caused. The most obvious source for solar influence on climate are changes in the total solar irradiance (TSI). Past TSI-changes were often reconstructed based on observations on sun-like stars[60]. These reconstructions hinted at century-scale variations in TSI of the order of about 5 W/m^2[61]. Recent observations, however, suggested that the apparently sun-like stars are in fact not very similar to the Sun[62]. As a consequence, it has now become even more questionable if past changes in total solar irradiance are of sufficiently large amplitude to explain the observed Sun-climate relations on centennial to millennial time scales.

In principle, other channels for solar influence on climate could account for these relations, for example changes in the ultra-violet frequency range of solar irradiance (which affect ozone and could thus modulate the propagation of planetary waves[63, 64, 65]) or, more hypothetic, variations in the the solar magnetic field (which possibly affect cloud formation by their effect on the flux of galactic cosmic rays[66, 67]). But it also cannot be entirely ruled out that the observed very small changes in total solar irradiance are indeed the dominant channel for solar influence on the Earth's climate, and that the climate is more sensitive to these changes than commonly assumed (because of some yet unknown feedback process).

To summarise this chapter, the time scale of the most dominant cycles in solar activity are presently fairly well-known, but the magnitude of the solar influence on the climate of the Earth is still very uncertain.

5 Spectral analysis

Time series of North Atlantic temperature reconstructions in the last glacial show a prominent spectral component corresponding to a frequency close to 1/1470 years^{-1} (see section 2.1.4). Solar variability, as a possible trigger for those climatic changes, shows prominent spectral components at frequencies near 1/210 years^{-1} and 1/87 years^{-1}, but lacks a frequency of 1/1470 years^{-1} (see section 4). This lack has often been regarded as a main argument against a solar driver of the glacial 1470-year climate cycle. In this thesis, this objection is tested. In other words, the main question considered here is: Is is possible that a forcing with spectral components close to that observed in proxies of solar variability can cause a prominent spectral peak at a frequency of 1/1470 years^{-1} in a time series of Greenland temperature, as simulated by a coupled climate model with boundary conditions of the Last Glacial Maximum?

In order to perform this analysis, a method for the detection of cycles and periodicities in a given time series is required. In the time series that are considered in this thesis, the signal-to-noise ratio is very high (noise is virtually absent). Moreover, most of the time series are periodic (with a known period) and can therefore be continued to infinity, despite their limited length. The time step in the time series is equidistant and the chronology is exact. For the analysis of such time series, standard Fourier series expansion is sufficient. Since noise is negligible and the length of the time series can be chosen such that the time series covers a full period, the Fourier spectra as obtained by this method reflect only the signal and are exact (apart from inaccuracies in the numerical calculation of the Fourier integrals). The specification of confidence limits is therefore not necessary here.

5.1 Fourier series expansion

In a Fourier series expansion, a periodic function $f(t)$ with period T is expressed in terms of sine- and cosine-functions with discrete frequencies $\omega_k = k \cdot \omega_0$ ($k \in \mathbb{N}$, $\omega_0 = 2\pi/T$)

$$F(t) = \frac{a_0}{2} + \sum_{k=1}^{\infty} a_k \cdot \cos(k\omega_0 t) + b_k \cdot \sin(k\omega_0 t). \tag{5.1}$$

The derivation of this formula, as well as of the following ones, is given in standard calculus textbooks. The function F is called the *Fourier series* of f, a_k and b_k are the *Fourier coefficients* of f, and ω_0 is the so-called *fundamental frequency* of f. The Fourier coefficients are computed according to the following relations

$$a_k = \frac{2}{T} \cdot \int_0^T \cos(k\omega_0 t) \cdot f(t) \cdot dt \tag{5.2}$$

$$b_k = \frac{2}{T} \cdot \int_0^T \sin(k\omega_0 t) \cdot f(t) \cdot dt. \tag{5.3}$$

From these two expressions, it is possible to obtain an amplitude-phase-notation, which is more useful for the calculation of the amplitude-spectrum of the function f than the notation given above. In the amplitude-phase-notation, F reads

$$F(t) = \frac{A_0}{2} + \sum_{k=1}^{\infty} A_k \cdot \cos(k\omega_0 t + \phi_k) \tag{5.4}$$

with the following expressions for the amplitude A_k and the phase ϕ_k, corresponding to the spectral component with the frequency $\omega_k = k \cdot \omega_0$

$$A_k = \sqrt{a_k^2 + b_k^2} \tag{5.5}$$

$$\phi_k = \arctan \frac{a_k}{b_k}. \tag{5.6}$$

These two expressions give the amplitude- and phase-spectra of f. Since f is periodic, the spectra are discrete (i.e. amplitudes of spectral components corresponding to frequencies different from $\omega_k = k \cdot \omega_0$ are zero).

When f is continuous and differentiable, F converges uniformly to f. In this case the Fourier series representation is unique: This means that if the function f can be written by any expression in the form as given by equation (5.1), then the coefficients a_k and b_k are necessarily given by the equations (5.2) and (5.3). These coefficients are thus the sought-after Fourier coefficients of f. Near points of discontinuity of the function f, the Fourier series F overshoots or undershoots[1]. This effect is due to the fact that the Fourier series does not converge uniformly at these points.

All amplitude-spectra which are presented in this thesis were numerically obtained with the formulae (5.2), (5.3) and (5.5). Phase-spectra are not investigated.

[1] This is the so-called *Gibbs phenomenon*.

5.2 Fourier spectra and non-linearity

For the purpose of time series analysis, Fourier-type spectra (amplitude- and/or power-spectra) are commonly computed to detect and analyse cyclic components in a given time series. In a linear system, the interpretation of these spectra is fairly straightforward since in this case the spectra of the forcing and of the system's response exhibit the same frequencies: Consider a system which is described by the time evolution of a single variable $y(t)$, for example global temperature, and which is driven by a forcing described by the function $x(t)$. If the system is linear (and time-invariant), a simple relation exists between the amplitude spectrum $X(\omega)$ of the forcing and the amplitude spectrum $Y(\omega)$ of the response

$$Y(\omega) = H(\omega) \cdot X(\omega) \tag{5.7}$$

where $H(\omega)$ is the Fourier transform of the so-called *transfer function*. As a consequence, the amplitude spectrum of the forcing and the one of the response show the same frequencies (unless $H(\omega) = 0$ for a certain value of ω). This means that if the response of a linear system exhibits a spectral component $Y(\omega)$ at a certain frequency ω, a component with the same frequency must also be present in the forcing.

In a non-linear system this simple relation between the amplitude-spectra of the forcing and of the system's response does not hold anymore. This makes the interpretation of Fourier-type spectra much more difficult and error-prone. To illustrate the potential effect of non-linear dynamics, two simple examples are now considered: In both examples, a sinusoidal forcing is applied, given by the expression

$$x(t) = \cos(\omega_0 t) \tag{5.8}$$

with the frequency $\omega_0 = 2\pi/T$ and the period $T = 1470$ years (see upper panel in figure 5.1). The amplitude spectrum of $x(t)$ only shows a single spectral component corresponding to a frequency $\nu_0 = \omega_0/2\pi = 1/1470$ years^{-1}, with an amplitude of one (upper panel in figure 5.2).

5.2.1 First example: $f(x) = x^2$

In the first example, the response $y(t)$ of a non-linear system to the forcing, denoted by $x(t)$, is given by

$$y_1(t) = [x(t)]^2 \tag{5.9}$$

(middle panel in figure 5.1). Since the relation

$$\cos^2(\omega t) = \frac{1}{2} + \frac{1}{2}\cos(2\omega t) \tag{5.10}$$

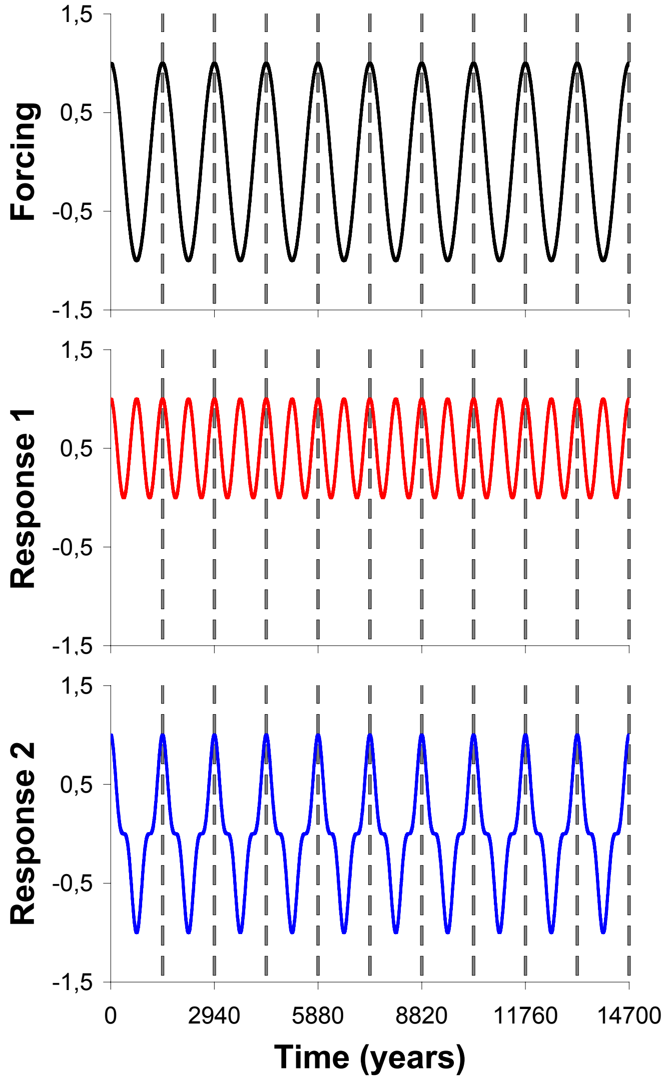

Figure 5.1: Forcing and response of a very simple non-linear system. Upper panel: Considered forcing (a cosine function with a period $T = 1470$ years and an amplitude $A = 1$). Middle panel: Response $y_1(t)$ to the forcing $x(t)$, assuming a relation $y_1 = x^2$. Lower panel: Response $y_2(t)$ to the forcing $x(t)$, assuming a relation $y_2 = x^3$. The dashed lines are spaced by 1470 years.

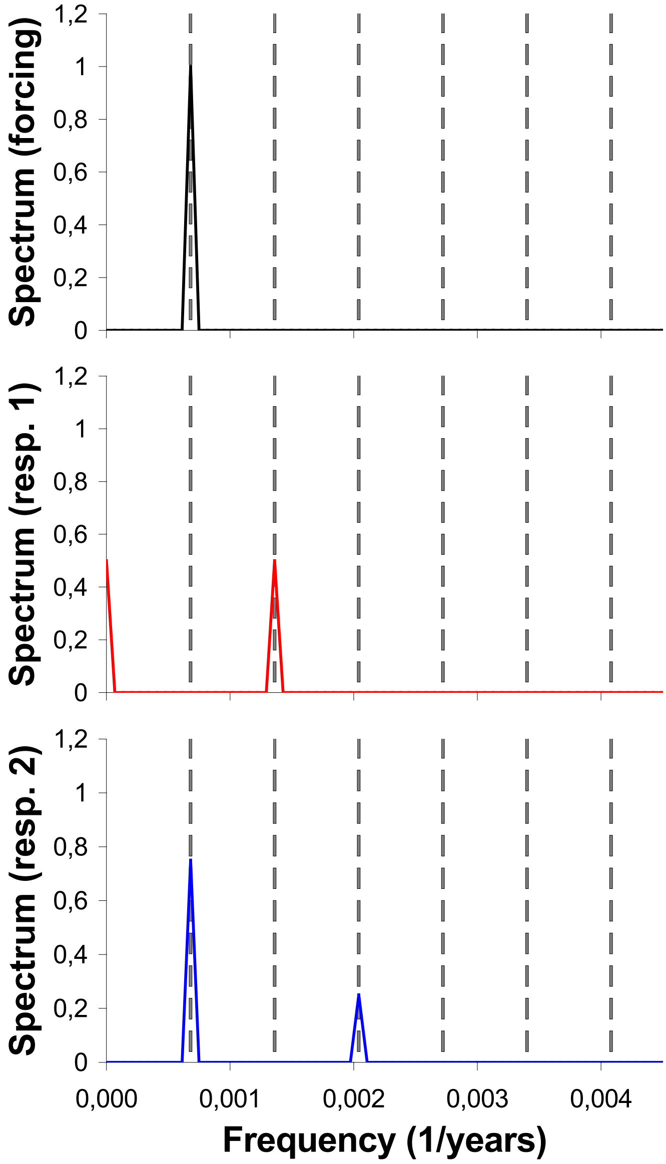

Figure 5.2: Amplitude spectrum of forcing and response.
Upper panel: Amplitude-spectrum of the forcing. The forcing $x(t)$, given by equation (5.8), exhibits a single spectral component with frequency $\nu_0 = 1/1470$ years^{-1}. Middle panel: Spectrum of $y_1(t)$ ($y_1 = x^2$). Lower panel: Spectrum of $y_2(t)$ ($y_2 = x^3$). The dashed lines are spaced by $1/1470$ years^{-1}.

holds, the spectrum of $y_1(t)$ (middle panel in figure 5.2) shows two peaks corresponding to frequencies of zero and of $2\nu_0 = 2/1470$ years^{-1}, with an amplitude of 0.5 for each component. This means that the response of a non-linear system can exhibit additional spectral components with frequencies that do not occur in the forcing. Moreover, the response $y_1(t)$ repeats every 735 years (middle panel in figure 5.1) whereas the forcing has a period of 1470 years. Since the period of $y_1(t)$ is 735 years, no spectral peak at $\nu_0 = 1/1470$ years^{-1} exists in the response (middle panel in figure 5.2). This means that the response of a non-linear system can also lack all of the frequencies that are present in the forcing.

5.2.2 Second example: $f(x) = x^3$

In the second example, the response of the system is considered to be

$$y_2(t) = [x(t)]^3 \tag{5.11}$$

(lower panel in figure 5.1). Since the relation

$$\cos^3(\omega t) = \frac{3}{4}\cos(\omega t) + \frac{1}{4}\cos(3\omega t) \tag{5.12}$$

holds, the spectrum of $y_2(t)$ (lower panel in figure 5.2) shows two peaks corresponding to frequencies of $\nu_0 = 1/1470$ years^{-1} and of $3\nu_0 = 3/1470$ years^{-1}, with an amplitude of 0.75 and 0.25, respectively. Again, the response of the non-linear system exhibits a spectral component that does not exist in the forcing.

Because of the potential differences between the spectra of the forcing and of the response, results of spectral analysis must be interpreted with extreme caution when non-linear relations are involved. This has important consequences for time series analysis performed on climatic variables, which often show a non-linear behaviour: The existence of statistically significant peaks in the Fourier spectra of climatic time series does not by itself imply that the same frequencies are also present in the forcing. Instead, the peaks might also be due to a non-linear response of the climate system to a forcing that shows a completely different spectral composition.

6 A new hypothesis to explain the glacial 1470-year climate cycle

In this chapter a new hypothesis is presented to explain the glacial 1470-year climate cycle, which is most pronounced in the North Atlantic region. In the next chapters, this hypothesis is tested with the climate model CLIMBER-2 (compare chapter 3) and with a very simple conceptual model, which is developed in order to interpret the model results obtained with CLIMBER-2.

6.1 Motivation of the hypothesis

Various hypotheses have already been proposed in order to explain the occurrence and the timing of abrupt glacial warming events in the North Atlantic region, the so-called Dansgaard-Oeschger (DO) events. As discussed in section 2.2, the suggested explanations either assume some external trigger for these events, or a self-sustained oscillation of the climate system. One of the main drawbacks of the current hypotheses is that none of them can give a plausible explanation for the regularity of the DO events as observed in the layer-counted part of the GISP2 ice-core[1] (see discussion in chapter 2). In this ice-core, a statistically significant spectral component of 1470 years was detected[2]. This climate cycle is manifested in the DO events, which are typically spaced by about 1470 years or integer multiples thereof[23, 31, 32] (with deviations which are less than about 150 years[32] for most events[2]).

6.1.1 A still undetected 1470-year forcing cycle?

In principle, this systematic pattern could be explained if the DO events were triggered by an external forcing cycle with a frequency of $1/1470$ years^{-1} (see section 2.2.2). Such a cycle, however, has not been detected. The strongest forcing cycles are either much longer or much smaller: The so-called *Milankovitch cycles*[3] on the

[1] the time-interval up to about 50000 years before present

[2] The only exceptions are the DO events labelled 4, 8 and 9, with deviations of about 250-500 years[32].

[3] Milankovitch cycles represent changes in solar radiation at the Earth's surface, due to variations in the Earth's orbit.

one hand have much longer periods of tens or hundreds of thousands of years. The known solar activity cycles on the other hand have much shorter periods of about 11, 87 and 210 years (compare chapter 4). Other forcing cycles exist in between[22], but these are also different from 1470 years. Moreover, they are much weaker than the Milankovitch cycles and the solar cycles, and are therefore less likely to trigger notable climatic changes. In any case, it seems plausible to rule out that the DO events are triggered by an unknown external forcing cycle with a frequency of about 1/1470 years^{-1}. The conclusion from this assumption is that DO events are either caused by internal processes only, or - at least to some part - by external forcings with spectral components corresponding to periods different from 1470 years.

6.1.2 Internal or external origin of the 1470-year climate cycle?

The notion of an external trigger of the DO events is supported by the apparently high regularity in the timing of DO events in the GISP2 ice-core, as well as by the statistical significance of the 1470-year spectral peak: In the case of a self-sustained oscillation, the period of that oscillation would be expected to depend on the climatic background, i.e. on the boundary conditions (continental ice-volume, sea level, orbital parameters, etc.). But over a time interval of tens of thousands of years these boundary conditions are highly variable, and the climate system probably passed through a number of different climate states. Consequently, the period of a self-sustained oscillation would be expected to be rather irregular over such a long interval. The DO events, however, were demonstrated to be fairly regular, at least in the layer-counted part of the GISP2 ice-core (see chapter 2). This regularity thus argues against a purely internal origin of the glacial 1470-year climate cycle.

But how could a 1470-year climate cycle be triggered by an external forcing without a 1470-year forcing cycle? It is important to notice that the lack of a 1470-year component in the spectral composition of a possible external forcing does not by itself imply that the forcing cannot repeat with a period of 1470 years: Any[4] function with a period of 1470 years can be expressed as a sum of sinusoidal components with frequencies ν_n of integer multiples of 1/1470 years^{-1} ($\nu_n = n \cdot \nu_0$, with $\nu_0 = 1/1470$ years^{-1} and $n \in \mathbb{N}$), see section 5.1. A forcing with frequencies larger than 1/1470 years^{-1} might thus still repeat with a period of 1470 years, provided that the forcing frequencies correspond to harmonics (i.e. to integer multiples) of the fundamental frequency ν_0. But a forcing with smaller frequencies cannot show a 1470-year period. This means that the 1470-year climate cycle might be much more easily explained by the high frequency solar forcing than by the low frequency Milankovitch cycles. Consequently, it is most promising to develop a hypothesis that

[4]more precisely, any continuous and differentiable

describes how the known solar cycles could explain the glacial 1470-year climate cycle. In the following section, my hypothesis is described.

6.2 Description of the hypothesis

6.2.1 Solar variability: Harmonics of a 1470-year cycle?

My hypothesis is based on the values for the periods of the known solar cycles: Apart from the obvious 11-year solar cycle (the Schwabe cycle), two other cycles are fairly well-known: the Gleissberg cycle (with a period of about 87 years[49]) and the DeVries cycle (period: about 210 years[52]), compare section 4. It is interesting to note that the periods of the two century-scale cycles are close to prime factors of 1470 years (1470/7 years = 210 years, 1470/17 years ≈ 86.5 years). These cycles could therefore represent the 7th and the 17th harmonic of a 1470-year fundamental frequency[5]. The sum $f(t)$ of two sinusoidal cycles with these periods

$$f(t) = \cos(2\pi t/T_1) + \cos(2\pi t/T_2) \tag{6.1}$$

(T_1 = 1470/7 years and T_2 = 1470/17 years) repeats with a period of 1470 years, although a frequency corresponding to that period is not explicitly present in that function (see figure 6.1).

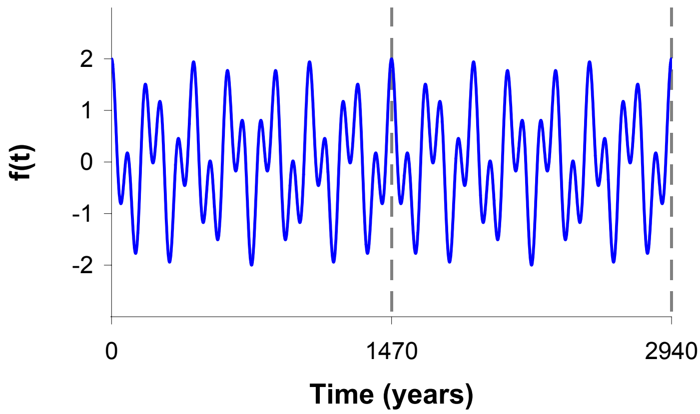

Figure 6.1: The sum of the two sinusoidal cycles.
Shown is the sum of two cosine cycles, with periods T_1=1470/7 years and T_2=1470/17 years, given by equation (6.1). The dashed lines indicate the period of 1470 years, with which the sum of the two cycles repeats.

[5]The term *fundamental frequency* does not imply that this frequency is present in the forcing.

What kind of climate response would be anticipated to result from this forcing? The answer to this question clearly depends on the degree of linearity of the relevant processes. Since the climatic conditions in the Holocene have been fairly stable compared with the last ice-age (abrupt and/or large-scale climate anomalies were far more frequent in the last glacial), it is plausible to assume that the Holocene climate response to the forcing would be of small amplitude and probably fairly linear. This means that the climate response would essentially show the same frequencies as the forcing (compare section 5.2). For glacial conditions, the climate response is more difficult to anticipate. But if the forcing were strong enough to trigger DO-like warming events with a duration of a few centuries, it would not be very surprising if these events showed the same 1470-year period as the forcing. My hypothesis is therefore that the glacial 1470-year climate cycle might have been caused by the two century-scale solar cycles.

6.2.2 How to test this hypothesis?

In the following chapters, this hypothesis is tested in detail. First, the response of a coupled climate model to this forcing (as well as to a more realistic representation of the solar cycles) is analysed in the next two chapters. The most appropriate class of models for this task is provided by the so-called EMICs (Earth System Models of Intermediate Complexity)[36], since more detailed GCMs (General Circulation Models) require much more computational time and are therefore not applicable for climate simulations on the multi-millennial time scale. With a suitable EMIC like CLIMBER-2 (see chapter 3), however, it is possible to perform a large number of systematic investigations over millennia or tens of millennia, and to test the hypothesis thoroughly.

But EMICs are already rather complex models, and it is often difficult to interpret their output correctly. In order to test the plausibility of the model results, a simpler model should thus be applied, for example a conceptual model. Such a model should only address processes that are essential to explain the output of the EMIC. On the one hand, the description of the considered processes should be as simple as possible, so that the behaviour of the conceptual model is still fairly easy to understand. On the other hand, the description should also be reasonably close to the one in the EMIC, so that both models agree in their key results. Such a conceptual model is designed and applied in chapter 9 in order to demonstrate the plausibility of the presented hypothesis.

7 Freshwater forcing of DO events in a coupled climate model

In this chapter it is demonstrated that the coupled climate model CLIMBER-2 (see chapter 3), can show abrupt switches in the glacial Atlantic thermohaline circulation when forced by two centennial-scale sinusoidal freshwater cycles. When the frequencies of the forcing cycles are chosen to be close to well-known and pronounced solar cycles, these switches can occur periodically, with a spacing of 1470 years or integer multiples of that value for many choices of the forcing parameters.

In the model, the simulated switches in the thermohaline circulation manifest themselves as warming events in the North Atlantic region, which reproduce many characteristic patterns of Dansgaard-Oeschger events. Because of the extreme non-linearity of these events, a glacial climate cycle in the North Atlantic region with a prominent frequency of 1/1470 years^{-1} can be obtained without a forcing frequency of 1/1470 years^{-1}. For Holocene conditions, no switches in the ocean circulation are triggered by the forcing. Therefore, the response of the model is much weaker and far more linear. As a consequence, a frequency of 1/1470 years^{-1} does not exist in the Holocene model response.

7.1 Set-up of the model experiments

In order to analyse if the glacial 1470-year climate cycle could be caused by century-scale cycles in solar activity, a forcing signal is considered which is the sum of two sinusoidal components. The periods of these two cycles are chosen to be 210 years and about 87 years. Following earlier simulations[16], this signal is incorporated in the model CLIMBER-2 as an anomaly of the freshwater fluxes into the North Atlantic region (latitude-belt 50-70°N). The amplitudes of the two cycles are chosen to be of the order of 0.01 Sverdrup, i.e. $10^4\ m^3/s$ or 10 mSv (1 mSv = 1 milli-Sverdrup). This value is fairly small: It is less than two percent of the present river discharge into the Atlantic ocean (which is about 0.6 Sverdrup), and it corresponds roughly to the present outflow of the Canadian river St. Lawrence into the North Atlantic (which is about 0.011 Sverdrup)[68].

In many aspects the approach is simplified: First of all, solar forcing is not considered directly (solar irradiance is fixed in the simulations). Besides, even if the freshwater fluxes to the North Atlantic were sensitive to solar forcing, it is an a priori assumption that the two solar frequencies are present in these fluxes. Although this assumption is plausible for the last glacial[1], its validity is not self-evident: Since the response of the freshwater fluxes to solar forcing might be non-linear, these fluxes might exhibit frequencies which are different from the solar frequencies. Another simplification is that sinusoidal cycles are considered in the forcing, with fixed amplitudes and frequencies. Solar variability, however, exhibits additional spectral components corresponding to the 11-year Schwabe cycle and to combination tones and harmonics of the known solar cycles[2]. It is important to stress that this approach is only taken here to demonstrate the basic principle of the hypothesis. More realistic profiles of the two cycles are considered later.

In addition to the two considered forcing cycles, a constant freshwater offset is also used in the forcing. The justification for this offset is as follows: DO events mainly occurred prior to about 30000 years before present (compare figure 2.1), which suggests that the North Atlantic climate was most unstable at that time. At LGM conditions (about 21000 years before present), however, DO events were almost absent. This implies that the North Atlantic "cold state" was probably more stable at the LGM. In line with that, the Atlantic thermohaline circulation in CLIMBER-2 has only one stable state for LGM conditions, namely the "stadial state" (corresponding to cold conditions in the North Atlantic region, compare section 3.2.1). As a consequence, the LGM is not the most favourable background climate for the occurrence of DO events, neither in reality nor in the model. But since a more appropriate climate state has not yet been simulated with the model, the LGM should nevertheless be used as the underlying background climate in the model simulations. To account for a more instable ocean circulation, it is thus essential to introduce a suitable perturbation of the LGM climate, with the purpose to slightly destabilise the density field of the North Atlantic compared with the LGM. This can be achieved by adding a negative freshwater anomaly (i.e. a salinity anomaly) to the North Atlantic. The role of this freshwater offset is therefore only to mimic a climate state in which DO events are more easily excitable in the model than at the LGM.

The total forcing F, which consists of the two sinusoidal cycles (F_1 and F_2) and the freshwater offset K, reads

$$F(t) = F_1(t) + F_2(t) + K \tag{7.1}$$

[1]Because of the large volume of the continental ice-sheets and of the North Atlantic sea-ice, a small temperature anomaly in the course of the solar cycles could have large effects on the mass balance of the ice and thus on the freshwater flux to the North Atlantic.

[2]This is due to the fact that the solar cycles are not sinusoidal. The Gleissberg cycle, for example, is known to be the amplitude-modulation of the 11-year Schwabe cycle[49].

with

$$F_1 = -A_1 \cdot \cos(\omega_1 t + \phi_1) \tag{7.2}$$

$$F_2 = -A_2 \cdot \cos(\omega_2 t + \phi_2). \tag{7.3}$$

The frequencies are chosen to be $\omega_1 = 2\pi/T_1$ and $\omega_2 = 2\pi/T_2$, with $T_1 = 1470/7$ years (= 210 years) and $T_2 = 1470/17$ years ($\approx$ 86.5 years). In this chapter, the special case of equal amplitudes and vanishing phases is considered (i.e. $A_1 = A_2 = A$, $\phi_1 = \phi_2 = 0$). In this case, the total forcing reads:

$$F = -A \cdot \cos(\omega_1 t) - A \cdot \cos(\omega_2 t) + K \tag{7.4}$$

This function is illustrated in figure 7.1.

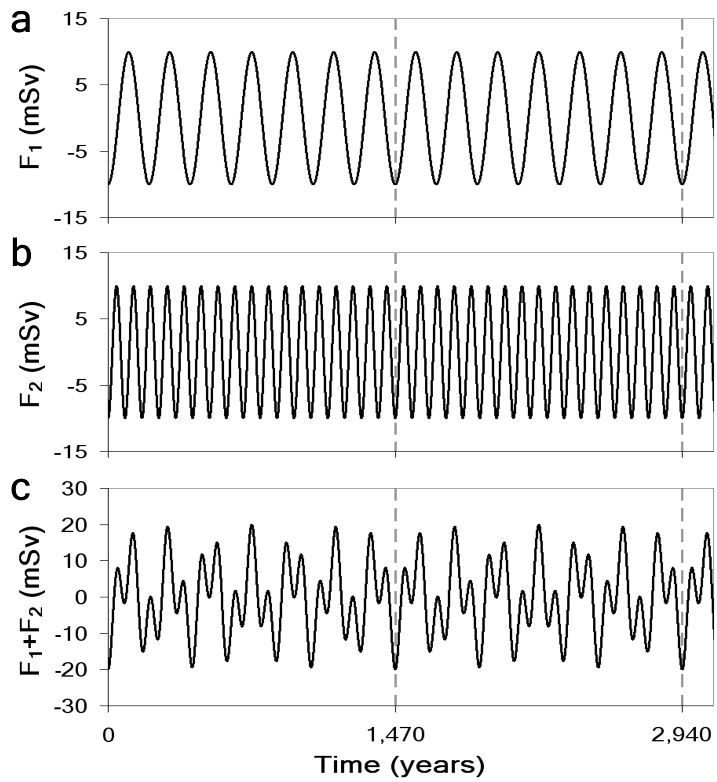

Figure 7.1: Applied freshwater forcing in the model study.
To represent the DeVries and Gleissberg solar cycles, two sinusoidal components are considered. a: DeVries component F_1 with period T_1 = 210 years. b: Gleissberg component F_2 with period $T_2 \approx$ 86.5 years. c: Sum of both components (F_1 + F_2). The dashed lines indicate the period of 1470 years in the forcing. In the figure, the amplitudes A_1 and A_2 are chosen to be 10 mSv, and the phases ϕ_1 and ϕ_2 to be 0. The offset K is not shown here. The figure is taken from [69].

The forcing repeats with a period of 1470 years, which is due to the sum of the two century-scale freshwater cycles. In the frequency domain (figure 7.2) only two spectral components are present, corresponding to the periods of 1470/7 years and 1470/17 years of the two forcing cycles. Since these two cycles are chosen to be sinusoidal, spectral components corresponding to combination tones ($\omega_1 + \omega_2$ and $\omega_1 - \omega_2$, for example) or harmonics ($n \cdot \omega_1$ and $n \cdot \omega_2$, with $n \in \mathbb{N}$) are not present. A spectral component corresponding to the forcing period of 1470 years explicitly does not exist.

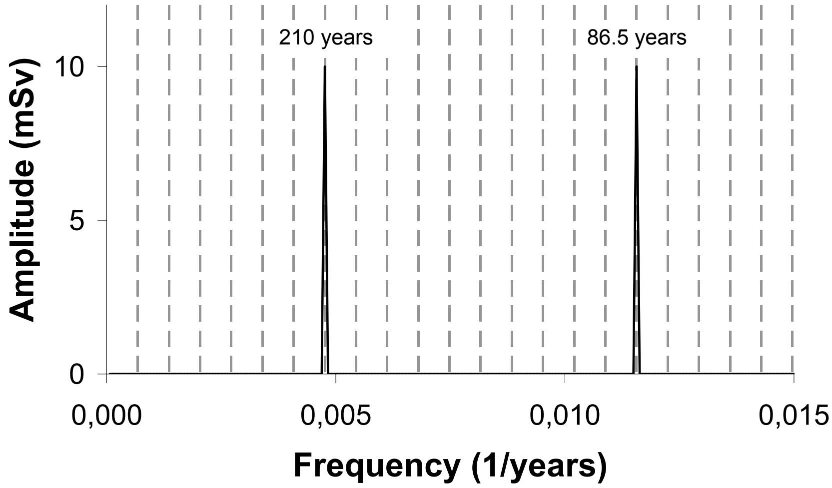

Figure 7.2: Amplitude-spectrum of the forcing.
Since two sinusoidal components with an amplitude of 10 mSv and with periods of 1470/7 years and 1470/17 years are considered, the forcing F_1+F_2 exhibits only two spectral components at frequencies of 7/1470 years^{-1} and 17/1470 years^{-1}. The amplitude of each of these components is 10 mSv. The dashed lines indicate multiples of 1/1470 years^{-1}. A spectral peak corresponding to the period of 1470 years is not present in the forcing.

In the following analysis the response of the climate model CLIMBER-2 to this forcing is investigated, for both Last Glacial Maximum and modern pre-industrial boundary conditions. By varying the two parameters of the forcing, the amplitude A and the offset K, the parameter space ("phase-space") of the forcing is screened over a large range. The model results will be discussed and interpreted in a later chapter, by comparison of CLIMBER's output with the results of a much simpler conceptual model.

7.2 LGM model response

In this section, it is shown that three fundamentally different patterns are possible for the glacial model response, depending on the magnitude of the freshwater offset K and on the amplitude A. For small amplitude values, the model ends up either in the glacial "cold" or "warm" state, corresponding to the stadial or interstadial mode of the glacial THC. For larger amplitudes, repeated oscillations between these two modes can be excited in a certain range of the forcing parameters A and K. In the model, these oscillations result in abrupt warming events in Greenland, similar to DO events. Within a continuous range of the two forcing parameters, the simulated DO events exhibit a period of 1470 years.

7.2.1 Small forcing amplitude

First, a vanishing forcing amplitude A is considered ($A = 0$ mSv). In this case, the forcing (equation 7.4) reduces to $F = K$. The forcing thus represents a constant shift in the freshwater flux to the North Atlantic. With only a small shift, the model remains in its initial THC mode, which is the stadial one. But when a larger negative offset in the freshwater flux to the North Atlantic is applied (i.e. a reduction, corresponding for example to an evaporation anomaly), the stadial mode of the THC becomes unstable, and the model switches to the interstadial mode, which now is stable. This switch is a threshold process. This means that a critical value K_{crit} for the freshwater offset exists which must be crossed in order to trigger a transition from the stadial into the interstadial mode (compare figure 7.3).

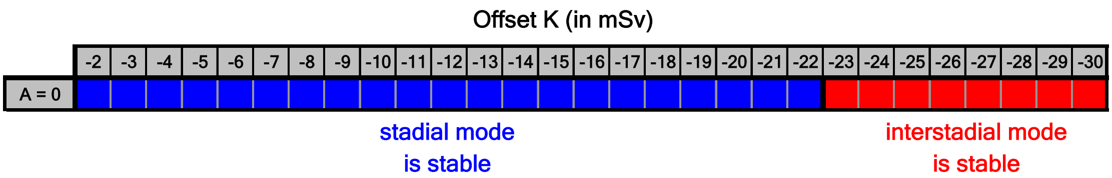

Figure 7.3: Phase space diagram for $A = 0$ mSv.
The figure schematically shows the stability of the THC, as simulated by the model CLIMBER-2 in response to the considered forcing. No periodic forcing component is used here (i.e. $A = 0$ mSv), and the freshwater offset K ranges between -2 and -30 mSv. Up to a critical value of this offset, the stadial mode of the THC is stable (shown in blue). For freshwater reductions beyond this critical value, only the interstadial mode is stable (shown in red). See text for further discussion.

For $K \geq$ -22 mSv, this critical value is not yet reached, and the stadial mode of the THC remains stable. But in the case of $K \leq$ -23 mSv, the stadial mode is not stable anymore because the reduction of the freshwater flux is large enough to cross the threshold and to trigger a switch into the interstadial mode of the THC. This means that in the case of $A = 0$ mSv, the critical value K_{crit} must lie between -22 mSv and -23 mSv.

For any value of the amplitude A between 0 mSv and 5 mSv, a similar pattern is found in the response of CLIMBER-2 to the forcing (see figure 7.4): For each given amplitude A, a unique critical offset-value K_{crit} exists at which the stadial mode becomes unstable, and the model switches into the interstadial mode. This critical value is not the same for different values of the forcing-amplitude A: When A is larger, a weaker (i.e. a less negative) offset can already trigger the transition from the stadial to the interstadial mode of the model.

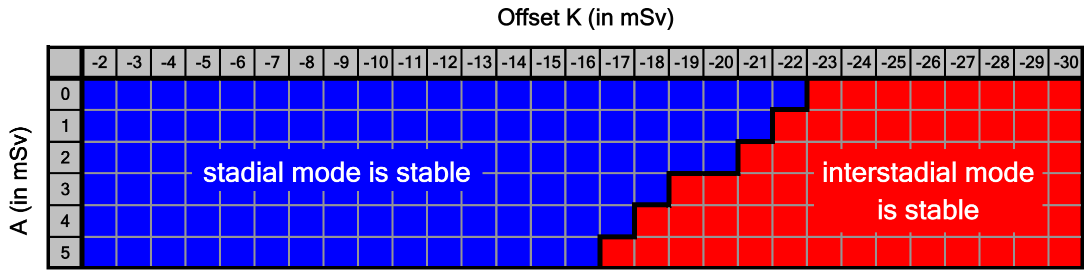

Figure 7.4: Phase space diagram for $A \leq 5$ mSv.
Stability of the simulated THC for forcing amplitudes up to 5 mSv and freshwater offsets K between -2 mSv and -30 mSv. The THC either remains in the stadial mode (blue area) or ends up in the interstadial one (red area).

The switch from the stadial mode to the interstadial one is accompanied by a large-scale reduction in North Atlantic winter sea-ice cover, and by simultaneous changes in other climatic variables, in particular by a massive increase in North Atlantic winter temperature. In the equilibrium of the interstadial mode, the simulated annual mean surface-air temperature in the model box comprising Greenland is about 3.5 Kelvin higher than in the stadial mode (with a seasonal warming by up to 11 Kelvin in February). Apart from this temperature change with the switch of the THC mode, the response of the model to the forcing is small (for $A = 5$ mSv, it is of the order of 0.4 Kelvin in annual mean Greenland temperature in the interstadial mode, and about 0.06 Kelvin in the stadial one) and almost linear (figure 7.5). This means that both in the stadial and in the interstadial mode, the spectral components which are present in the model response are very similar to the ones in the forcing.

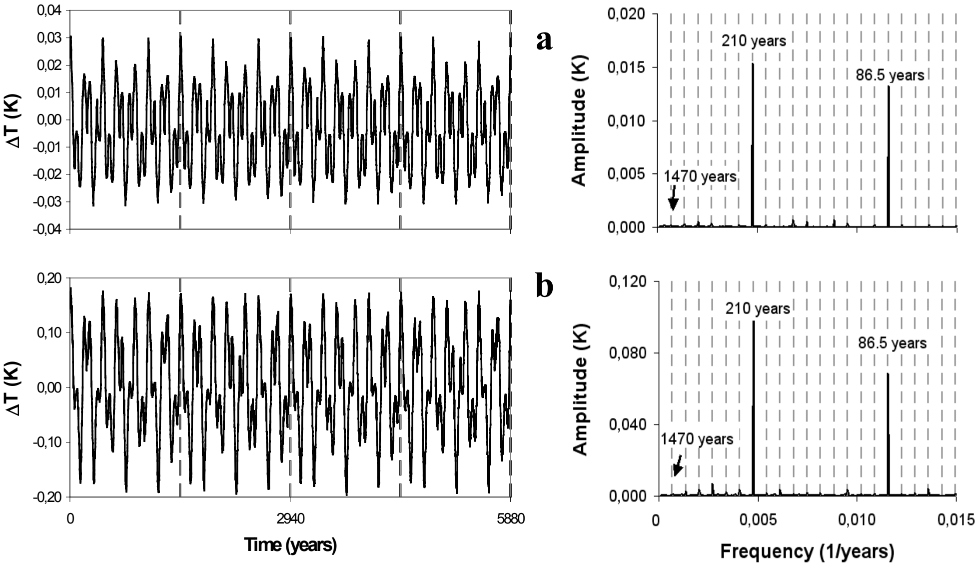

Figure 7.5: Model response for $A = 5$ mSv.
The figure shows the time evolution of the simulated annual mean Greenland surface air temperature anomalies (left column) and their amplitude-spectrum (right column) in response to the forcing. The chosen forcing amplitude is 5 mSv. The freshwater offset K is -2 mSv (a) and -30 mSv (b). Since the model response to the forcing is almost linear, the amplitude spectra of the response are very similar to the spectrum of the forcing (figure 7.2). Note that in panel b, the time-average of Greenland temperature is about 3.5 Kelvin higher than in panel a, due to the switch in the THC.

7.2.2 Larger forcing amplitude

For larger forcing amplitudes ($A \geq 6$ mSv), the pattern in the model response is fundamentally different: For a given value of A, two critical offset-values $K_{crit,1}$ and $K_{crit,2}$ now exist ($K_{crit,1}$, $K_{crit,2} < 0$ and $|K_{crit,1}| \leq |K_{crit,2}|$). As before, the stadial mode of the THC is stable for small negative freshwater-offsets K (with $|K| < |K_{crit,1}|$). For large negative offsets (with $|K| > |K_{crit,2}|$), the interstadial is stable. But for intermediate values ($|K_{crit,1}| < |K| < |K_{crit,2}|$), none of the two modes is stable: The model rather shows repeated oscillations between both modes. These oscillations manifest themselves as a sequence of abrupt warming and cooling events in the North Atlantic region, similar to DO-events.

In this regime of the forcing parameters, which is referred to as the *DO regime* in the following, large-amplitude temperature anomalies in Greenland (of the order of five Kelvin) are triggered by the forcing. The magnitude of the temperature response in the other two regimes, where either the stadial or the interstadial mode is stable (in the following referred to as *cold* and *warm regime*, respectively), is much smaller, see figure 7.6.

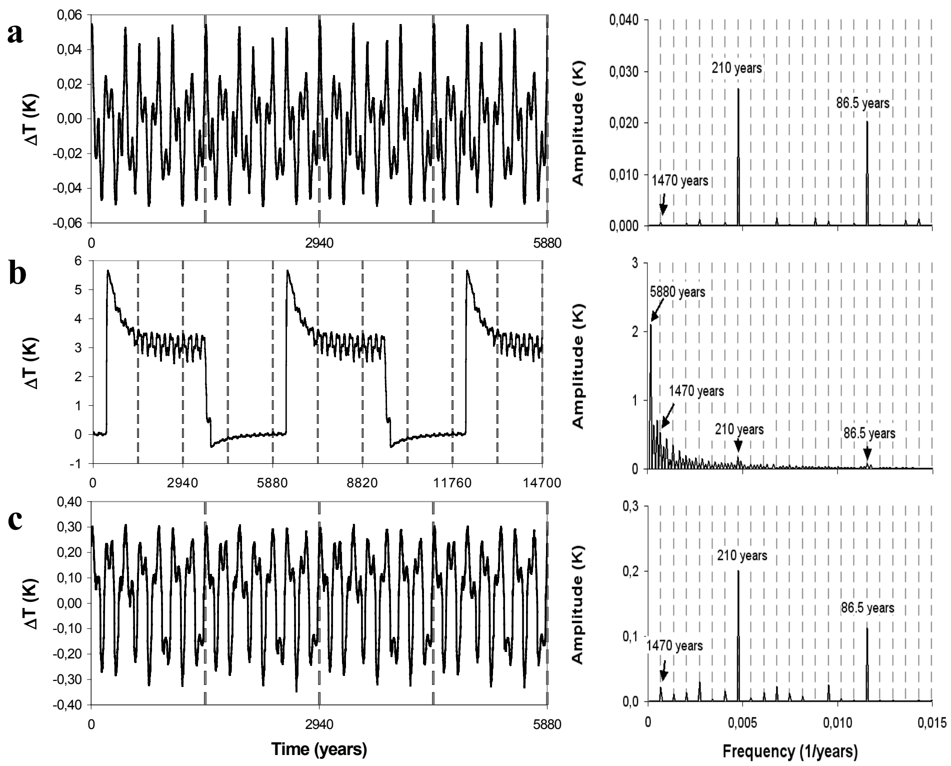

Figure 7.6: Model response for $A = 6$ mSv.
The figure shows the time evolution of the simulated Greenland surface air temperature anomalies (left column) and their amplitude-spectrum (right column) in response to the forcing. The chosen forcing amplitude is 6 mSv. The freshwater offset K is -2 mSv (a), -17 mSv (b) and -30 mSv (c). Panel a corresponds to the *cold regime*, panel b to the *DO regime*, panel c to the *warm regime*. Note that the spectral component corresponding to a frequency of zero is not shown in the spectrum, since this component represents only a constant temperature offset.

Moreover, the time scale of the climate response in the DO regime is very different from the one in the cold and warm regime: In those two regimes, the climate response is very similar to the forcing. Consequently, it shows most variability on the century-scale (see panels a and c in figure 7.6). In the DO regime, however, the climate response occurs mainly on the millennial or multi-millennial scale, i.e. much slower than the forcing (panel b in figure 7.6). The response of the model is thus highly non-linear in this regime, while it is fairly linear in the other two regimes. Note that the DO regime in the model response starts at a critical amplitude $A_{crit} \approx 6$ mSv, and becomes broader with larger amplitude (figure 7.7).

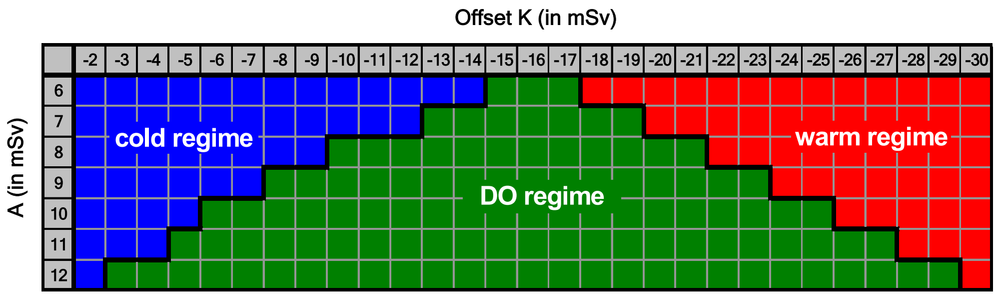

Figure 7.7: Phase space diagram for $A \geq 6$ mSv.
Stability of the simulated THC for forcing amplitudes of 6-12 mSv and freshwater offsets K between -2 mSv and -30 mSv. Three different cases are possible for the model response. 1) Cold regime: The THC ends up in the stadial mode (blue area). 2) Warm regime: The THC ends up in the interstadial mode (red area). 3) DO regime: The THC repeatedly oscillates between the stadial and the interstadial modes (green area). See text for discussion.

In the DO regime, the simulated oscillations between the two modes of the THC occur fairly regular: Successive switches from the stadial to the interstadial mode typically have a uniform spacing in the millennial range. This spacing depends on the forcing parameters, i.e. on the values for the amplitude A and the freshwater offset K. When the offset is fixed and the forcing amplitude is increased, the warming events occur more frequently and last for a shorter time (figure 7.8). As can be seen in that figure, the duration of the warming events in Greenland can range from a few centuries to a couple of millennia, depending on the chosen values of A and K. Since the applied climate model CLIMBER-2 does not explicitly resolve "noisy" inter-annual climate variability, the simulated DO events repeat almost periodically for a given combination of the forcing parameters[3].

Figure 7.8 shows that the forcing amplitude A can be chosen such that the simulated warm events in Greenland show a spacing of 1470 years (panels e, f) or integer multiples thereof (panels a, c). It is important to notice that the existence of a 1470-year period in the model response does not imply that the warming events

[3]In some cases, however, the events are not strictly periodic due to the existence of small-magnitude intrinsic noise in the model (see panel g in figure 7.8, for example.)

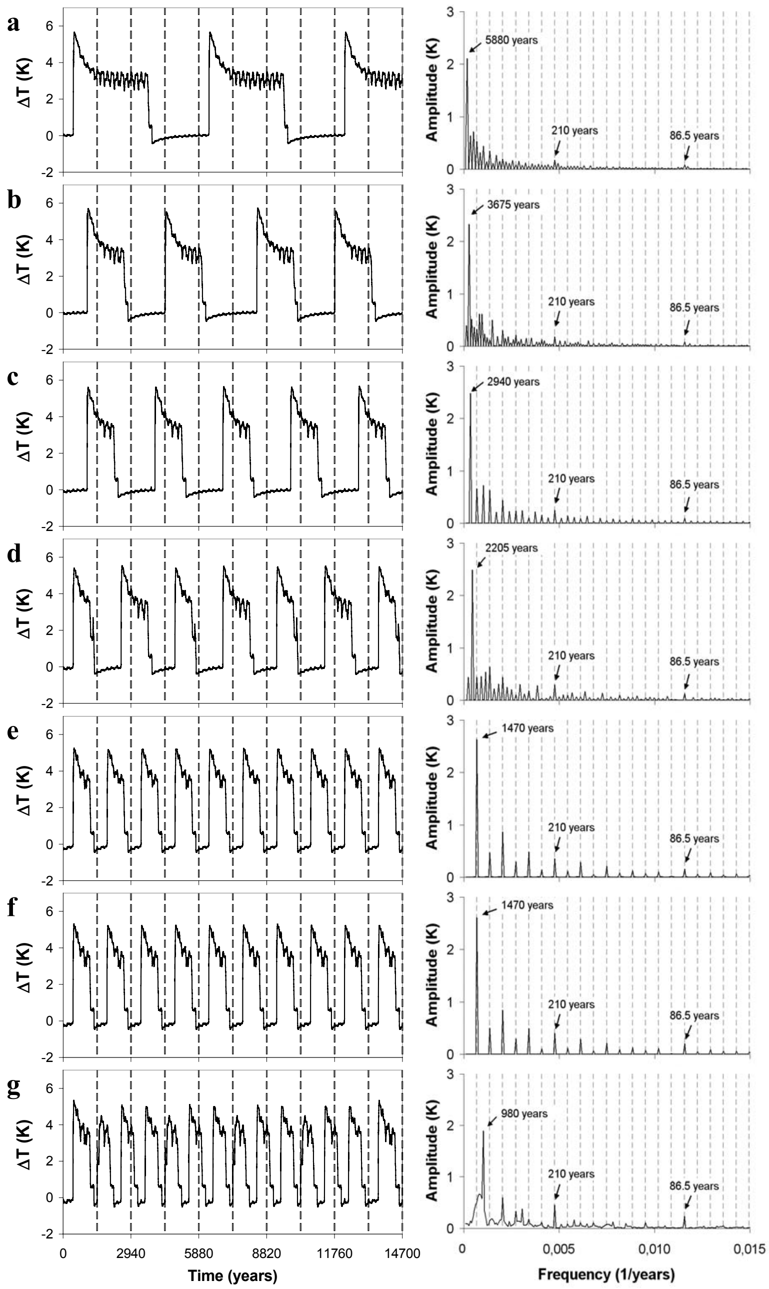

Figure 7.8: **Model response for K = -17 mSv.**
Left: simulated annual mean surface air temperature anomaly in Greenland for A = 6 mSv (a), 7 mSv (b), 8 mSv (c), 9 mSv (d), 10 mSv (e), 11 mSv (f), 12 mSv (g). The curves represent continuous 14700-year segments from longer model runs. The dashed lines show the position of the first order minima (i.e. the salinity maxima) in the forcing. Right: Amplitude-spectrum. The dashed lines represent multiples of 1/1470 years^{-1}.

are triggered by the first order minima in the forcing (i.e. the salinity maxima), which occur at t = n·1470 years ($n \in \mathbb{N}$). Instead, they can also be triggered by the second-order minima (at t ≈ 430 years, t ≈ 1040 years) and sometimes even by the third order minima (at t ≈ 610 years, t ≈ 860 years). Because of this, the spacing of successive warming events can also be different from integer multiples of 1470 years, with possible deviations up to about 500 years (see panel b in figure 7.8, for example).

In the case when the model response is strictly periodic, the amplitude-spectrum of the response is discrete (a, b, c, d, e, f) and the non-vanishing spectral components are equidistant in the frequency space[4]. When the model response is not strictly periodic, the spectrum is continuous (g). Owing to the high degree of non-linearity in the response of the THC to the forcing, prominent millennial-scale spectral components exist in the output of the climate model (see panel a, for example). Note that these frequencies are not present in the forcing (figure 7.2): The forcing only exhibits spectral components corresponding to periods of 210 years and 86.5 years. It is not surprising that these spectral components are also present in the model response (figure 7.8). But it is surprising that a number of other components in the model response exhibit much larger amplitudes than the two forcing frequencies, even though they are not present in the forcing. A good example is the pronounced 1470-years peak, which is present in the amplitude spectrum of the model response for $A = 10$ mSv and $A = 11$ mSv (panels e and f in figure 7.8): The spectral amplitude that corresponds to this peak is of the order of 3 Kelvin, and therefore about ten times larger than the amplitudes of the 210-year and 86.5-year peaks.

It is a very robust result that the forcing, which lacks any millennial-scale spectral components, can excite temperature changes in Greenland which exhibit prominent millennial-scale spectral components of large amplitude. This finding is fundamental for the explanation of the glacial 1470-year climate cycle: Because a 1470-year spectral component has not yet been observed in a possible external trigger, external forcing of the DO events has often been ruled out. But the model study presented here shows that this objection does not hold: A millennial scale climate cycle in the glacial North Atlantic, and in particular a 1470-year cycle, can in fact be excited by a forcing which only exhibits spectral components corresponding to periods much shorter than 1470 years. This 1470-year climate cycle in the model output does not only occur for a particular value of the offset K in the forcing. It rather appears for many combinations of the two forcing parameters A and K, as can be see in figure 7.9.

[4]This is due to the fact that the simulated climate cycle is far from sinusoidal. As a consequence, the amplitude spectrum is composed of a fundamental frequency and additional harmonics at integer multiples of the fundamental frequency (compare chapter 5.1).

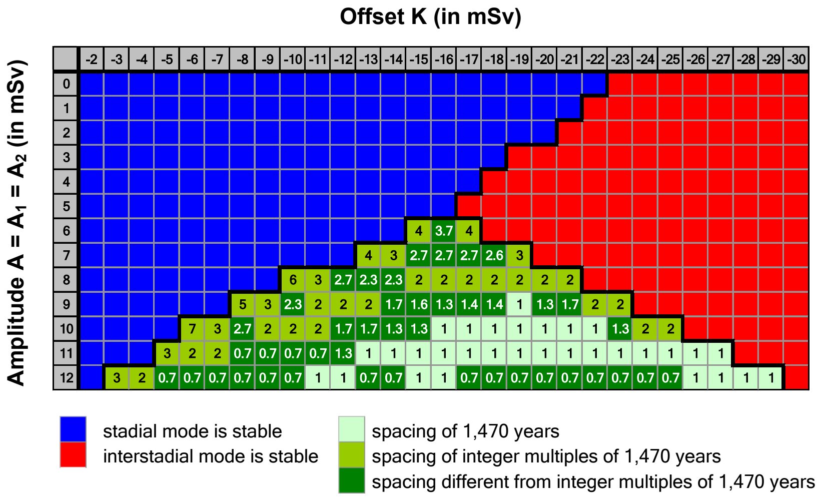

Figure 7.9: Phase space diagram for $A \leq 12$ mSv.
Stability of the simulated THC for forcing amplitudes up to 12 mSv and freshwater offsets K between -2 mSv and -30 mSv. *Cold regime*: blue area. *Warm regime*: red area. *DO regime*: green area. The numbers in this regime denote the most frequently occurring temporal spacing between successive DO events (for each combination of A and K), in multiples of 1470 years. The figure is taken from [69].

The numbers in that figure show the main period in the model response (i.e. the most frequently occurring value of the temporal spacing between successive warm events) for a given combination of the two forcing parameters. With K = -17 mSv, for example (figure 7.8), the main period in the model response is 4·1470 years for A = 6 mSv, 2.3·1470 years or 2.7·1470 years for A = 7 mSv[5], 2· 1470 years for A = 8 mSv, 1.4·1470 years or 1.6·1470 years for A = 9 mSv, 1·1470 years for A = 10 mSv and A = 11 mSv, and about 0.7·1470 years for A = 12 mSv[6].

In the phase-space diagram (figure 7.9), a couple of characteristics of the simulated warm events are noteworthy, which will be discussed in more detail in chapter 9:

- The warm events can only occur for a sufficiently large forcing amplitude A. For amplitudes $A \leq 5$ mSv, at least one stable mode of the THC exists, and repeated warming events consequently do not occur. For $A \geq 6$ mSv,

[5] As can be seen from figure 7.8, for A = 7 mSv the events show the following pattern: After a spacing of 2.3·1470 years between two events, the next event follows after 2.7·1470 years.

[6] In this case, the majority of the simulated events is spaced by roughly 0.7·1470 years. But other values can also occur (see figure 7.8)

DO events occur in a certain range of freshwater offset-values K. This range becomes broader with a larger forcing amplitude.

- For many combinations of the forcing parameters A and K, the warm events are spaced by 1470 years of integer multiples of this value.
- A glacial 1470-year climate cycle in the model occurs within a continuous area of the forcing parameter-space.
- Deviations from this prevalent 1470-year time scale are possible for the spacing of successive DO events in the model. These deviations can be as much as about 500 years (i.e. about 0.3·1470 years).
- For a fixed offset K, the period in the model response tends to decrease with a larger forcing amplitude A.
- For a fixed amplitude A, the period in the model response shows a minimum value for offsets values near -20 mSv (corresponding to the interior of the DO regime). For these values, the period in the model response is almost insensitive to small changes of the freshwater offset K. When K is chosen to be closer to the borders to the cold or warm regimes, the period in the model response increases[7].
- A millennial-scale response of the model occurs throughout the entire DO regime in figure 7.9. Although only century-scale forcing cycles exist, the response of the model is not on the centennial time scale.

7.3 Modern (pre-industrial) response

For pre-industrial boundary conditions, the response of the model to the forcing is fundamentally different from the glacial response since the THC is much more stable in the Holocene[16]. Therefore, the forcing cannot trigger transitions between different modes of the THC, and cannot cause large-scale warming or cooling events in the North Atlantic region. As a consequence, the model response to the forcing (figure 7.10) is much weaker and also far more linear than for glacial boundary conditions. The modern temperature response in Greenland lacks spectral components corresponding to millennial-scale periods. The amplitude-spectrum of the model response instead shows pronounced cycles of 210 years and 86.5 years (figure 7.10), i.e. it exhibits a structure that is very similar to the spectrum of the forcing[8].

[7] apart from a certain area which is located at amplitude values A of 11 and 12 mSv and offset values K of about -10 mSv

[8] The existence of small spectral peaks corresponding to periods different from 210 years and 86.5 years is due to the fact that the model response in not perfectly linear.

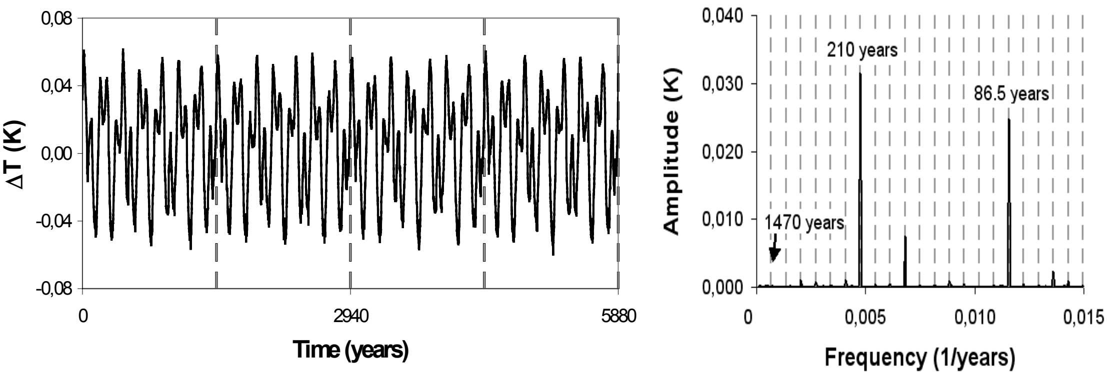

Figure 7.10: Pre-industrial model response for $A = 10$ mSv.
Left panel: simulated annual mean surface air temperature anomaly in Greenland for $A = 10$ mSv (pre-industrial boundary conditions). Right panel: Amplitude-spectrum. The dashed lines represent multiples of 1/1470 years^{-1}. Apart from the 210-year and the 86.5-year peak, a smaller peak is present at a period of 147 years. This peak represents a combination tone of the two forcing cycles (10/1470 years^{-1} = 17/1470 years^{-1} - 7/1470 years^{-1}). The existence of this peak, which is not present in the forcing (figure 7.2), shows that the model response to the forcing is not entirely linear.

To summarise, it was shown in this chapter that different regimes exist in the glacial response of the climate model CLIMBER-2 to the applied century-scale freshwater forcing: For small forcing amplitudes, the model ends up either in a cold (*stadial*) mode of the Atlantic THC, or in a warm (*interstadial*) one, depending on the chosen freshwater offset K. In both cases, only small temperature changes (of the order of tens of Kelvin) are triggered by the cyclic forcing components. For sufficiently large forcing amplitudes, none of the two modes is stable, and oscillations between both modes are triggered by the forcing. In this case, much larger temperature anomalies (about 5 Kelvin) occur in the North Atlantic region. These anomalies manifest themselves as abrupt warming events, similar to DO events. For many choices of the forcing parameters A and K, the warming events show a spacing of 1470 years or integer multiples thereof.

It was also shown that the 1470-year time scale in the model response only occurs for glacial boundary conditions. A 1470-year climate response was not found for pre-industrial boundary conditions. For these, the THC is more stable, and switches between different modes cannot be triggered by the forcing. The model response to the forcing is therefore much smaller and also virtually linear. While the almost linear model response for pre-industrial boundary conditions is not very surprising, the glacial response of CLIMBER-2 to the forcing might be unexpected. In any case, the systematic patterns in the glacial response require a more thorough investigation and interpretation. The interpretation will be given is the chapter after next. But before, the stability of the simulated 1470-year glacial climate cycle with respect to changes of the forcing structure will be investigated in the next chapter.

8 Stability analysis

In the previous chapter, the hypothesis that was suggested in order to explain the glacial 1470-year climate cycle was tested in a very simplified way. The main limitation of the analysis that was performed so far is that the two solar cycles are represented in the forcing in a very idealised way: Both forcing cycles were considered to be sinusoidal, with fixed frequencies in the ratio of 7:17. The amplitudes of the two cycles were already varied simultaneously over some range, but their ratio was also fixed, at a value of 1:1. Both forcing phases were set to zero. In addition to that, the 11-year Schwabe cycle was not considered in the forcing, although it is very prominent in records of solar activity. Moreover, short-term climate variability ("noise") was not present in the simulations, since the applied model only resolves large-scale, time-average climatic variables, but not the more "noisy" inter-annual variability.

In this chapter, additional tests of the hypothesis are performed: First, the stability of the simulated 1470-year climate cycle with respect to variations of the forcing parameters (phases, amplitudes, frequencies) is investigated[1]. Noise is considered in the forcing as an additional non-periodic component in the freshwater flux to the North Atlantic. Finally, the 11-year solar Schwabe cycle is also incorporated in the forcing, and the two century-scale solar cycles are implemented as non-sinusoidal cycles. It is shown that in all of these cases, a robust 1470-year model response can still be obtained.

8.1 Forcing parameters

The most general expression for a periodic function with only two spectral components ω_1 and ω_2 ($\omega_1 = 2\pi/\mathrm{T}_1$, $\omega_2 = 2\pi/\mathrm{T}_2$) reads (compare section 5.1):

$$F(t) = F_1(t) + F_2(t) + K \tag{8.1}$$

$$F_1 = -A_1 \cdot \cos(\omega_1 t + \phi_1) \tag{8.2}$$

$$F_2 = -A_2 \cdot \cos(\omega_2 t + \phi_2) \tag{8.3}$$

[1]The dependence of the model results on the freshwater offset K was already investigated in the last chapter. This analysis is thus not repeated here.

In this expression, A_1 and A_2 are the amplitudes of the two cycles, T_1 and T_2 are the two periods, ϕ_1 and ϕ_2 are the phases.

Since F_1(t) repeats with a period of T_1, the relation $F_1(t+T_1) = F_1(t)$ holds for all values of t. Similarly, $F_2(t+T_2) = F_2(t)$ is valid since $F_2(t)$ has a period of T_2. If it is possible to find values n_1 and n_2 (n_1, $n_2 \in \mathbb{N}$) with

$$n_1 \cdot T_1 = n_2 \cdot T_2 = T \tag{8.4}$$

then both F_1 and F_2 repeat every T years. This means that $F(t)$ has a period of T. Equation (8.4) is fulfilled when the two periods T_1 and T_2 are rational numbers[2]. Since F is periodic in this case, Fourier series expansion (section 5.1) can be applied to calculate the amplitude-spectrum of the function $F(t)$. In the following investigations, I will therefore restrict myself to forcing functions for which condition (8.4) holds.

In the previous chapter, it was assumed that the two frequencies $1/T_1$ and $1/T_2$ are fixed at values of 7/1470 years^{-1} respectively 17/1470 years^{-1}. The forcing amplitudes A_1 and A_2 were considered to be equal, and the phases ϕ_1 and ϕ_2 were assumed to be zero. In this chapter, the glacial response of the model CLIMBER-2 will be investigated for a forcing type given by the equations (8.1 to 8.4). Moreover, the effect of changes in each of the six forcing parameters on the stability of the simulated 1470-year climate cycle will be examined.

8.1.1 Forcing phases

In this part of the analysis, it will be investigated how a shift in the phase relation of the two forcing cycles affects the simulated 1470-year climate cycle. To do so, the model response is analysed for 20 different values of the phase ϕ_1 of the 210-year cycle ($\phi_1 = 0.00 \cdot 2\pi,\ 0.05 \cdot 2\pi,\ 0.10 \cdot 2\pi,\ \dots,\ 0.95 \cdot 2\pi$). The second forcing phase ϕ_2 is not varied, since any of the two phases can be set to zero by a shift of the time-axis[3]. The other forcing parameters (A_1, A_2, T_1, T_2) are fixed at the following values: $A_1 = A_2 = 10$ mSv, $T_1 = 1470/7$ years $= 210$ years, $T_2 = 1470/17$ years $\approx$ 86.5 years.

Figure 8.1 shows that for different values of ϕ_1 (for all 20 values, as a matter of fact), CLIMBER-2 shows abrupt warming events in the North Atlantic region, spaced by 1470 years. The difference in the model output for different forcing phases is only the phase of the simulated events: When ϕ_1 is changed, the abrupt warming events are shifted in time, but their spacing still remains 1470 years (see figure 8.1). It is interesting to realize that although ϕ_1 is continuously varied, the phase of the simulated climate cycle can only take discrete values, i.e. the abrupt

[2] This means that both periods can be written in the form $T_i = p_i/q_i$, with p_i and $q_i \in \mathbb{N}$.
[3] $\cos(\omega t + \phi) = \cos(\omega t')$, with $t' = t + \phi/\omega$

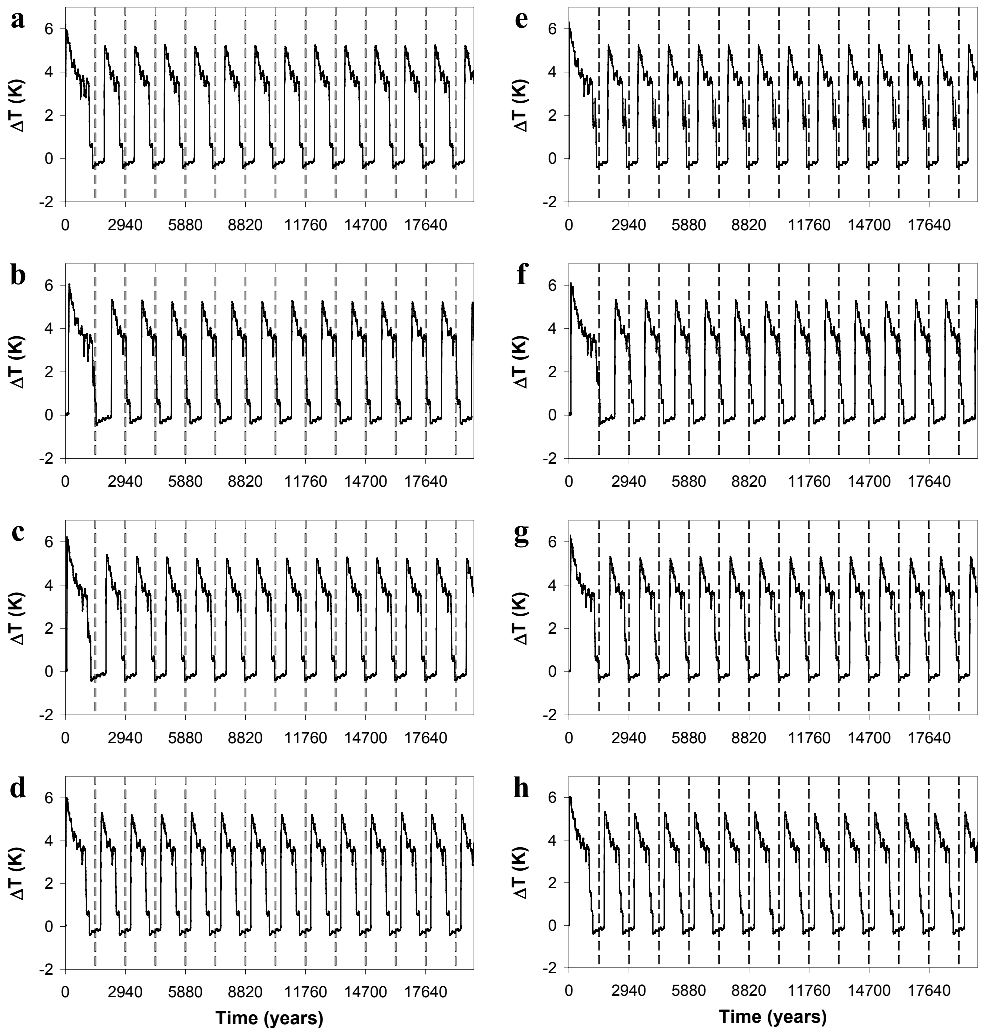

Figure 8.1: Model response for different phases ϕ_1.
The figure shows the simulated anomaly in the annual mean surface air temperature in the model box comprising Greenland. The amplitudes A_1 and A_2 of both forcing cycles are chosen to be 10 mSv. The additional freshwater offset K is -17 mSv (a-d) and -19 mSv (e-h), respectively. The phase ϕ_1 of the 210-year cycle is 0 (a, e), $\pi/2$ (b, f), π (c, g) and $3\pi/2$ (d, h). In all cases, the model response to the forcing shows a very pronounced and regular 1470-year cycle.

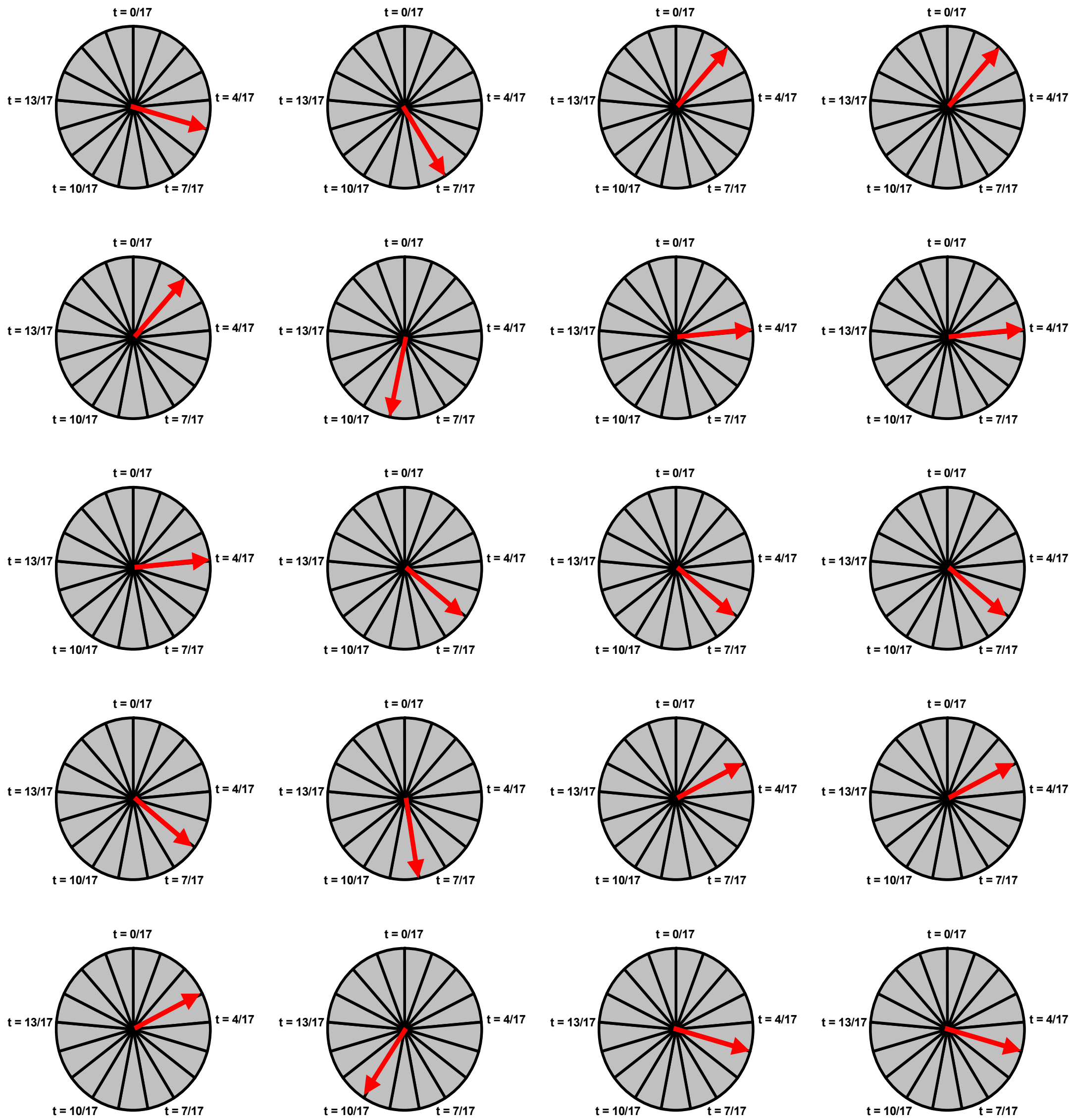

Figure 8.2: Phase relation of the simulated warming events.
Phase relation between the forcing and the simulated 1470-year climate cycle for various values of the forcing phase ϕ_1. First row (from left to right): $\phi_1 = 0$, $\phi_1 = 1\pi/10$, $\phi_1 = 2\pi/10$, $\phi_1 = 3\pi/10$. Second row: $\phi_1 = 4\pi/10$, $\phi_1 = 5\pi/10$, $\phi_1 = 6\pi/10$, $\phi_1 = 7\pi/10$. Third row: $\phi_1 = 8\pi/10$, $\phi_1 = 9\pi/10$, $\phi_1 = 10\pi/10$, $\phi_1 = 11\pi/10$. Forth row: $\phi_1 = 12\pi/10$, $\phi_1 = 13\pi/10$, $\phi_1 = 14\pi/10$, $\phi_1 = 15\pi/10$. Fifth row: $\phi_1 = 16\pi/10$, $\phi_1 = 17\pi/10$, $\phi_1 = 18\pi/10$, $\phi_1 = 19\pi/10$. The red arrows indicate the time step (in multiples of 1470 years) at which the warming events occur. Note that only discrete phases are possible for the simulated 1470-year cycle: The events only occur at multiples of 1470/17 years. See text for more discussion.

warming events can only occur near integer multiples of 1470/17 years. No event is ever triggered in between these values. This means that the abrupt warming events in the North Atlantic region always coincide with one of the minima of the 86.5-year freshwater-forcing cycle. The relevant minimum, however, is not the same for different values of ϕ_1. This is why the phase of the simulated 1470-year climate cycle is not fixed when the forcing phase ϕ_1 is varied (compare figure 8.1).

This shift in the phase of the simulated 1470-year climate cycle can be clearly seen in figure 8.1. In the left column of that figure (i.e. in the panels a-d), the DO events in the North Atlantic region are always spaced by 1470-years, independent of the chosen forcing phase ϕ_1. This means that for all values of ϕ_1, the simulated events occur at times $t = t_0(\phi_1) + n{\cdot}1470$ years[4], (n $\in \mathbb{N}$). But the timing of the events is not the same for all values of ϕ_1, since $t_0(\phi_1)$ can be different for different values of ϕ_1: For $\phi_1 = 0$, for example, the warming events occur at times $t \approx 435$ years + $n{\cdot}1470$ years, see panel a in figure 8.1. This implies that $t_0(\phi_1 = 0) \approx$ 435 years. The value of 435 years is close to 5/17·1470 years. This means that for $\phi_1 = 0$ the simulated warming events occur at $t \approx (5/17{+}n){\cdot}1470$ years. When these times are plotted in a phase-diagram (with 0 representing $t_0 = 0$ years and 1 representing $t_0 = 1470$ years), the simulated events for $\phi_1 = 0$ therefore all correspond to a value of 5/17. This value is indicated by the red arrow in figure 8.2. Similarly, the following values are obtained from figure 8.1: 9/17 for $\phi_1 = \pi/2$ (i.e. $t_0[\phi_1 = \pi/2] \approx 780$ years), 6/17 for $\phi_1 = \pi$ (i.e. $t_0[\phi_1 = \pi] \approx 520$ years) and 3/17 for $\phi_1 = 3\pi/2$ (i.e. $t_0[\phi_1 = 3\pi/2] \approx 260$ years).

Since the shift in the forcing phase ϕ_1 only affects the phase of the simulated climate cycle, but not the spacing of successive warming events, the occurrence of the 1470-year climate cycle is completely insensitive to the choice of the forcing phases. This insensitivity is found for many offset values K, not just for the particular case of K = -17 mSv, compare figure 8.1. Because the period of the simulated glacial climate cycle does not depend on ϕ_1 and ϕ_2, these phases are omitted in the following analysis (i.e. both phases are set to zero, as was done in the previous chapter).

8.1.2 Forcing frequencies

In this part of the analysis, it will be investigated how a shift in the frequency of the two forcing cycles affects the simulated 1470-year climate cycle. To do so, the model response is first analysed for a simultaneous shift of both forcing frequencies (i.e. the ratio of 7/17 between the two frequencies is fixed). Afterwards, each forcing frequency is varied on its own, while the second frequency is fixed (i.e. the ratio

[4] Deviations from this regular behaviour only occur during the first millennia of the model runs, before the model settles in a regular 1470-year oscillation mode.

between the two frequencies is also varied). Both forcing amplitudes are considered to be equal (i.e. $A_1 = A_2 = 10$ mSv). The forcing phases are taken to be zero.

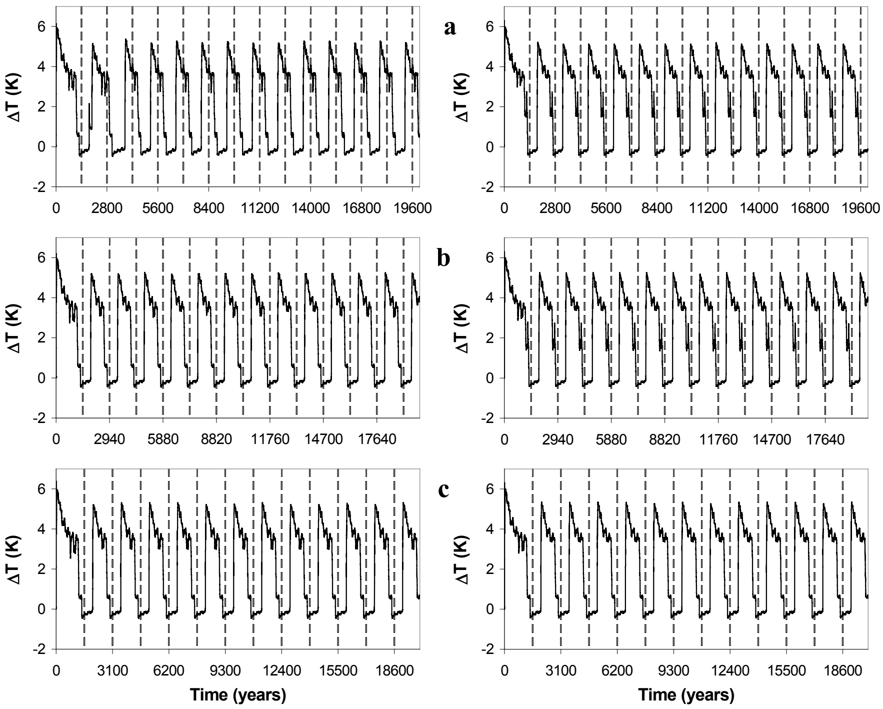

Figure 8.3: Model response for different forcing frequencies.
The figure shows the simulated anomaly in the annual mean surface air temperature in the model box comprising Greenland. The freshwater offset K is chosen to be -17 mSv (left column) and -19 mSv (right column). The periods T_1 and T_2 of the two forcing cycles are: $T_1 = 1400/7$ (=200) years and $T_2 = 1400/17$ ($\approx$82) years (a), $T_1 = 1470/7$ (=210) years and $T_2 = 1470/17$ ($\approx$86.5) years (b), $T_1 = 1550/7$ (=221) years and $T_2 = 1550/17$ ($\approx$91) years (c). The dashed lines represent multiples of 1400 years (a), 1470 years (b) and 1550 years (c).

In the first part of the investigation, the two forcing periods are simultaneously varied over a range of 1400/7 to 1550/7 years (200 to 221.4 years) and 1400/17 to 1550/17 years (82.4 to 91.2 years), respectively. Figure 8.3 shows the time-evolution of Greenland temperature in the model, for six different combinations of the forcing frequencies and the freshwater offset K. The figure shows that the simulated warming events exhibit a very similar pattern in all six cases (and, as a matter of fact, for all frequency-values as given above): When different forcing frequencies are used, the main difference in the model response is that the spacing of the simulated events is scaled. Since a simultaneous change of the two forcing frequencies corresponds to a scaling of the model's time axis, it is not surprising that the time axis of the model output (i.e. the spacing between successive warm events) is also scaled.

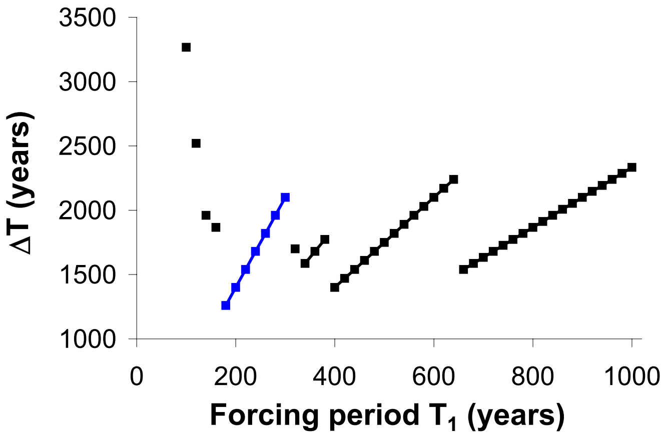

Figure 8.4: Spacing of successive warm events, as a function of T_1.
The figure shows the spacing ΔT between successive warming events in the model output, as a function of the first forcing period T_1 (with T_1 ranging from 100 years to 1000 years). The forcing period T_2 ($\mathrm{T}_2 = 7/17 \cdot \mathrm{T}_1$) is synchronously changed with T_1. In certain ranges (as shown in blue, for example), linear relations exist between the spacing of the events in the model response and the period of the forcing. As before, the chosen freshwater offset K is -17 mSv.

Within certain ranges of the forcing period T_1, this scaling is linear (see the blue line in figure 8.4, for instance): A change of ten percent in the two forcing periods T_1 and T_2, for example, causes a shift of ten percent in the spacing of successive warming events in the model output. This means that a very regular climate cycle with a period of approximately 1470 years can still be obtained when both forcing frequencies are simultaneously varied over a fairly large range.

Having shown that the glacial 1470-year climate cycle is stable with respect to synchronous changes of the two forcing frequencies, the stability of this climate cycle is now investigated with respect to variations of only one forcing frequency. The frequency of the relevant cycle is changed in equidistant frequency steps of $0.1/1470 \cdot \text{years}^{-1}$. The second forcing cycle is held at a fixed period (1470/7 years respectively 1470/17 years). The stability analysis is performed for two different values of the forcing amplitudes, i.e. for $A_1 = A_2 = 10$ mSv and for $A_1 = A_2 = 11$ mSv. The considered freshwater offset K is -17 mSv.

Figure 8.5 shows the spacing of successive warm events in the model output over the entire range of considered forcing frequencies. From the figure, it can be seen that a strictly periodic 1470-year model response can only be obtained when both

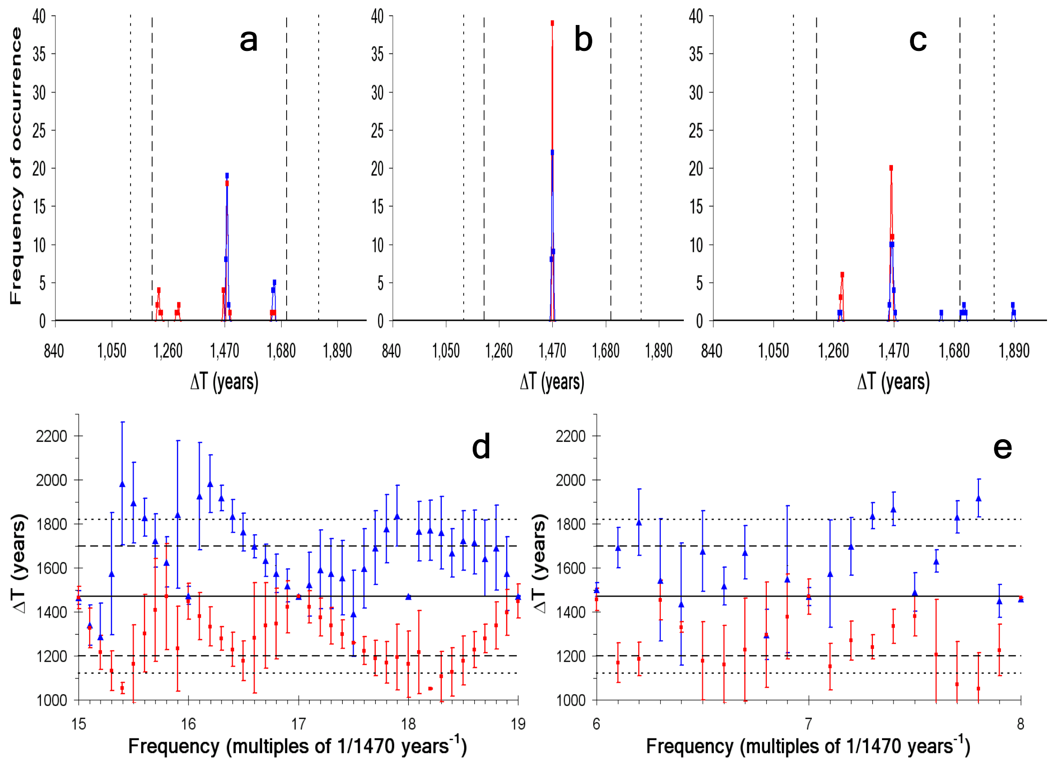

Figure 8.5: Stability with respect to changes of one forcing frequency
For the freshwater offset K = -17 mSv and a forcing amplitude A ($A = A_1 = A_2$) of the two forcing cycles (blue: A = 10 mSv, red: A = 11 mSv), a-c show the frequency distribution of the spacing ΔT between successive warming events over 60000 years in the model simulation. The forcing periods T_1 and T_2 are chosen as follows: $T_1 = 1470/7$ (= 210) years, $T_2 = 1470/16.9$ (≈ 87) years (a); $T_1 = 1470/7$ years, $T_2 = 1470/17$ (≈ 86.5) years (b); $T_1 = 1470/7$ years, $T_2 = 1470/17.1$ (≈ 86) years (c). Panels d and e show the mean value and the standard deviation of the spacing ΔT for: $T_1 = 1470/7$ years, T_2 ranging from 1470/15 (≈ 98) to 1470/19 (≈ 77) years (d); T_1 ranging from 1470/6 (≈ 245) to 1470/8 (≈ 184) years, $T_2 = 1470/17$ years (e). The dashed lines represent ΔT = 1200 years and ΔT = 1700 years. The dotted lines represent ΔT = 1470 years ± 350 years. The solid line in the panels d and e indicates ΔT = 1470 years. See text for further discussion. The figure is taken from [70].

forcing periods are identical to integer factors of 1470 years (panel b in figure 8.5). When the periods are different from these values (i.e. different from the ratio 7/17), the simulated warming events still occur with an average spacing which is fairly close to 1470 years (panels a and c in figure 8.5). When the forcing frequencies are varied over some range, the average spacing between successive warm events in the simulation typically changes by up to 300-400 years (panels d and e in figure 8.5). This change is consistent with the spacing of the observed DO events: Two studies on the regularity of the glacial 1470-year climate cycle suggest that the DO events, as seen in the GISP2 ice-core, deviate by up to 270 years[5], or by up to 350 years[6], from a strict period of 1470 years. Note that the average spacing between successive events in the simulation is typically smaller than 1470 years for an amplitude of 11 mSv, and typically larger than 1470 years for an amplitude of 10 mSv. The average spacing between the simulated events would thus even be closer to 1470 years if small variations in the forcing amplitude (between 10 and 11 mSv) were applied.

To summarise, even if the periods of the two solar cycles are not fixed, the two cycles could still trigger abrupt warming events in the North Atlantic region, with an average period of 1470 years for these events. For a large range of forcing frequencies, the deviations of the simulated climate cycle from a 1470-year period are consistent with the regularity of the observed DO events. In the context of the presented hypothesis, the 1470-year glacial climate cycle, as simulated by the model, is thus sufficiently stable with respect to variations of the two forcing frequencies.

8.1.3 Forcing amplitudes

In the previous chapter, the model response to the forcing was already investigated for a large range of forcing amplitudes. It was shown that abrupt glacial warming events with a period of 1470 years can be triggered for various values of the forcing amplitudes, with $A_1 + A_2$ ranging from 2·9 mSv to 2·12 mSv (see figure 7.9)[7]. In that analysis, however, the ratio of the two forcing amplitudes was fixed at a value of 1:1 (i.e. A_1 and A_2 were considered to be equal).

In this part of the analysis, the stability of the simulated 1470-year climate cycle with respect to changes in the ratio of the two forcing amplitudes is analysed. The sum $A_1 + A_2$ of the amplitudes is fixed at a value of 20 mSv. The forcing periods are chosen to be 1470/7 years (=210 years) and 1470/17 years ($\approx$ 86.5 years). The

[5] This pattern is indicated by the dashed lines in figure 8.5. These lines correspond to a spacing of 1200 years and of 1700 years. These values are very close to the spacing observed between the DO events labelled 3 and 4, and between the events labelled 6 and 7, see [32].

[6] This pattern is indicated by the dotted lines in figure 8.5. The dotted lines correspond to the approximate maximum lag between canonical DO events and a 1470-year template, compare [31].

[7] For amplitudes $A = A_1 = A_2 > 12$ mSv, it is still possible to chose the freshwater offset K such that the warming events in the model repeat with a period of 1470 years.

forcing phases are again considered to be zero. The model response to the forcing is investigated for three different freshwater offset-values (K = -17 mSv, K = -19 mSv and K = -21 mSv).

Figure 8.6 shows the temporal spacing between successive warming events, which is obtained when the ratio of the two forcing amplitudes is varied over a large range. In the case when only a single cycle is considered in the forcing (i.e. for $A_1 = 0$ or $A_2 = 0$), the simulated warming events still evolve on the millennial scale, but a very regular 1470-year spacing is not present.

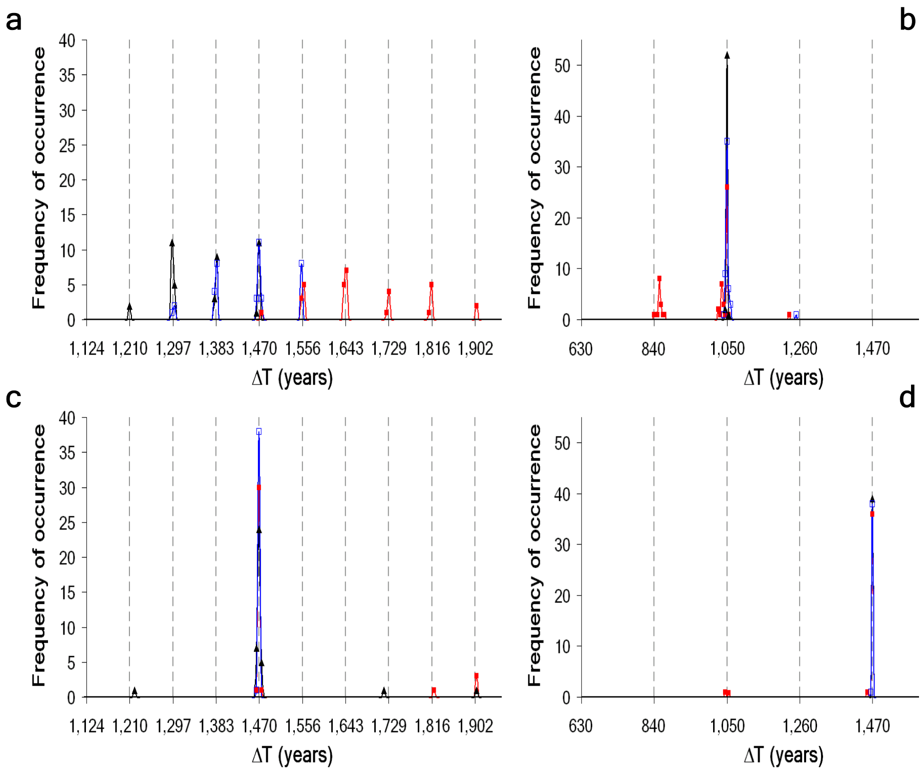

Figure 8.6: Model response for different forcing amplitude-ratios. The figure shows the frequency distribution of the temporal spacing ΔT (in years) between successive warm events in simulations running over 60000 years. The chosen offset K is: -17 mSv (blue), -19 mSv (black) and -21 mSv (red). The applied amplitudes (with $A_1 + A_2 = 20$ mSv) are: $A_1 = 0$ mSv, $A_2 = 20$ mSv (a). $A_1 = 20$ mSv, $A_2 = 0$ mSv (b). $A_1 = 4$ mSv, $A_2 = 16$ mSv (c). $A_1 = 16$ mSv, $A_2 = 4$ mSv (d). The dashed lines indicate integer multiples of 86.5 years (a, c) and 210 years (b, d), respectively. The figure is taken from [70].

With only the 86.5-year cycle in the forcing (panel a), the warming events are distributed over a much larger range than in the case when both forcing cycles are considered. With only the 210-year cycle (panel b), the events are fairly regular, but in this case, the spacing of successive events is typically 1050 years, rather than 1470 years. When both forcing cycles are used, however, their amplitude-ratio can be varied over a very large range (from $A_1/A_2 = 0.25$ to $A_1/A_2 = 4$, see panels c and d) without losing the very sharp 1470-year peak in the frequency distribution of the spacing between successive warming events. This means that when both forcing cycles are used, the simulated 1470-year climate cycle is almost insensitive to changes in the ratio of the two forcing-amplitudes.

8.2 Noise in the forcing

It has already been mentioned that the climate system model CLIMBER-2 does not explicitely resolve short-term climate variability (see chapter 3). Only the large-scale, time-average climatic fields (temperature, pressure, etc.) and their variations are simulated by the model. Since no "noisy" component of climate variability is present in the model output, the simulated warming events were so far almost identical copies of some prototypical event. For the DO events, as recorded in ice-cores from Greenland, this is not the case: Although different DO events have a couple of characteristics in common on the centennial and millennial scale, they clearly look different and exhibit substantial noise-like variability on shorter time scales. This suggests that the events were, at least to some extent, influenced by "noisy" short-term variability.

In this part of the analysis, the stability of the simulated 1470-year glacial climate cycle is investigated with respect to an additional noise-like component in the freshwater forcing. The total forcing reads:

$$F(t) = F_1(t) + F_2(t) + K + N(t) \tag{8.5}$$

$$F_1 = -A_1 \cdot \cos(\omega_1 t) \tag{8.6}$$

$$F_2 = -A_2 \cdot \cos(\omega_2 t) \tag{8.7}$$

with amplitudes $A_1 = A_2$, periods $T_1 = 1470/7$ (=210) years and $T_2 = 1470/17$ ($\approx$86.5) years, phases $\phi_1 = \phi_2 = 0$, freshwater offset values K and noise $N(t)$. Since the noisy component $N(t)$ is used to mimic unresolved short-term climate variability, white noise is applied[8] rather than red noise, which has lower amplitudes for short-term spectral components. $N(t)$ is computed for each year, and is then considered to be constant over the course of the year. The magnitude of the noise is given by its standard deviation σ.

[8] The expression *white* means that the amplitude is the same for all frequencies

In this section, the response of the climate model to the forcing, as given by equation (8.5) is analysed. First, the two amplitudes A_1 and A_2 are considered to be equal, and the stability of the simulated 1470-year climate cycle with respect to changes in the noise level σ is investigated. Afterwards, σ is fixed, and the robustness of the 1470-year cycle with respect to changes in any of the two forcing amplitudes A_1 and A_2 is studied.

8.2.1 Different noise levels, fixed forcing amplitude

In the first part of the analysis, the forcing amplitudes are chosen to be equal, i.e. $A_1 = A_2 = A$. An offset K = -17 mSv is used. Three different noise levels are considered (σ = 10 mSv, σ = 25 mSv, σ = 30 mSv).

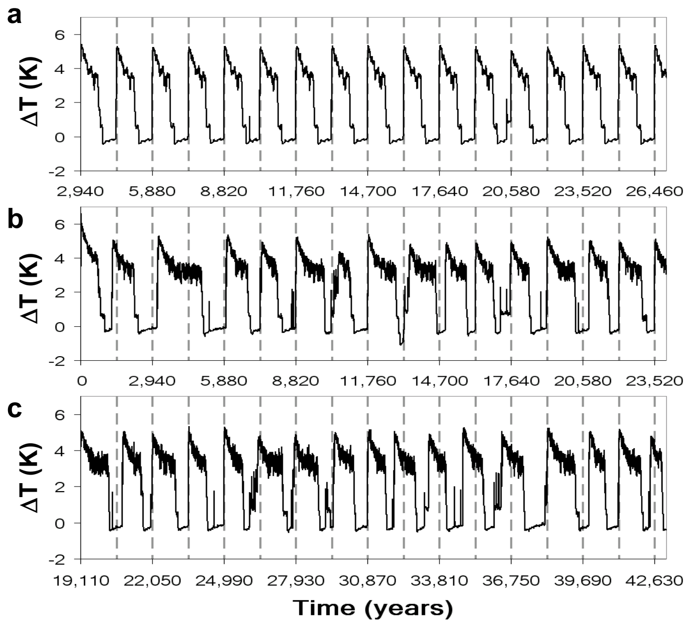

Figure 8.7: Simulated warming events with additional white noise. The figure shows the simulated anomalies ΔT in Greenland surface air temperature, with white noise included in the forcing. The amplitude A of the two forcing cycles and the standard deviation σ of the noise are chosen as follows: A = 10 mSv, σ = 10 mSv (a). A = 6 mSv, σ = 25 mSv (b). A = 4 mSv, σ = 30 mSv (c). The dashed lines indicate the first order minima in the forcing (i.e. the maxima in the salinity flux), with a period of 1470 years. All curves are segments of longer (60000 years) model runs. The figure is taken from [70].

As shown in figure 8.7, for each of these noise levels it is possible to chose the forcing amplitude A such that a fairly regular, roughly 1500-year quasi-cycle is obtained in the model response, at least over some tens of thousands of years (which corresponds to a continuous sequence of about 20 DO events). When the noise level is low, the 1470-year climate cycle can be extremely regular, and different events look almost identical (panel a in figure 8.7). For higher noise levels, a smaller amplitude of the two forcing cycles is required to produce a 1470-year quasi-period in the model response (panels b and c). In this case, the spacing between successive warming events can still be close to 1470 years (or integer multiples thereof) over an interval up to tens of millennia. Moreover, different events can look very different when noise is considered. Note that in panel c, the amplitude A of the forcing cycles is reduced by a factor of 2.5 compared with panel a. Noise can thus act as a very efficient amplifier mechanism for a periodic signal, in line with results of a study performed by Ganopolski and Rahmstorf [24]. Very similar results can also be obtained with other values of the forcing parameters (i.e. with $K \neq$ -17 mSv).

8.2.2 Fixed noise level, different forcing amplitudes

An important consequence of this amplification is demonstrated in figure 8.8. When noise is present in the forcing, much smaller amplitudes of the two forcing cycles are already sufficient to produce a 1470-year climate cycle in the model output: In the figure, $A_1 + A_2$ varies around 10 mSv, compared with a value of roughly 20 mSv in the case without noise (figure 7.9). In order to obtain a 1470-year time scale in the model response, the forcing amplitudes can be varied over a larger percentage-range when noise is also considered: In this case, the amplitudes $A_1 + A_2$ can be between 8 mSv and 14 mSv (figure 8.8), which corresponds to a percentage-range of roughly (14-8)/10 = 60 percent. Without noise, the forcing amplitudes can only be varied between $2{\cdot}10$ mSv and $2{\cdot}11$ mSv (see figure 7.9[9]). This is a percentage-range of only about (22-20)/20 = 10 percent. Again, similar results can also be obtained with other values of the freshwater offset K.

To summarise, additional noise does not spoil the robustness of the glacial 1470-year climate cycle, as simulated by CLIMBER-2: A fairly regular 1470-year cycle can still be obtained when noise is included in the freshwater flux to the North Atlantic. With noise, different warming events look different, and smaller amplitudes of the two forcing cycles are already sufficient to produce a roughly 1470-year quasi-period in the glacial model response. Moreover, the stability of the simulated 1470-year climate cycle with respect to relative (i.e. percentage) variations of the two forcing amplitudes increases in the presence of noise.

[9]The interval $2{\cdot}10$ to $2{\cdot}11$ mSv corresponds to the freshwater offset K = -17 mSv in that figure.

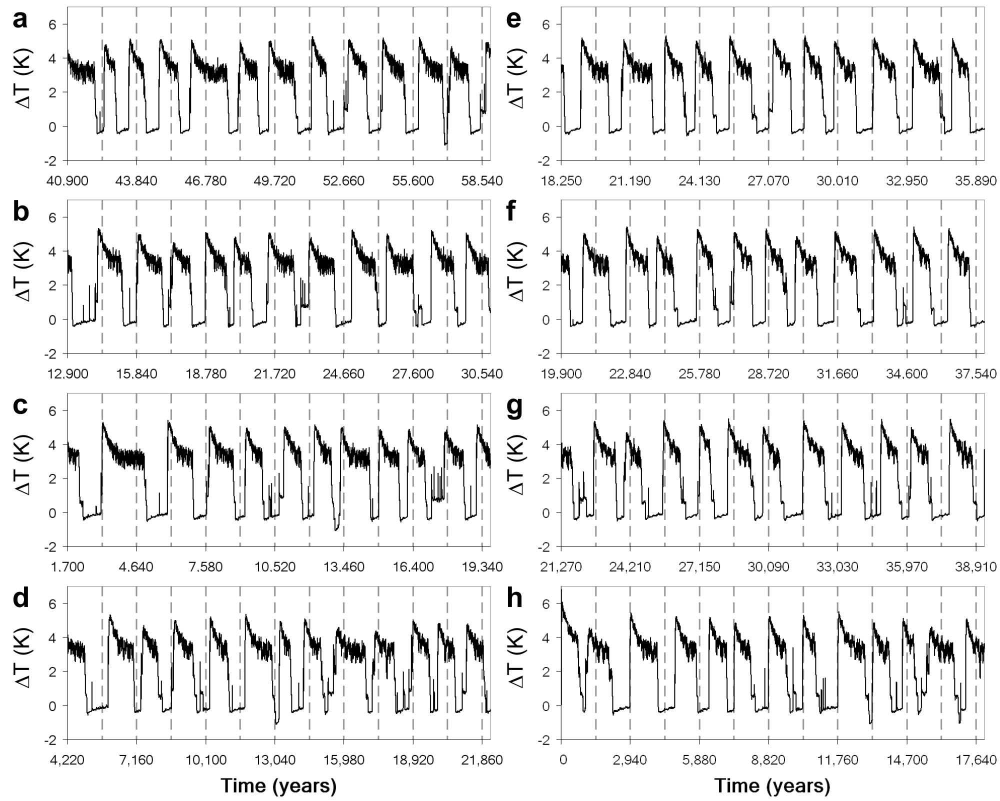

Figure 8.8: Simulated warming events with additional white noise. The figure shows the simulated changes ΔT in Greenland surface air temperature, for various forcing amplitudes A_1 and A_2. The noise level is $\sigma = 25$ mSv. A_1 and A_2 are chosen to be: $A_1 = 0$ mSv, $A_2 = 8$ mSv (a). $A_1 = 2$ mSv, $A_2 = 8$ mSv (b). $A_1 = 4$ mSv, $A_2 = 8$ mSv (c). $A_1 = 6$ mSv, $A_2 = 8$ mSv (d). $A_1 = 8$ mSv, $A_2 = 0$ mSv (e). $A_1 = 8$ mSv, $A_2 = 2$ mSv (f). $A_1 = 8$ mSv, $A_2 = 4$ mSv (g). $A_1 = 8$ mSv, $A_2 = 6$ mSv (h). The dashed lines are spaced by 1470 years. The lines were chosen such that they coincide best with the start of the simulated warming events. All curves are segments of longer (60000 years) model runs. The figure is taken from [70].

8.3 More realistic forcing profiles

In the previous tests of the hypothesis, only two forcing cycles were considered. These cycles, with periods close to the so-called DeVries and Gleissberg solar cycles, were treated as sinusoidal. Both of these simplifications, however, are problematic: First of all, solar activity exhibits more than just the DeVries and Gleissberg cycles. At least the 11-year Schwabe cycle is also of solar origin. Second, the known solar cycles are not sinusoidal (see chapter 4). The Gleissberg cycle, for example, is the amplitude-modulation of the Schwabe cycle. And the DeVries cycle was suggested to be the amplitude-modulation of the Gleissberg cycle[49]. In line with this, solar activity exhibits a large number of spectral components (possibly harmonics and combination tones of the known cycles), compare chapter 4. But the bi-sinusoidal forcing type that was applied in the previous analysis shows only two spectral components (see figure 7.2). This forcing profile is therefore a highly simplified approximation of the known solar cycles. As a consequence, it might be suspected that a more realistic implementation of the solar cycles in the freshwater fluxes does not produce a regular and pronounced 1470-year climate cycle in the glacial response to the forcing.

In this section, the response of CLIMBER-2 to a more realistic representation of the solar cycles in the applied freshwater forcing is investigated. First, the Gleissberg cycle is implemented as the amplitude-modulation of an additional cycle with a period of about 11 years, representing the Schwabe cycle. Second, the DeVries cycle is implemented as the amplitude-modulation of the Gleissberg cycle. As before, the periods of the DeVries and the Gleissberg cycles are chosen to be $T_1 = 1470/7$ (= 210) years and $T_2 = 1470/17$ ($\approx$ 86.5) years, respectively. For simplicity, noise is not considered in the forcing anymore.

8.3.1 More realistic Gleissberg component

To represent the Gleissberg cycle more realistically, the 86.5-year forcing cycle is considered to be the modulation of a 10.8-year cycle. For simplicity, the DeVries cycle is still considered as an additional sinusoidal cycle. The total freshwater forcing F_{tot} reads:

$$F_{tot}(t) = F_1(t) + F_2(t) + K \tag{8.8}$$

$$F_1 = -A_1 \cdot \cos(\omega_1 t) \tag{8.9}$$

$$F_2 = -A_2 \cdot |\cos(\omega_2 t/2)| \cdot |\cos(\omega_3 t/2)| \tag{8.10}$$

with A_1 = 10 mSv, A_2 = 30 mSv, $\omega_1 = 2\pi/T_1$, $\omega_2 = 2\pi/T_2$, $\omega_3 = 2\pi/T_3$ (T_3 = 1470/136 years $\approx$ 10.8 years) and K = -5 mSv (see panel a in figure 8.9)[10].

[10] $|\cos(\omega t/2)|$ is used since $|\cos(\pi t/T)|$ has a period of T.

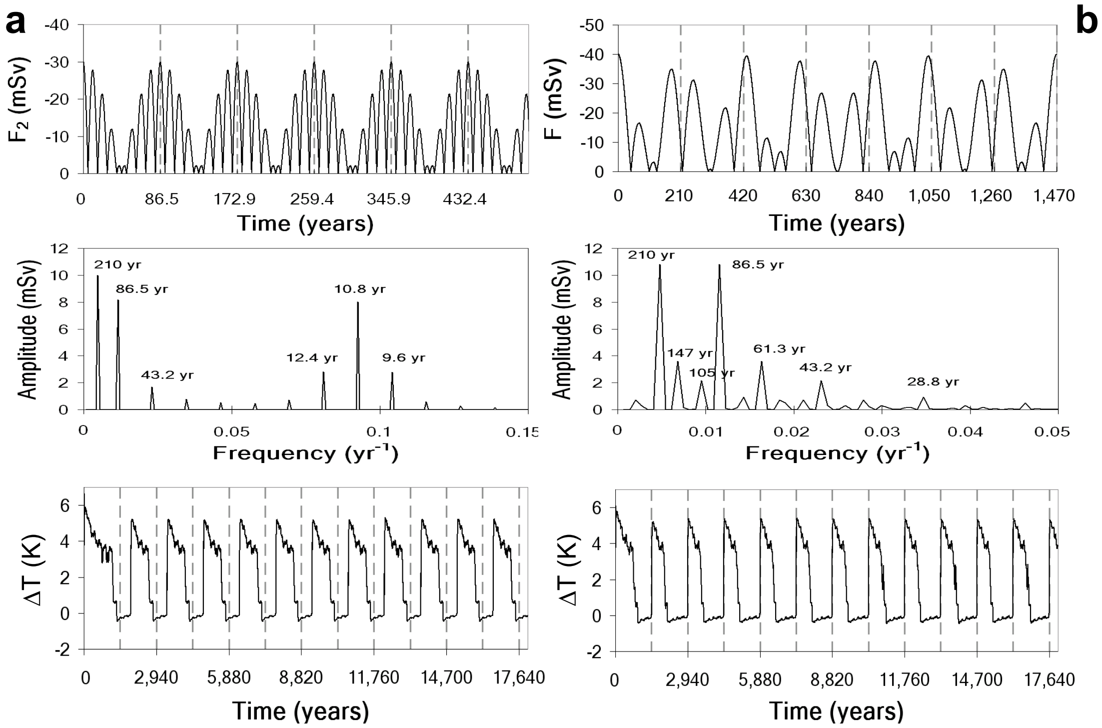

Figure 8.9: Model response to non-sinusoidal forcing profiles
Left column (a): 86.5-year ("Gleissberg") forcing cycle implemented as an amplitude-modulation of an additional 10.8-year ("Schwabe") forcing cycle. Upper row: Combined Gleissberg/Schwabe forcing component F_2. Middle row: Fourier spectrum of $F_1 + F_2$. Numbers above peaks are years. Lower panel: Model response. Right column (b): 210-year ("DeVries") forcing cycle implemented as amplitude-modulation of the 86.5-year ("Gleissberg") forcing cycle. Upper row: Combined DeVries/Gleissberg forcing component F. Middle row: Fourier spectrum of F. Lower panel: Model response. See text for discussion. The figure is taken from [69].

In the frequency domain, the forcing exhibits a pronounced spectral peak at a period of 210 years, corresponding to the sinusoidal component F_1. Pronounced peaks also exist at periods of about 86.5 years and 10.8 years. These peaks are the dominant components of the combined Gleissberg/Schwabe forcing component F_2. Further peaks exist at periods of $86.5/n$ years (n = 2,3,4,...). These peaks correspond to harmonics of the 86.5-year spectral component and occur because the 86.5-year cycle is non-sinusoidal. The most prominent of these harmonics correspond to periods of about 43.2 years (the second harmonic, with n=2), about 12.4 years (n=7) and about 9.6 years (n=9). Note that the 10.8-year cycle is also a harmonic of the 86.5-year cycle (with n=8), since its period is chosen to be 1470/(17·8) years. The 12.4-year and the 9.6-year peaks are fairly prominent, since they correspond to combination tones of the two main forcing frequencies (1/12.4 years^{-1} $\approx$ 1/10.8 years^{-1} - 1/86.5 years^{-1}, 1/9.6 years^{-1} $\approx$ 1/10.8 years^{-1} + 1/86.5 years^{-1}). A 1470-year peak is not explicitly present in the amplitude-spectrum.

Despite the lack of such a spectral peak, the model response to the forcing exhibits periodic warming events in the North Atlantic region, with a spacing of 1470 years. This shows that a stable 1470-year glacial climate cycle can still be obtained when the 86.5-year forcing cycle is implemented as the amplitude-modulation of an additional 10.8-year forcing cycle. The non-sinusoidal profile of the Gleissberg cycle in the solar data therefore does not by itself argue against the hypothesis.

8.3.2 More realistic DeVries component

To represent the DeVries cycle more realistically (see [49]), the 210-year forcing cycle is taken to be the modulation of the 86.5-year cycle. For simplicity, the Schwabe cycle is neglected. The total freshwater forcing F_{tot} reads:

$$F_{tot}(t) = F(t) + K \tag{8.11}$$

$$F = -A_1 \cdot |\cos(\omega_1 t/2)| \cdot |\cos(\omega_2 t/2)| \tag{8.12}$$

with $A_1 = 40$ mSv, $\omega_1 = 2\pi/\mathrm{T}_1$, $\omega_2 = 2\pi/\mathrm{T}_2$ and $K = 5$ mSv (see panel b in figure 8.9).

As in the previous cases, the forcing exhibits prominent spectral components at periods of 210 years and 86.5 years. Further peaks exist, for example at periods of 105 years and 43.2 years (corresponding to the second harmonics of the 210-year cycle and the 86.5-year cycle, respectively) as well as at periods of 147 years and 61.3 years (corresponding to combination tones of the two forcing frequencies: 1/147 years^{-1} $\approx$ 1/86.5 years^{-1} - 1/210 years^{-1}, 1/61.3 years^{-1} $\approx$ 1/86.5 years^{-1} + 1/210 years^{-1}). As before, a 1470-year spectral peak is not present in the forcing.

Despite the lack of such a peak, the model response to the forcing again exhibits periodic warming events in the North Atlantic region, with a spacing of 1470 years. This shows that a stable 1470-year glacial climate cycle can also be obtained when the 210-year forcing cycle is implemented as the amplitude-modulation of the 86.5-year forcing cycle. A possible non-sinusoidal profile of the DeVries/Gleissberg cycles therefore also does not argue against the hypothesis. It is interesting to note that the combined DeVries/Gleissberg forcing type agrees much better with Fourier spectra as obtained from proxies of solar activity than the bi-sinusoidal forcing type that was considered in the last chapter: As can be seen in figure 4.2, records of past ^{14}C-variations in the atmosphere not only exhibit pronounced spectral components with periods near 210 years and 87 years, but also spectral peaks corresponding to periods of about 148 years, 104 years, 60 years and 45 years. These values agree fairly well with the spectral peaks in panel b of figure 8.9, which occur at periods of about 147 years, 105 years, 61 years and 43 years.

As a summary of this section, it was shown that a non-sinusoidal character of the solar activity cycles does not by itself argue against the hypothesis that is presented in this thesis in order to explain the glacial 1470-year cycle. When the Gleissberg cycle is implemented as the amplitude-modulation of an about 11-year freshwater cycle, it is still possible to simulate abrupt warming events with a period of 1470 years. A periodic 1470-year climate cycle can also be obtained when the DeVries cycle is implemented as the amplitude-modulation of an about 86.5-year freshwater cycle. In contrast to the bi-sinusoidal forcing types, the non-sinusoidal forcings show a fairly good agreement in the spectral domain with the Fourier spectra from proxies of solar activity.

8.4 Summary of the stability analysis

To conclude this chapter, the stability studies as described above revealed that the simulated 1470-year climate cycle is a robust feature of the glacial model response of CLIMBER-2 to the forcing. A 1470-year time scale in the model output can still be obtained when

- the forcing parameters (the phases, amplitudes and frequencies) are varied over some range
- noise is included in the forcing
- more realistic (i.e. non-sinusoidal) forcing profiles are described.

This means that the 1470-year response of the climate model to the forcing is a very stable result of the analysis.

From this analysis, however, it is not yet evident why the model responds with a 1470-year time scale to the century-scale forcing. Although the simulated 1470-year glacial climate cycle is stable according to the investigations as performed in this chapter, this stability might seem to be counter-intuitive. Moreover, this cycle might even be an artefact of the model. It is therefore essential to analyse why the century-scale forcing causes the stable millennial-scale cycle in the model response. This will be done in the next chapter: It will be shown that the stability of the glacial model output is a plausible consequence which results from two characteristics of the thermohaline circulation. To interpret the results as obtained in the last two chapters with the climate model CLIMBER-2, a simple conceptual model of the glacial THC will be designed in the next chapter. With this model, it will then be shown that a 1470-year climate response to the forcing is in fact expected, given the dynamics of the THC in the last glacial.

9 A conceptual model of DO-events

In this chapter, the model results which were presented in the last two chapters are interpreted. The previous analysis, which was performed with the coupled climate model CLIMBER-2, showed that in the model DO-like warming events can be triggered in the last glacial by century-scale forcing cycles, with periods close to two known solar cycles. Within a large forcing-parameter range, the simulated warming events are typically spaced by about 1470 years or integer multiples thereof. In the previous two chapters, however, the plausibility of the 1470-year time scale in the glacial model response to the century-scale forcing was not explicitly discussed. The simulated 1470-year climate cycle might therefore seem to be counter-intuitive.

Here, a very simple conceptual model is presented in order to explain the output of the much more complex model CLIMBER-2. The response of this conceptual model to the forcing is then compared with the response of CLIMBER-2 (which was discussed in the previous two chapters). It is shown that the conceptual model is able to mimic many key features of the output of CLIMBER-2. The similarities in the response of both models to the same forcing strongly suggest that the glacial 1470-year cycle, as simulated by CLIMBER-2, is not an artefact. Instead, a 1470-year climate cycle of DO-like warming events is in fact expected to be triggered by the forcing, provided that these warming events are caused by highly non-linear switches in the thermohaline circulation.

9.1 Description of the conceptual model

The conceptual model, which is applied in the following, describes a system that consists of two states (*cold* and *warm*), analogous to the stadial and interstadial modes of the thermohaline circulation (THC) in CLIMBER-2. As long as no freshwater forcing acts, both states are considered to be stable. When the forcing is applied, transitions between both states can be excited, provided that the forcing is sufficiently strong.

The first assumption for the dynamics of the conceptual model is that these transitions are threshold processes. This implies that a transition from the warm to the cold state occurs instantaneously each time the forcing crosses a certain threshold $T_{W \rightarrow C}$. Similarly, a transition from the cold to the warm state is triggered instantaneously each time the forcing crosses a second threshold $T_{C \rightarrow W}$. This assumption accounts for the dynamics of the transitions between the two modes of the THC in CLIMBER-2, which evolve very rapidly over only a few years and are triggered by a threshold process, i.e. by changes in deep convection.

The second assumption for the dynamics of the conceptual model is that the two thresholds do not remain constant after a transition into the relevant state of the model. Instead, they are gradually decreasing: The threshold $T_{W\to C}$, which has positive values, since transitions into the stadial mode are triggered by positive freshwater anomalies, is at maximum value $T_{W\to C}(t{=}0)$ directly after a transition from the cold to the warm state and then declines exponentially with a limiting value $T_{W\to C}(t{=}\infty)$, see figure 9.1.

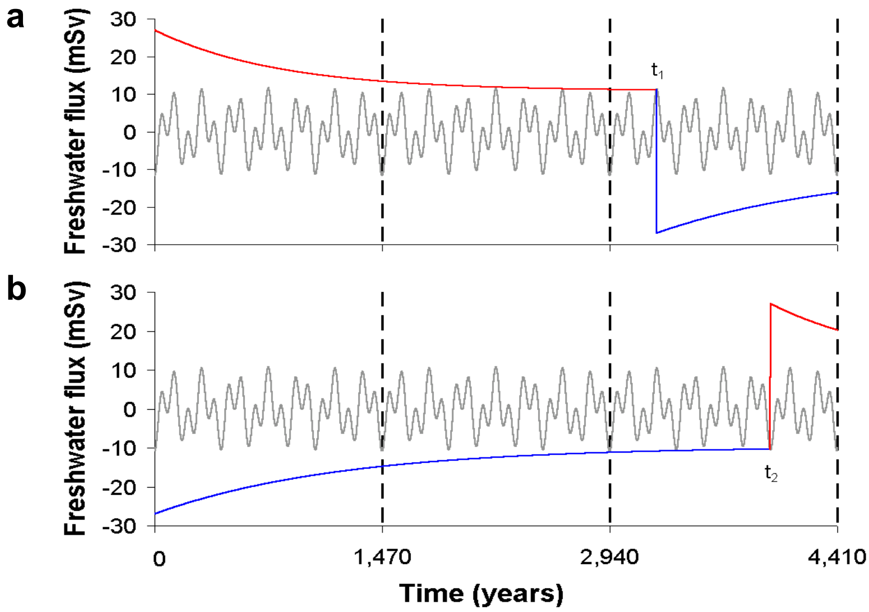

Figure 9.1: Time-evolution of the conceptual model.
Each time the forcing (grey, in mSv) crosses a certain threshold (coloured line, in mSv), a transition between the two model states is triggered. Panel a: Transition from the warm (red) to the cold (blue) state. The model is started in the warm state at time t = 0 years. The relevant threshold $T_{W\to C}$ decreases exponentially until the forcing crosses this threshold, which is the case at time t_1, and the model then flips into the cold state. Panel b: Transition from the cold to the warm state. The model is started in the cold state at time 0 years. The relevant threshold $T_{C\to W}$ likewise increases (i.e. $|T_{C\to W}|$ decreases exponentially) until the forcing crosses this threshold, which is the case at time t_2, and the model then flips into the warm state. The figure is taken from [70].

The threshold $T_{C\to W}$, which has negative values since the interstadial mode is excited by negative freshwater anomalies, similarly is at minimum value $T_{C\to W}$(t=0) directly after the transition from the warm to the cold state, and $|T_{C\to W}|$ then decreases exponentially with a limiting value $|T_{C\to W}(t{=}\infty)|$, see figure 9.1. The two thresholds read:

$$T_{W\to C}(t) = [T_{W\to C}(t=0) - T_{W\to C}(t=\infty)] \cdot \exp(-t/\tau_{W\to C}) + T_{W\to C}(t=\infty) \quad (9.1)$$

$$T_{C\to W}(t) = [T_{C\to W}(t=0) - T_{C\to W}(t=\infty)] \cdot \exp(-t/\tau_{C\to W}) + T_{C\to W}(t=\infty) \quad (9.2)$$

where t indicates the time after the last transition into the relevant state.

The assumption of a *relaxation time* τ accounts for the long characteristic time scale of the THC: After a switch of the mode, the THC requires some time of adjustment before the spatial structure of the oceanic density field is such that the next switch can be triggered by the forcing. This adjustment process is expressed by the time-dependence of the two thresholds in the conceptual model. During the adjustment process, denoted by the relaxation times $\tau_{W\to C}$ and $\tau_{C\to W}$, the thresholds are therefore gradually being reduced[1]. Note that waiting times larger than 1470 years between successive transitions are not compatible with constant threshold values: If the forcing (figure 7.1) does not cross a constant threshold within the first 1470 years, it never will, due to the 1470-year period of the forcing. Consequently, the waiting times of several multiples of 1470 years, which occur in the response of CLIMBER-2 (figure 7.9), show that the thresholds in that model also decrease with time.

When started in the cold state, this state of the conceptual model remains stable if and only if the forcing never crosses the threshold $T_{C\to W}$(t). For the forcing as given by the expression

$$F = -A \cdot \cos(\omega_1 t) - A \cdot \cos(\omega_2 t) \quad (9.3)$$

with $\omega_1 = 2\pi/T_1$ (T_1 = 1470/7 years = 210 years) and $\omega_2 = 2\pi/T_2$ (T_2 = 1470/17 years $\approx$ 86.5 years), this is the case for $2A \leq |T_{C\to W}(t{=}\infty)|$. Otherwise, i.e. for $2A > |T_{C\to W}(t{=}\infty)|$, a transition from the cold to the warm state is excited at some time. In this case, the model either ends up in the warm state (for $2A \leq T_{W\to C}[t{=}\infty]$) or shows periodic oscillations between both states (for $2A > T_{W\to C}[t{=}\infty]$). Therefore, this simple model is able to reproduce the existence of the three different regimes (cold regime, warm regime, Dansgaard-Oeschger regime), as seen in the response of CLIMBER-2 (figure 7.9). Note that the location of these regimes in the amplitude-parameter range[2] depends only on the choice of $T_{C\to W}(t{=}\infty)$ and $T_{W\to C}(t{=}\infty)$.

[1] $\tau_{W\to C}$ and $\tau_{C\to W}$ would be expected to be of the order of about 1000 years.
[2] given by all possible values for the amplitude A

To compare the output of both models, the freshwater offset K, which was applied in the forcing of CLIMBER-2 to mimic changes in the background climate, needs to be transformed into these two parameters of the conceptual model. The offset is thus not considered in the forcing of the conceptual model anymore. The reason for this approach is as follows: For each value of K, the two parameters $\mathrm{T}_{C\to W}(\mathrm{t}=\infty)$ and $\mathrm{T}_{W\to C}(\mathrm{t}=\infty)$ can be chosen such that the conceptual model reproduces the existence of the three regimes in the response of CLIMBER-2, as well as their position in the amplitude-parameter space. For K = -17 mSv, for example, $\mathrm{T}_{C\to W}(\mathrm{t}=\infty)$ and $\mathrm{T}_{C\to W}(\mathrm{t}=\infty)$ must lie within the following intervals: -10 mSv $<$ $\mathrm{T}_{C\to W}(\mathrm{t}=\infty) \leq$ -8 mSv and 10 mSv $\leq$ $\mathrm{T}_{W\to C}(\mathrm{t}=\infty) <$ 12 mSv. With this choice it is assured that the conceptual model, when started in the cold state, remains there for amplitude values $A \leq 4$ mSv, ends up in the warm state for A = 5 mSv, and shows periodic oscillations between both states for $A \geq 6$ mSv, just like CLIMBER-2 (see figure 7.9).

In the following, the response of CLIMBER-2 for a fixed offset (K = -17 mSv) is compared with the response of the conceptual model. The six parameters of that model are chosen as follows: $T_{W\to C}(t = 0)$ = 27 mSv, $T_{C\to W}(t = 0)$ = -27 mSv, $T_{W\to C}(t = \infty)$ = 11.2 mSv, $T_{C\to W}(t = \infty)$ = -9.7 mSv, $\tau_{W\to C}$ = 800 years, $\tau_{C\to W}$ = 1200 years. Note that $\mathrm{T}_{C\to W}(\mathrm{t}=\infty)$ and $\mathrm{T}_{W\to C}(\mathrm{t}=\infty)$ are well within the ranges mentioned above. $|\mathrm{T}_{C\to W}(\mathrm{t}=0)|$ is taken to be equal to $\mathrm{T}_{W\to C}(\mathrm{t}=0)$, for simplicity. The adjustment times $\tau_{W\to C}$ and $\tau_{C\to W}$ are both of the order of about 1000 years, which is typically for the THC. $\tau_{C\to W}$ is chosen to be larger than $\tau_{W\to C}$ since the cold mode of the THC in CLIMBER-2 decays more slowly than the warm one.

Figure 9.2 shows the response of the conceptual model, which is started in the cold state just like CLIMBER-2, for five values of A. As mentioned above, the model remains in the cold state for A = 4 mSv and ends up in the warm state for A = 5 mSv. For $A \geq 6$ mSv, periodic oscillations between both states occur. The duration of the warm and cold intervals decreases with larger amplitude A. This is a characteristic feature of the conceptual model that is independent of the choice of the six model parameters. With the parameter-values mentioned above, the model can reproduce the spacing of the DO events as simulated by CLIMBER-2 (compare figure 7.9). It is important to mention that for different choices of the six free parameters of the conceptual model, both models still shows general agreement, for example a frequency conversion[3] between forcing and response and a dependence of the period in the model response on the forcing amplitude A. Furthermore, it is not only for the offset value K = -17 mSv that the conceptual model is able to mimic the dynamics of CLIMBER-2. As will be shown later, the parameters $\mathrm{T}_{C\to W}(\mathrm{t}=\infty)$ and $\mathrm{T}_{W\to C}(\mathrm{t}=\infty)$ can be adjusted such that the conceptual model shows agreement with CLIMBER-2 for many freshwater-offset values K.

[3]This means that the model response shows millennial-scale spectral components which are not present in the forcing.

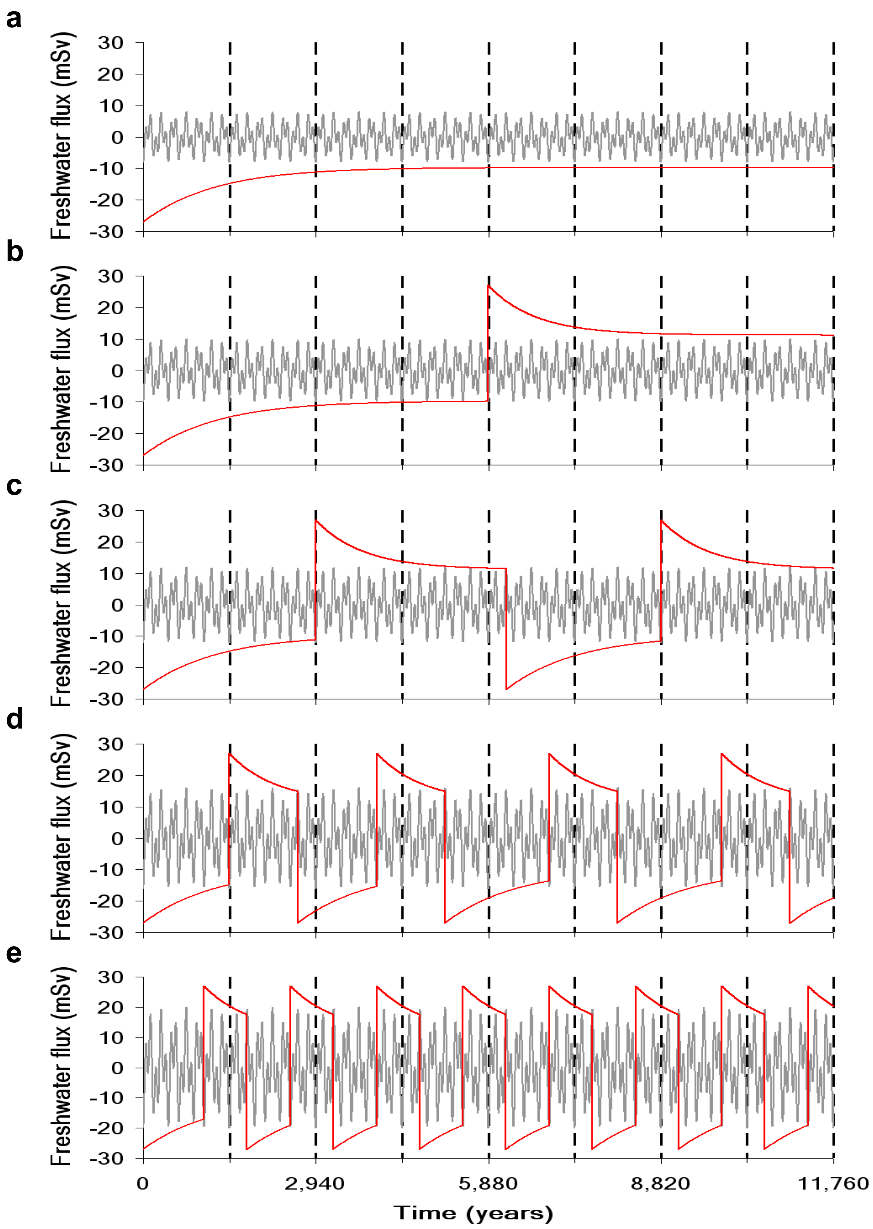

Figure 9.2: Response of the conceptual model to the forcing.
The forcing (grey, in mSv) is given by equation (9.3), compare figure 7.1. The amplitude A is: 4 mSv (a), 5 mSv (b), 6 mSv (c), 8 mSv (d), 10 mSv (e). The model response is illustrated by the time-evolution of the threshold (red, in mSv). The dashed lines indicate the first order minima in the forcing (i.e. the maxima in the salinity flux), with a period of 1470 years. The period in the response of the conceptual model (c-e) agrees with the period in the response of CLIMBER-2 (for K = -17 mSv, see figure 7.9). The figure is taken from [70].

9.2 Parameter-space of the model

In the previous section, the response of the conceptual model to the forcing[4] was already compared with the response of CLIMBER-2[5]. This comparison, however, was only performed for a specific choice of the threshold parameters $T_{C\to W}(t=\infty)$ and $T_{W\to C}(t=\infty)$, corresponding to the freshwater offset K = -17 mSv.

In this section, the conceptual model is generalised so that it can be used to mimic the response of CLIMBER-2 for all possible freshwater offsets, not just for K = -17 mSv. The model's phase space diagram is then compared with the one that was obtained with CLIMBER-2 (figure 7.9). It is shown that the conceptual model is able to reproduce many characteristic features that exist in the response of CLIMBER-2 to the forcing, for example the occurrence of three different regimes in the model output. In this chapter, these regimes are interpreted in terms of a bifurcation in the model dynamics. The similarity between both model outputs suggests that the conceptual model successfully captures the main features of the dynamics of DO events as given by the much more complex model CLIMBER-2.

9.2.1 Generalisation of the conceptual model

In order to generalise the conceptual model, so that its output can be compared with the output of CLIMBER-2 for all offset values K, an offset $C = K + 17$ mSv could be added to the forcing $F = -A \cdot \cos(\omega_1 t) - A \cdot \cos(\omega_2 t)$ of the conceptual model. In this approach, the model thresholds $T_{W\to C}$ and $T_{C\to W}$ remain unchanged, and the forcing F is transformed

$$\begin{aligned} T'_{W\to C}(t) &= T_{W\to C}(t) \\ T'_{C\to W}(t) &= T_{C\to W}(t) \\ F'(t) &= F(t) \; + \; K \; + \; 17 \; mSv. \end{aligned} \tag{9.4}$$

Note that equation (9.4) implies that $F'(t) = F(t)$ for K = -17 mSv, i.e. no transformation of the forcing is required in this case (and in fact, no such transformation was considered above).

In the following, a slightly different approach is taken, in which the forcing remains the same for different offset-values K, but the model thresholds $T_{C\to W}(t)$ and $T_{W\to C}(t)$ are transformed

[4] The forcing of the conceptual model exhibits only two century-scale cycles, but no additional offset, compare equation (9.3)

[5] In order to mimic changes in the background climate conditions, an additional offset K was used in the forcing of the climate model, compare equation (7.4).

$$
\begin{aligned}
T''_{W\to C}(t=0) &= T_{W\to C}(t=0) - K - 17\ mSv \\
T''_{W\to C}(t=\infty) &= T_{W\to C}(t=\infty) - K - 17\ mSv \\
T''_{C\to W}(t=0) &= T_{C\to W}(t=0) - K - 17\ mSv \\
T''_{C\to W}(t=\infty) &= T_{C\to W}(t=\infty) - K - 17\ mSv \\
F''(t) &= F(t).
\end{aligned} \tag{9.5}
$$

This is more convenient for the following model investigations. Besides, it is also more intuitive since the offset K was introduced to mimic changes in the background climate, and these changes would be expected to affect the position of the thresholds in the "real" climate system. As will be shown now, this approach is possible since both transformation (9.4, 9.5) lead to the same dynamics of the conceptual model.

The starting point are the following four possible relations between the transformed forcing F'' and the transformed model thresholds $T''_{W\to C}(t)$ and $T''_{C\to W}(t)$

$$
\begin{aligned}
F''(t) &> T''_{W\to C}(t) \\
F''(t) &\leq T''_{W\to C}(t) \\
F''(t) &< T''_{C\to W}(t) \\
F''(t) &\geq T''_{C\to W}(t).
\end{aligned} \tag{9.6}
$$

These relations govern the dynamics of the conceptual model, since in the model it only matters whether or not the relevant threshold is crossed by the forcing at a given time. To show that the transformations (9.4) and (9.5) are equivalent, it is thus necessary to demonstrate that the above relations also hold when T'', $T''_{W\to C}$ and $T''_{C\to W}$ are replaced by T', $T'_{W\to C}$ and $T'_{C\to W}$. To do that, The starting point are the relations (9.6): Substituting (9.5), (9.1) and (9.2) into these relations yields

$$
\begin{aligned}
F(t) &> T_{W\to C}(t) - K - 17\ mSv \\
F(t) &\leq T_{W\to C}(t) - K - 17\ mSv \\
F(t) &< T_{C\to W}(t) - K - 17\ mSv \\
F(t) &\geq T_{C\to W}(t) - K - 17\ mSv.
\end{aligned} \tag{9.7}
$$

These relations can be rewritten as

$$
\begin{aligned}
F(t) + K + 17\ mSv &> T_{W\to C}(t) \\
F(t) + K + 17\ mSv &\leq T_{W\to C}(t) \\
F(t) + K + 17\ mSv &< T_{C\to W}(t) \\
F(t) + K + 17\ mSv &\geq T_{C\to W}(t)
\end{aligned} \tag{9.8}
$$

or, with transformation (9.4)

$$\begin{aligned} F(t)' &> T'_{W\rightarrow C}(t) \\ F(t)' &\leq T'_{W\rightarrow C}(t) \\ F(t)' &< T'_{C\rightarrow W}(t) \\ F(t)' &\geq T'_{C\rightarrow W}(t). \end{aligned} \tag{9.9}$$

This means that the expressions (9.6) and (9.9) are indeed equivalent. This result is not very surprising: Transformation (9.4) implies that the forcing is shifted by K+17 mSv, and the model thresholds are unchanged. And transformation (9.5) means that the forcing is unchanged, but the thresholds are shifted by -K-17 mSv. The main difference between both transformations is thus a shift in the freshwater axis, but such a shift does not affect the dynamics of the conceptual model. Since the transformations (9.4) and (9.5) are equivalent, the dynamics of the conceptual model is the same in both approaches. This means that instead of changing the forcing of the model according to equation (9.4) for a different offset value K, it is also possible to modify the threshold parameters according to equation (9.5), and to leave the forcing unchanged.

From equation (9.5) and from the choice of the model parameters in the previous section[6], it follows that the four parameters of the two thresholds in the conceptual model must be chosen in the following way, in order to compare the model output with the output of CLIMBER-2 for a given value of the offset K:

$$\begin{aligned} T_{C\rightarrow W}(K, t=0) &= -44\ mSv\ -\ K \\ T_{C\rightarrow W}(K, t=\infty) &= -26.7\ mSv\ -\ K \\ T_{W\rightarrow C}(K, t=0) &= 10\ mSv\ -\ K \\ T_{W\rightarrow C}(K, t=\infty) &= -5.8\ mSv\ -\ K \end{aligned} \tag{9.10}$$

Note that in the case of K = -17 mSv, which was considered in the previous section, this transformation gives exactly the parameter values which were used in that section. This means that the transformation (9.10) is well-defined. With the expressions given in (9.10), it is now possible to compute the response of the conceptual model for all offset-values K.

9.2.2 Phase-space diagram of the conceptual model

Figure 9.3 shows the phase-space diagram of the conceptual model. This diagram illustrates the response of the model to the forcing as given by equation (9.3), for all possible combinations of A and K in the intervals $0 \leq A \leq 12$ mSv and -30 mSv

[6] These values were: $T_{W\rightarrow C}(t=0)$ = 27 mSv, $T_{C\rightarrow W}(t=0)$ = -27 mSv, $T_{W\rightarrow C}(t=\infty)$ = 11.2 mSv, $T_{C\rightarrow W}(t=\infty)$ = -9.7 mSv.

$\leq K \leq$ -2 mSv. For each value of K, the parameters of the conceptual model are calculated according to the relations (9.10)[7]. The comparison of this figure with the phase-space diagram that was obtained with CLIMBER-2 (figure 7.9) shows many similarities:

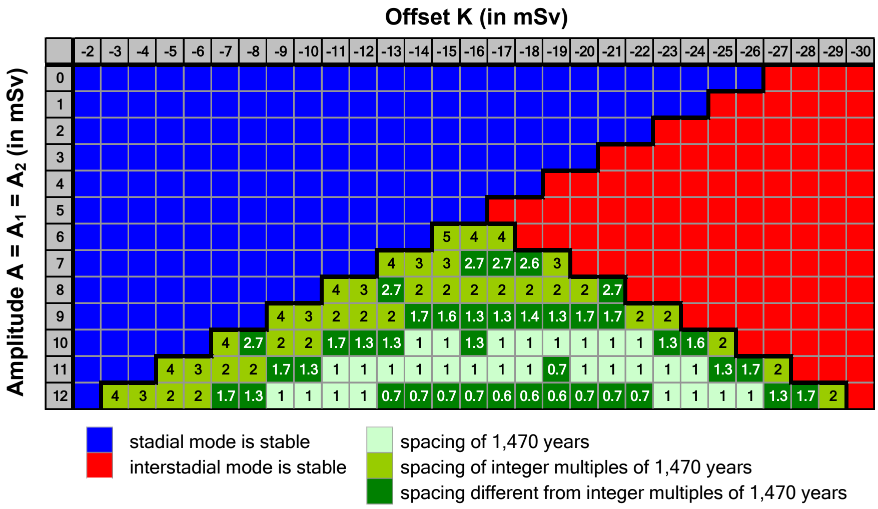

Figure 9.3: Phase space diagram for $A \leq 12$ mSv.
Schematic response of the conceptual model to the forcing for amplitudes A up to 12 mSv and freshwater offsets K between -2 mSv and -30 mSv. *Cold regime*: blue area. *Warm regime*: red area. *DO regime*: green area. The numbers in this regime denote the most frequently occurring temporal spacing between successive DO events (for each combination of A and K), in multiples of 1470 years. The conceptual model is started in the cold state, since CLIMBER-2 is initially also in the cold state for LGM boundary conditions.

- The conceptual model reproduces the existence of three different regimes in the response to the forcing: A *cold* regime in which the cold state of the model is stable, a *warm* regime in which the model ends up in the warm state, and a *DO* regime in which the forcing triggers periodic oscillations between both model states.
- The conceptual model fairly well reproduces the position of these three regimes in the forcing-parameter space of CLIMBER-2.
- The main stability properties of the three regimes in the model output of CLIMBER-2 are reproduced by the conceptual model: For amplitude-values

[7]The relaxation times $\tau_{W \to C} = 800$ years and $\tau_{C \to W} = 1200$ years are assumed to be independent of the offset K.

A of less than 6 mSv, the conceptual model is bi-stable, and repeated warming events do not occur yet. For values of 6 mSv or more, the events occur in a certain range of offset-values K. This range gets broader with larger forcing amplitude. For a fixed value of K, the period in the response of the conceptual model decreases with a larger forcing amplitude A, in agreement with CLIMBER-2. Moreover, the period of the oscillations between both model states is smallest in the interior of the DO regime. When K is chosen to be near the borders to the cold or warm regimes, the period in the output of the conceptual model increases, similar to the pattern that was found with CLIMBER-2.

- In the conceptual model, a spacing of 1470 year between successive events occurs for many combinations of the forcing parameters and within a continuous range of the phase space.
- Deviations from this prevailing 1470-year (or multiples thereof) time scale are possible. The deviations are very similar to the ones in the output of CLIMBER-2 (i.e. they are most often in the range of 500 years).
- A millennial-scale response of the conceptual model occurs throughout the entire DO regime. In no part of the phase-space is the model response on the centennial time scale.

Some mismatches, however, can be found when the patterns in the output of both models are compared in detail:

- For small values of A, the cold regime in the conceptual model extends further than the cold regime in CLIMBER-2. For example, in the conceptual model the border between both regimes lies around $K \approx$ -26.5 mSv for $A = 0$ mSv. In the climate model, however, the border is around $K \approx$ -22.5 mSv.
- In the conceptual model, the region with a 1470-year model response is slightly shifted in the K-space, towards larger (i.e. less negative) offset-values.
- A couple of combinations of the forcing parameters A and K exist for which the period in the response of both models does not agree.

Given the high simplicity of the conceptual model, however, the agreement between both models is surprisingly good: The model has just six free parameters. And only two of these, namely $T_{C\rightarrow W}$(t=0) and $T_{W\rightarrow C}$(t=0) can be chosen completely arbitrarily. The other four parameters are not entirely free to chose, since their approximate values can be inferred to some extent. The most realistic range for the two relaxation times $\tau_{W\rightarrow C}$ and $\tau_{C\rightarrow W}$, for example, can be estimated from the physical meaning of these two parameters: They represent characteristic time scales of the thermohaline circulation and would therefore be expected to be of the order of 1000 years. And the possible range for $T_{W\to C}$(t=∞) and $T_{C\to W}$(t=∞) is rather small, since these two parameters can be directly estimated from the phase-space diagram of CLIMBER-2 (as discussed in the section 9.1).

As discussed above, the pattern in the output of both models for forcing amplitudes A of up to 5 mSv is fundamentally different from the pattern for amplitudes of at least 6 mSv: While the model is bi-stable for small amplitudes (i.e. the models ends up either in the cold or in the warm mode), periodic oscillations between both modes can be excited for $A \geq 6$ mSv. This means that some bifurcation exists in the model response. The origin of this bifurcation was not yet discussed. The conceptual model as presented here gives an explanation for the existence of this bifurcation: In this model, oscillations between both states occur when the forcing amplitude A is large enough to cross both model thresholds. This condition is fulfilled for

$$\begin{aligned} -2A &< T_{C\to W}(t=\infty) \\ 2A &> T_{W\to C}(t=\infty). \end{aligned} \tag{9.11}$$

With the expressions given in equation (9.10) it follows that these oscillations occur in the conceptual model when

$$\begin{aligned} 2A &> 26.7\ mSv + K \\ 2A &> -5.8\ mSv - K \end{aligned} \tag{9.12}$$

both hold. A minimum value A_{bif} exists, and correspondingly a value K_{bif}, for which

$$\begin{aligned} 2A &= 26.7\ mSv + K \\ 2A &= -5.8\ mSv - K \end{aligned} \tag{9.13}$$

are fulfilled at the same time. These values are

$$\begin{aligned} A_{bif} &= 5.225\ mSv \\ K_{bif} &= -16.25\ mSv. \end{aligned} \tag{9.14}$$

The location in the phase-space that is given by the coordinates (A_{bif}, K_{bif}) represents the bifurcation point of the conceptual model.

For offset values $K > K_{bif}$ (i.e. -2 mSv $\geq K \geq$ -16 mSv in figure 9.3), the upper expression in relation (9.12) is more stringent. When this relation is not fulfilled, a transition from the cold state to the warm state of the model cannot occur, because the threshold $T_{C \to W}$ is never crossed. A forcing with an amplitude $A = 5$ mSv, for example, and offset-values K as mentioned above cannot fulfil this condition, since $A < A_{bif}$. This is why the conceptual model, when started in the cold state, remains in this state for the relevant points in the phase-space (blue area in figure 9.3). In this case, it does not matter whether or not the lower expression in relation (9.12), which governs the transition from the warm state to the cold state, holds: Since the model never switches to the warm state, it is not relevant if the warm state is stable or not.

In the opposite case, when $K < K_{bif}$ (i.e. -17 mSv $\geq K \geq$ -30 mSv in figure 9.3), the lower expression in relation (9.12) is more stringent. When this relation is not fulfilled, a transition from the warm state to the cold state cannot occur, because the threshold $T_{W \to C}$ is never crossed. A forcing with amplitude A of 5 mSv and offset-values K as mentioned above cannot fulfil this condition, since $A < A_{bif}$. Nevertheless, the upper relation in (9.12) can still hold. If this is the case, the conceptual model switches its state and ends up in the warm state (red area in figure 9.3). The existence of the three regimes in the phase-space diagram of the conceptual model is thus plausible. Given the good agreement in the main features of the phase-space diagrams as obtained with both models, it is very likely that the same principle can also explain the existence of the bifurcation in CLIMBER-2.

9.3 Stability of the 1470-year cycle in the model

The stability of the 1470-year climate cycle in the response of the CLIMBER-2 to the forcing was already investigated in the previous chapter. In this chapter, the conceptual model is used for similar tests. It is shown that the 1470-year cycle in the model output is also stable with respect to changes in the forcing parameters (i.e. the phases, frequencies and amplitudes of the two forcing cycles). In this part of the analysis, the parameters of the conceptual model are chosen as above (for the case of K = -17 mSv). A bi-sinusoidal forcing type is considered, given by:

$$F(t) = F_1(t) + F_2(t) \tag{9.15}$$

$$F_1 = -A_1 \cdot \cos(\omega_1 t + \phi_1) \tag{9.16}$$

$$F_2 = -A_2 \cdot \cos(\omega_2 t + \phi_2) \tag{9.17}$$

compare section (8.1). A_1 and A_2 are the amplitudes of the two cycles, T_1 and T_2 are the periods, ϕ_1 and ϕ_2 are the phases. After considering this forcing type, it is discussed why a stable 1470-year climate cycle can also be obtained when a non-sinusoidal forcing profile is used.

9.3.1 Variations of the forcing phases

In this part of the analysis, the sensitivity of the 1470-year cycle in the response to the forcing is analysed for different phase relations between the two phases ϕ_1 and ϕ_2. A_1 and A_2 are chosen to be 10 mSv, T_1 is taken to be 1470/7 (=210) years, T_2 is 1470/17 ($\approx$86.5) years. ϕ_2 is chosen to be zero. Twenty different values are considered for ϕ_1 (0, 0.1π, ..., 1.9π).

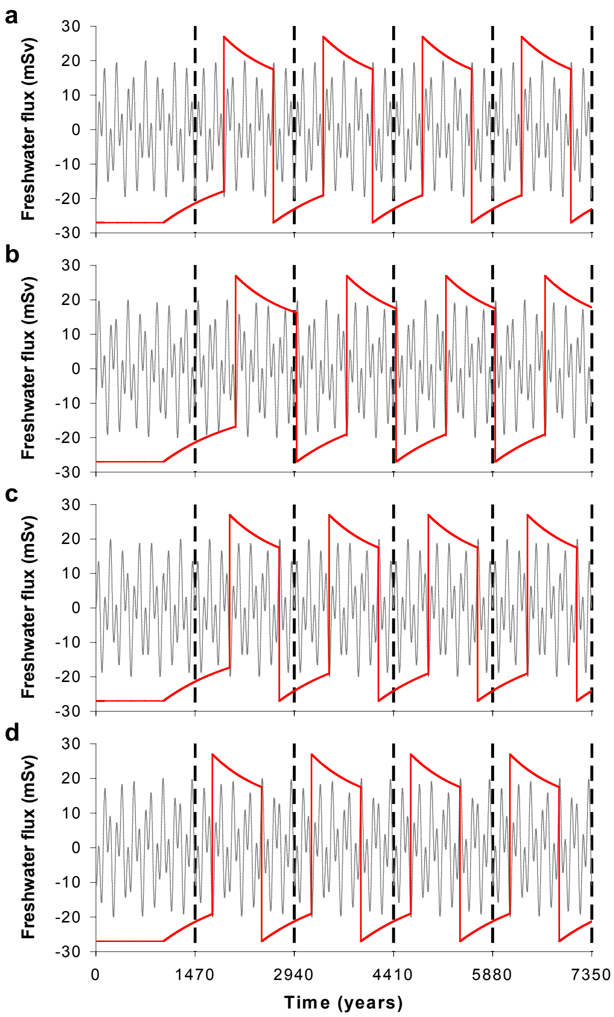

Figure 9.4: Model response for different phases ϕ_1.
The phase ϕ_1 of the 210-year forcing cycle is chosen to be 0 (a), $\pi/2$ (b), π (c) and $3\pi/2$ (d). Note that the model is started at t = 1000 years (for $t \leq 1000$ years, the model thresholds are fixed).

For all of these values, the conceptual model exhibits periodic oscillations between both model states, with a period of 1470 year. Figure 9.4 shows the simulated events for four values of ϕ_1. As in the output of CLIMBER-2, the start and the end of the events in the conceptual model is shifted in time when different forcing phases are applied. In figure 9.4, the dynamical evolution of the model is started at time $t = 1000$ years (prior to that time, the model thresholds are fixed at their initial values). The reason why this is done is that without this shift in the time axis of the conceptual model, the 1470-year cycle in the response of that model is shifted in time compared with the cycle in the response of CLIMBER-2[8]. The value of 1000 years is chosen to achieve agreement in the timing of the events for $\phi_1 = 0$, as simulated with both models[9]. Both models also agree in the timing of the events for many other values of ϕ_1 (and the time axis of the conceptual model was not adjusted to obtain this agreement).

The phase relation of the 1470-year cycle in the output of the conceptual model is shown in figure 9.5, for all chosen values of ϕ_1. As in CLIMBER-2 (figure 8.2), the onset of the simulated events always occurs at discrete time intervals, close to integer multiples of 1470/17 years. The reason for this behaviour of the conceptual model is the threshold character of the switches between both model states: Transitions from the cold to the warm state can only be triggered when the forcing crosses the threshold $T_{C \to W}$. These transitions, however, occur when both forcing cycles have very low values[10]. When one cycle has a low value, but the other cycle has a high value, the two cycles average out to some degree, and a transition is not triggered. Since the minima of the second forcing cycle occur every 1470/17 years, it is not very surprising that the switch from the "cold" to the "warm" state can only occur close to these minima.

The comparison of the phase relation in the output of CLIMBER-2 (figure 8.2) with the phase relation in the response of the conceptual model (figure 9.5) shows a very good agreement between both models: For almost all values of ϕ_1 (apart from $\phi_1 = 2/10\pi$ and $\phi = 9/10\pi$), the switch to the warm mode of the conceptual model occurs at the correct time interval (i.e. at the same peak of the 86.5-year forcing cycle as in CLIMBER-2). How significant is the agreement? The phase diagrams (figures 8.2 and 9.5) can be considered as a sequence of twenty phase-values $\Phi_0, \Phi_1, ..., \Phi_{19}$, where Φ_i denotes the phase of the 1470-year cycle in the model response to the forcing[11] for a forcing-phase ϕ_i which is given by $\phi_i = i \cdot \pi/10$.

[8]This is because the initial conditions in both models are different. Therefore, it takes slightly different time intervals before the output of both models becomes stationary. This eventually leads to a phase shift in the response of both models to the same forcing. This phase shift can be compensated by a roughly 1000-year shift in the time axis of the conceptual model.

[9]The events in the panels a of figure 8.1 and 9.4 start and end at very similar time steps. This would not be the case without the shift in the time axis.

[10]because this transition is triggered by negative freshwater anomalies

[11]or, more precisely, the timing of the switch from the cold state to the warm state

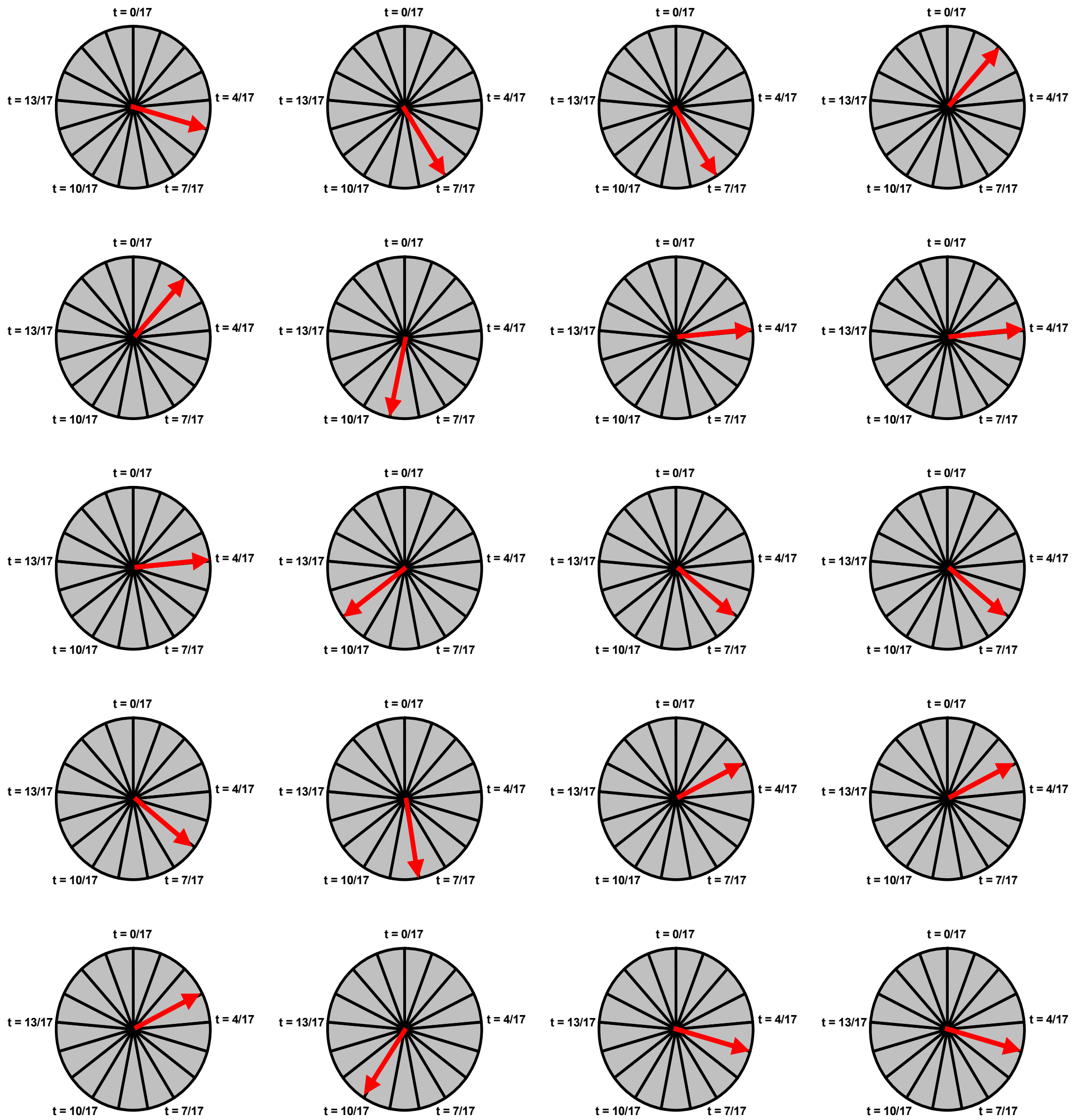

Figure 9.5: Phase diagram of the simulated warming events.
Phase relation between the forcing and the simulated 1470-year climate cycle as simulated with the conceptual model, for various values of the forcing phase ϕ_1. First row (from left to right): $\phi_1 = 0$, $\phi_1 = 1/10\pi$, $\phi_1 = 2/10\pi$, $\phi_1 = 3/10\pi$. Second row: $\phi_1 = 4/10\pi$, $\phi_1 = 5/10\pi$, $\phi_1 = 6/10\pi$, $\phi_1 = 7/10\pi$. Third row: $\phi_1 = 8/10\pi$, $\phi_1 = 9/10\pi$, $\phi_1 = 10/10\pi$, $\phi_1 = 11/10\pi$. Forth row: $\phi_1 = 12/10\pi$, $\phi_1 = 13/10\pi$, $\phi_1 = 14/10\pi$, $\phi_1 = 15/10\pi$. Fifth row: $\phi_1 = 16/10\pi$, $\phi_1 = 17/10\pi$, $\phi_1 = 18/10\pi$, $\phi_1 = 19/10\pi$. The red arrows indicate the time (in multiples of 1470 years) at which the abrupt warming events occur in the model. Note that only discrete phases are possible for the simulated 1470-year cycle: The warming events always occur at multiples of 1470/17 years.

Since the switch to the warm state can only be triggered at a minimum of the 86.5-year cycle, Φ_i can take seventeen possible values: $\Phi_i = 2\pi \cdot n/17$, with n = 0,1,2,...,16. The sequence of the twenty model-output phases can thus be written as a sequence of twenty n-numbers: n_{Φ_0}, n_{Φ_1},...,$n_{\Phi_{19}}$. Consequently, the phase diagram of CLIMBER-2 can thus be expressed as the sequence

$$[n]_{CLIMBER} = [5, 7, 2, 2, 2, 9, 4, 4, 4, 6, 6, 6, 6, 8, 3, 3, 3, 10, 5, 5] \tag{9.18}$$

Similarly, the phase diagram of the conceptual model can be written as

$$[n]_{CONCEPT} = [5, 7, 7, 2, 2, 9, 4, 4, 4, 11, 6, 6, 6, 8, 3, 3, 3, 10, 5, 5] \tag{9.19}$$

These two sequences agree in 18 out of 20 elements. Since the shift in the time-axis of the conceptual model was chosen such that the model agrees in its phase Φ_0 with CLIMBER-2, the agreement in n_{Φ_0} is only the result of the tuning process. Thus, the conceptual model only reproduces 17 out of 19 elements by its predictive skill.

A measure for the statistical significance of the agreement between both models is the probability P that a randomly generated sequence $[n_{\Phi_1}, ..., n_{\Phi_{19}}]$ agrees in at least the same number of element (i.e. in 17, 18, or 19 out of 19) with the sequence $[n]_{CLIMBER}$. Assuming that n_{Φ_i} can take 17 possible values (0-16), that each of these value has the same probability (1/17), and that the values n_{Φ_i} (i = 1-19) are independent of each other, this probability can be deduced from the binomial distribution:

$$P(n) = \binom{N}{n} p^n (1-p)^{N-n} \tag{9.20}$$

with N=19 and p=1/17. P is given by P(17)+P(18)+P(19). From equation (9.20) it follows that P is of the order of 10^{-19}. This means that the agreement between both models is extremely good, and that it is virtually impossible that this agreement is only by chance.

9.3.2 Variations of the forcing frequencies

In the previous chapter, it was shown that a synchronous change of the two forcing frequencies ω_1 and ω_2 over some range, corresponding to a scaling of the time axis of the forcing, leads to a scaling of the period in the output of CLIMBER-2. This scaling was found to be linear within certain frequency-ranges (figure 8.4). Very similar results are found for the output of the conceptual model. In this analysis, vanishing forcing phases ϕ_1 and ϕ_2 are considered ($\phi_1 = \phi_2 = 0$), and the two forcing amplitudes are taken to be equal ($A_1 = A_2 = 10$ mSv). Similar to the response of the climate model, various intervals for the forcing frequencies ω_1 and ω_2 exist in which the period in the model response is linearly scaled when the frequencies are changed (figure 9.6). The piecewise linearity implies that a roughly

1470-year period in the output of the conceptual model is still obtained when both forcing frequencies are simultaneously changed over some range.

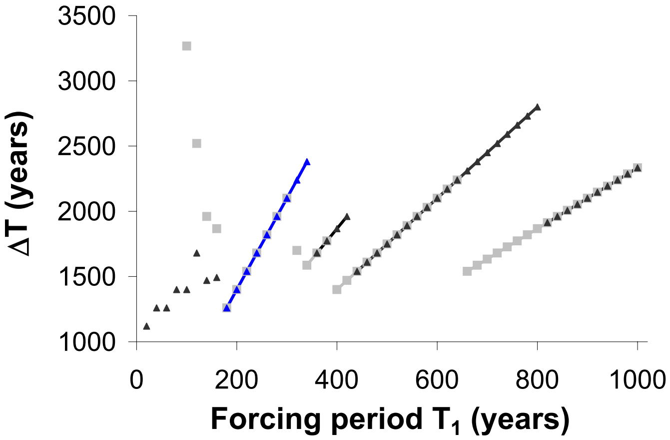

Figure 9.6: Spacing of successive warm events, as a function of T_1. The figure shows the spacing ΔT between successive warming events in the model output, as a function of the first forcing period T_1 (with T_1 ranging from 20 years to 1000 years). The forcing period T_2 is synchronously changed with T_1 ($T_2 = 7/17 \cdot T_1$). In certain ranges (as shown in blue, for example), linear relations exist between the spacing of the events in the model response and the period of the forcing. The black and blue curves show the output of the conceptual model. The grey curve illustrates the output of the climate model CLIMBER-2, as given in figure 8.4.

While the agreement between both models is fairly good for longer forcing cycles (i.e. for larger periods), an important mismatch exist when shorter (decadal-scale) cycles are used: In this case, DO-like events with a spacing of 1000-1500 years are still obtained in the conceptual model. But in the climate model, the spacing between successive events is much larger. Moreover, for very short forcing cycles, oscillations between both climate states do not occur anymore in CLIMBER-2. The reason for this mismatch is that in order to trigger switches between both states of the conceptual model, the thresholds need to be crossed only during an infinitesimal short time-interval. But in the climate model, the thresholds must be crossed over a time-interval of finite length, which is certainly more realistic. This means that the effect of shorter forcing cycles is damped in that model, and consequently larger forcing amplitudes must be used in order to trigger oscillations between both climate states. This damping is illustrated in figure 9.7.

As can be seen in the figure, for each period T_1 a value A_{crit} for the forcing amplitude exists which marks the beginning of the DO regime in CLIMBER-2 (this

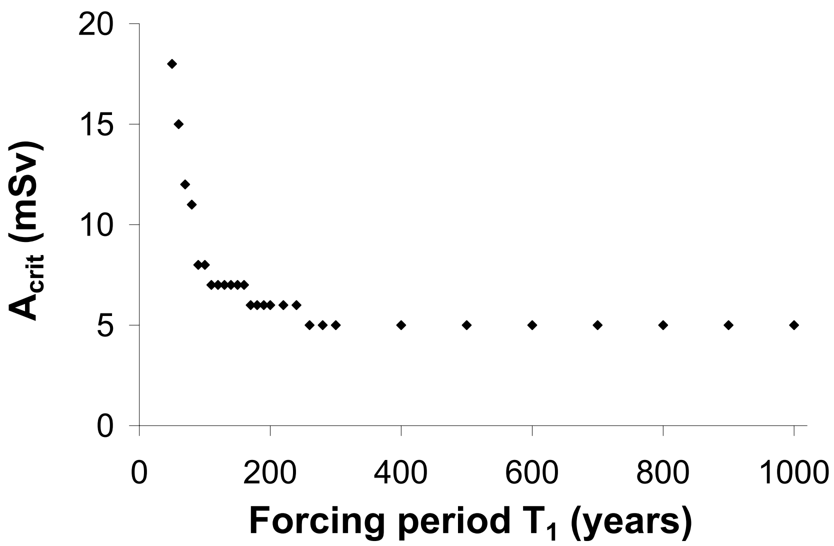

Figure 9.7: Damping of short forcing cycles in CLIMBER-2.
This figure illustrates the location of the DO regime in the period-amplitude space of CLIMBER-2: For a given period T_1 (with $T_2 = 7/17 \cdot T_1$), switches between both model states are triggered if the forcing amplitude A is larger than a critical value $A_{crit}(T_1)$. A_{crit} is indicated by the black diamonds. For smaller amplitudes, the model ends up in a stable mode. See text for discussion.

means that repeated oscillations between both THC modes occur for $A > A_{crit}$). A_{crit} depends on the forcing period: For $T_1 \geq 260$ years, oscillations between both THC modes in CLIMBER-2 can already be excited with a forcing amplitude $A \geq 5$ mSv (this means that 4 mSv $\leq A_{crit} < 5$ mSv). But for $T_1 = 60$ years, for example, oscillations do not yet occur for $A = 14$ mSv (i.e. 14 mSv $\leq A_{crit} < 15$ mSv). In the conceptual model $A_{crit} = 1/2 \cdot \max[T_{W\to C}(t = \infty), |T_{C\to W}(t = \infty)|]$ holds. When $T_{W\to C}(t = \infty)$ and $T_{C\to W}(t = \infty)$ are assumed to be independent of the forcing periods T_1 and T_2, A_{crit} is thus also independent of T_1 and T_2, and consequently damping of short forcing cycles does not exists in the conceptual model.

Both models also agree fairly well when only one forcing period is modified (with the second period being fixed at either 1470/7 years of 1470/17 years). This can be seen by a comparison of figure 8.5 (panels d and e) with figure 9.8. The figure shows that within a large range of forcing frequencies, the spacing between successive events in the conceptual model is not far from 1470 years, similar to the output of CLIMBER-2. The spacing is typically larger than 1470 years for forcing amplitudes $A = 10$ mSv and smaller than 1470 years for $A = 11$ mSv, in agreement with the results of the climate model. Moreover, the conceptual model reproduces the mean spacing between successive warming events, as simulated by CLIMBER-2,

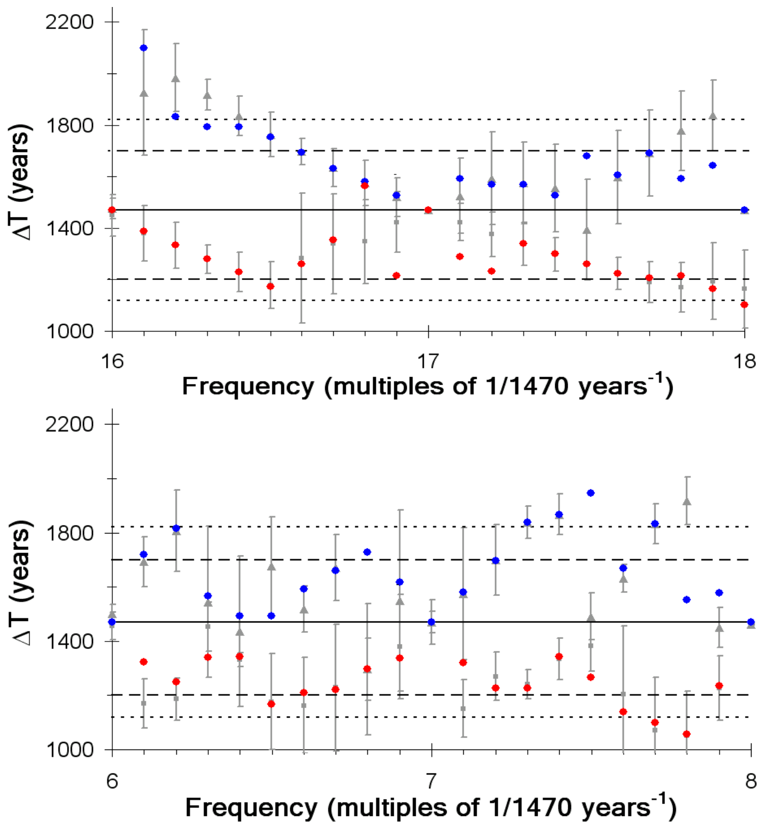

Figure 9.8: Model output for changes in only one forcing frequency
Shown is the mean value of the spacing ΔT between successive switches from the cold to the warm state of the conceptual model for: $T_1 = 1470/7$ years, T_2 ranging from 1470/16 (≈ 92) to 1470/18 (≈ 82) years (upper panel); T_1 ranging from 1470/6 (≈ 245) to 1470/8 (≈ 184) years, $T_2 = 1470/17$ years (lower panel). Blue: $A_1 = A_2 = 10$ mSv. Red: $A_1 = A_2 = 11$ mSv. Grey curves correspond to the model output of CLIMBER-2 (see figure 8.5). The dashed lines represent ΔT = 1200 years and ΔT = 1700 years. The dotted lines represent ΔT = 1470 years ± 350 years. The solid line indicates ΔT = 1470 years. See also figure 8.5.

for many values of the forcing frequencies. In some cases (for example in the upper panel at frequency-values of 16.9/1470 years^{-1}, 17.1/1470 years^{-1} and 17.2/1470 years^{-1}), however, mismatches between both models outputs exist. To some degree, these mismatches might be reduced by a fine-tuning of the conceptual model, for instance by a slightly different choice of the model parameters $T_{W\to C}(t = 0)$ and $T_{C\to W}(t = 0)$. This, however, is beyond the scope of this thesis. Note that the mean spacing of the warming events, as simulated with the conceptual model, is typically within the ranges given by the dashed and dotted lines in figure 9.8. This means that the spacing is consistent with the observed deviations of the DO events, as inferred from Greenland ice-core data (compare figure 8.5 and the discussion of that figure). Thus, the simulated 1470-year cycle in the response of the conceptual model to the forcing is also fairly robust with respect to changes in each of the two forcing frequencies.

9.3.3 Variations of the forcing amplitudes

The stability of the simulated 1470-year cycle with respect to changes of the forcing amplitude A (with $A = A_1 = A_2$) was already shown in the phase-space diagram of the conceptual model, figure 9.3. Now, the robustness of the 1470-year cycle is investigated with respect to changes in the ratio A_1/A_2 of the two forcing amplitudes (with $A_1 + A_2 = 20$ mSv). The phases ϕ_1 and ϕ_2 are set to zero. The forcing periods are chosen to be $T_1 = 1470/7$ years and $\mathrm{T}_2 = 1470/17$ years. Figure 9.9 shows the period in the output of the conceptual model as a function of A_1.

As long as both cycles are present in the forcing (i.e. in the case of $A_1 \neq 0$ mSv and $A_1 \neq 20$ mSv), the response of the conceptual model exhibits a 1470-year cycle. When only the 86.5-year forcing cycle is considered (in the case of $A_1 = 0$ mSv), the switches to the warm state occur with a period of 13/17·1470 years (≈1124 years). With only the 210-year cycle (in the case of $A_1 = 20$ mSv), the model response has a period of 6/7·1470 years (≈1260 years). For all other values, the period is 1470 years. The robustness of this 1470-year cycle is thus comparable with the stability of the 1470-year cycle in the climate system model CLIMBER-2 (figure 8.6). Note that both models disagree in the period of the model response for $A_1 = 0$ mSv and $A_1 = 20$ mSv: For $A_1 = 20$ mSv, the period in the response of the climate model is only 5/7·1470 years = 1050 years (i.e. the period is shorter in that model), compare panel b in figure 8.6. And for $A_1 = 0$ mSv, no distinct period exists in the output of CLIMBER-2. Instead, the spacing of the simulated DO events can take various discrete values, namely integers of 1470/17 years: 15/17·1470 years, 16/17·1470 years, 17/17·1470 years and 18/17·1470 years (see the blue curve in panel a of figure 8.6). This means that for $A_1 = 0$ mSv, the spacing between successive events in the climate model is larger than in the conceptual model.

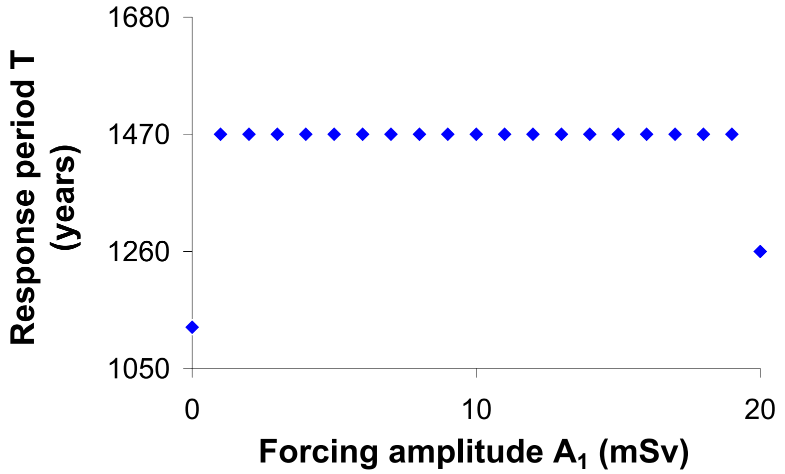

Figure 9.9: Period in the model output for different ratios A_1/A_2. The figure shows the period in the response of the conceptual model (i.e. the spacing between successive warming events) as a function of the forcing amplitude A_1 (with A_2 = 20 mSv - A_1). See text for discussion.

This effect is probably due to the damping of shorter forcing cycles in the climate model (compare section 9.3.2): It was shown above that switches between both THC modes are more difficult to trigger by a decadal-scale forcing. It is thus not surprising that the response of the climate model to a 86.5-year cycle is somewhat slower than the one of the conceptual model. For the same reason, it is also plausible that the response of CLIMBER-2 to a 210-year cycle is somewhat faster than the one of the conceptual model. In addition to that, the lack of any intrinsic variability in the conceptual model can explain why the response of that model to a 86.5-year cycle shows a very distinct period, whereas various discrete values are found for the spacing of the simulated events in the climate model: Because of the intrinsic variability in CLIMBER-2, the salinity changes in the North Atlantic region are not strictly periodic, even when a periodic anomaly of the freshwater fluxes is prescribed. When a sufficiently short forcing cycle is considered, it is thus possible that a shift of the THC mode in CLIMBER-2 can sometimes be triggered slightly earlier than usual (i.e. one forcing peak earlier than under normal conditions) and sometimes slightly later (i.e. one forcing peak later than under normal conditions). Since internal variability does not exist in the conceptual model, the simulated events in that model are perfectly regular. In any case, both models agree in that the simulated 1470-year climate cycle is very robust when the ratio of the forcing amplitudes A_1 and A_2 is changed over a large range.

9.3.4 Non-sinusoidal forcing cycles

It was shown in the previous chapter that the simulation of a 1470-year climate cycle in the model CLIMBER-2 does not require sinusoidal forcing cycles (compare section 8.3). Instead, a non-sinusoidal profile of the applied freshwater cycles can also give a very regular 1470-year cycle in the output of that model. Given the dynamics of the switches between the two modes of the THC this is not surprising:

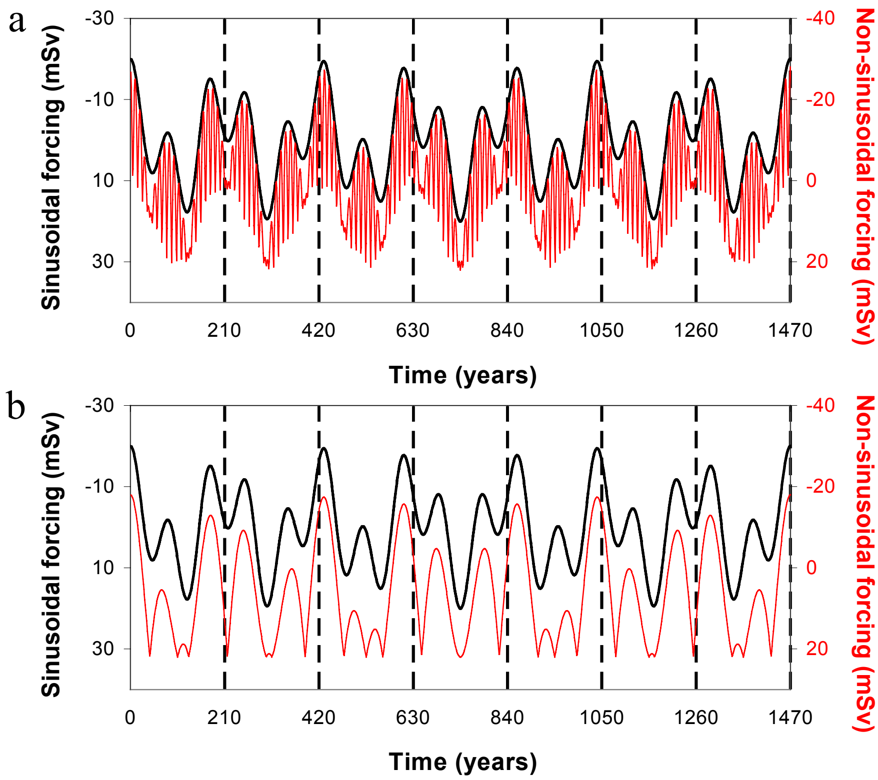

Figure 9.10: Considered sinusoidal and non-sinusoidal forcing profiles
Shown is the comparison between the sinusoidal forcing (black), as used in chapter 7 (see figure 7.1) and the non-sinusoidal ones (red), as applied in the previous chapter (figure 8.9). The non-sinusoidal curve in panel a corresponds to the case in panel a of figure 8.9, and the non-sinusoidal curve in panel b to the one in panel b of that figure. Note that for convenience, the freshwater axis for the non-sinusoidal profiles is shifted by 10 mSv compared to the one for the sinusoidal profiles. Compared with the profiles used in chapter 8, a constant freshwater offset of 17 mSv is added to all curves (so that the time-average of the black curve is 0 mSv instead of -17 mSv).

Since the abrupt warming events are caused by negative peaks in the forcing (i.e. by negative freshwater anomalies), and since the general structure of these peaks is very similar for the considered sinusoidal and non-sinusoidal forcing types (figure 9.10), the warming events are indeed expected to occur at the same peaks in the forcing, no matter which forcing type is used. It thus comes out as no surprise that the considered non-sinusoidal forcing types can also produce a glacial 1470-year cycle in the output of CLIMBER-2.

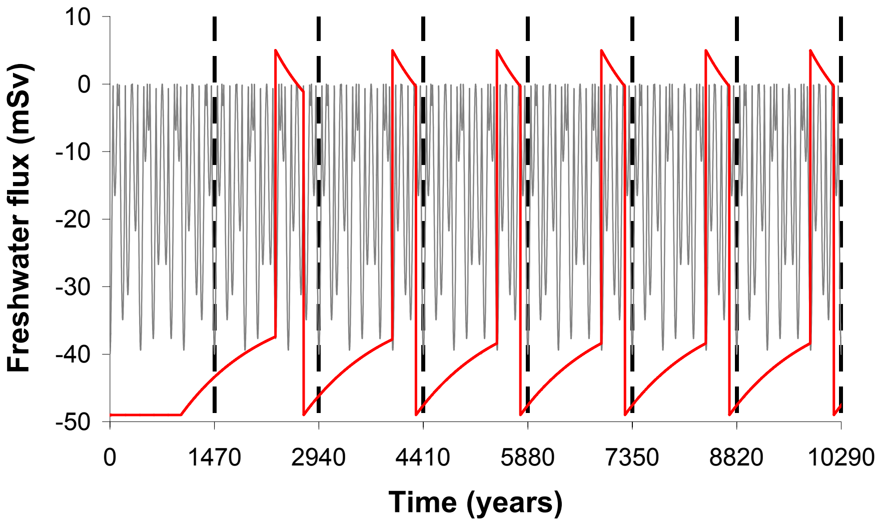

Figure 9.11: Response of the conceptual model to a non-sinusoidal forcing Shown is the response of the model (red) to the non-sinusoidal forcing type as illustrated in panel b of figure 9.10 (given by equation 8.11). The forcing (grey) consists of a 86.5-year cycle, which is amplitude-modulated by a 210-year cycle. Note that the freshwater axis is inverted compared with figure 9.10 and that the freshwater offset has been converted into the model thresholds according to the relations 9.5.

Since a damping of high forcing frequencies exists in the climate model, but not in the conceptual model (compare 9.3.2), it is questionable if the latter model can give a realistic response to the non-sinusoidal forcing type as shown in panel a of figure 9.10. In that forcing type (*Gleissberg cycle implemented as amplitude-modulation of the Schwabe cycle*) a decadal-scale oscillation is included, and this oscillation is probably to fast to be realistically represented in the conceptual model. But the second forcing type (*DeVries cycle implemented as amplitude-modulation of the Gleissberg cycle*), as shown in panel b of that figure, is of the same time scale as the sinusoidal forcing. The effect of this cycle should therefore be more realistically represented in the conceptual model. Figure 9.11 shows the response of the conceptual model to this forcing type[12]. As can be seen from that figure, the period in the response of the model is also 1470 years. This means that in the conceptual model, a 1470-year cycle can also be triggered by non-sinusoidal forcing cycles, in agreement with the results that were already obtained with CLIMBER-2.

9.3.5 Noise in the forcing

In the previous chapter, it was shown that a fairly regular 1470-year cycle of abrupt warming events can still be obtained in CLIMBER-2 when noise is incorporated in the forcing (see section 8.2). In order to simulate a 1470-year cycle in the presence of noise, it was shown to be possible to reduce the amplitude of both forcing cycles substantially. This means that noise, in a way, acts as an amplifier. In the context of the conceptual model, this amplification is not surprising: When the forcing consists of two components, a random component and a periodic one, the model threshold can be crossed by the total forcing (i.e. by the sum of both components), although the periodic component alone is too small to cross the threshold. Moreover, since the total forcing is more likely to cross the threshold during the peaks of the periodic component, the simulated switches in the THC can still be rather regular, despite the presence of noise. It is thus a direct consequence of the threshold behaviour that in the presence of noise, fairly regular events can be triggered by a smaller periodic forcing.

Note that a realistic representation of white noise is difficult to achieve in the conceptual model, since white noise also contains a lot of variablity in the high-frequency range. But these spectral components in the forcing are not damped in the conceptual model, in contrast to CLIMBER-2 (compare 9.3.2). This means that the conceptual model probably shows an unrealistically high sensitivity to white noise.

9.3.6 Summary of the model analysis

To summarise, a very simple conceptual model of DO events was presented in this chapter. This model is based on two plausible assumption, namely on a high degree of non-linearity of these climatic shifts, and on the existence of a characteristic time scale of the order of 1000 years. In response to the century-scale freshwater forcing, the conceptual model showed abrupt shifts between two climate states (labelled *cold* and *warm*), which evolve on the millennial time scale. Within a large area of the forcing parameter-space, these shifts occur with a period of 1470 years. It was shown that the conceptual model reproduces many features of the response of CLIMBER-2 to the forcing, for example the robustness of the simulated 1470-year cycle with respect to changes of the forcing parameters (phases, frequencies

[12] The threshold parameters are chosen according to equation 9.10, with K = 5 mSv.

and amplitudes). The similarities between both models suggest that the response of CLIMBER-2 is a result of the high degree of non-linearity that is inherent in the transitions between the two modes of the THC, and of the long characteristic timescale of the THC, which prevents a faster (i.e. a century-scale) model response.

Other concepts which might be suggested to explain the response of the climate model would show much more disagreement. For example, if the simulated 1470-year climate cycle resulted solely from the existence of such a climate mode in the model, the amplitude-dependence of the period in the model response would remain unexplained (figure 7.8). Similarly, the concept of a harmonic oscillation is not applicable since the response of such oscillators shows the same spectral components as the forcing, due to the linearity of the processes. The response of CLIMBER-2, however, is shifted in the frequency space compared to the forcing. The conceptual model, on the other hand, is able to reproduce these features of the output of the climate model. The overall agreement between both models strongly suggests that the robust 1470-year cycle in the output of CLIMBER-2 is physically plausible (and not a model artefact, for example).

Given the extreme simplicity of the conceptual model, the detailed agreement between both models is astonishing. The main reason for this agreement is the focus on the time scale of the simulated climate shifts. This time scale is determined by the slowest of all relevant processes, i.e. by the millennial-scale build-up of a large-scale instability in the THC. In order to obtain a detailed agreement between both model outputs, the conceptual model therefore needs to account only for the dynamics of the THC, i.e. for its threshold behaviour and for its characteristic time scale. Were the model designed to mimic the spatial pattern or the magnitude of the signature of DO events in the atmosphere, atmosphere-ocean-ice interactions would also need to be included in the conceptual model. A realistic representation of these interactions, however, is probably impossible to achieve in such a simple model. But since here the focus is only on the time scale of the climate response, such processes do not explicitly need to be considered to mimic the response of CLIMBER-2. In any case, the agreement between both models shows that the conceptual model can provide a very useful tool to interpret the dynamics of CLIMBER-2, which itself is already too complex to give a definite answer to the question why the simulated DO events show a 1470-year time scale when the model is forced by century-scale cycles.

10 Summary, interpretation, discussion

In this chapter, the results that were obtained in the previous chapters are interpreted. Based on these results, the strengths and weaknesses of the new hypothesis are discussed. At the end of the chapter a very short outlook for future work is given.

10.1 Summary and interpretation

10.1.1 A new hypothesis for the glacial 1470-year climate cycle

In chapter 6, a new hypothesis was presented in order to explain the glacial 1470-year quasi-cycle, which is apparently inherent in the Dansgaard-Oeschger (DO) events. According to this hypothesis, the 1470-year climate cycle in the North Atlantic region could result from the combined effect of two pronounced solar cycles, with periods of about 210 years and 87 years.

10.1.2 First tests of the hypothesis with a climate model

In chapter 7, a first test of this hypothesis was performed with the coupled model CLIMBER-2, a climate system model of intermediate complexity. This model is the most suitable tool for the analysis: First, fairly realistic DO events have already been simulated with this model[16, 24, 40, 41]. Second, more detailed general circulation models (GCMs) are not applicable for such tests, since they require far too much computational time.

In the test, it was shown that for boundary conditions of the Last Glacial Maximum, abrupt shifts between two different modes of the Atlantic thermohaline circulation can be triggered by a century-scale perturbation of the freshwater fluxes to the North Atlantic. These shifts manifest themselves as abrupt warming events in the North Atlantic region which reproduce many features of the observed DO events, in particular the characteristic progression of Greenland temperature in the course of the events, the phase relation of the Antarctic temperature changes, and the global response to the events[16]. It was shown that when the two century-scale solar cycles are implemented as a freshwater anomaly in the North Atlantic, the simulated DO events occur on the millennial time scale. For many choices of the forcing parameters the events show a regular spacing of 1470 years or integer multiples of that value. It was also demonstrated that similar temperature shifts do not occur in the model for modern (pre-industrial) boundary conditions, since the THC is more stable in the Holocene than in the last glacial. The modern preindustrial response to the forcing is therefore much smaller and far more linear. This means that it exhibits spectral contributions which are very similar to the ones in the forcing, i.e. pronounced components with periods of 210 years and about 86.5 years. These spectral components were indeed found in a couple of climate records[2, 55, 56]. A spectral component corresponding to a 1470-year period, however, is not present in the modern preindustrial model response, in agreement with many climate archives from the Holocene.

10.1.3 Stability of the simulated 1470-year climate cycle

In the second part of the tests with CLIMBER-2, the stability of this 1470-year cycle was investigated (chapter 8). For a sinusoidal implementation of the two forcing cycles it was shown that, as expected, the 1470-year climate cycle in the glacial model output is insensitive to changes in the phase relation of the forcing cycles: A shift in the phase of any of the two forcing cycles only results in a phase-shift of the 1470-year climate cycle, but not in a modification of its period.

A simultaneous shift of the two forcing frequencies over some range, corresponding to a scaling of the forcing's time-axis, results in a likewise shift of the period in the model output, corresponding to a scaling of the model's time-axis. A very regular climate cycle with a period of about 1500 years can thus still be obtained when both forcing frequencies are shifted in the frequency-range, provided that their ratio remains the same. It was further demonstrated in chapter 8 that the simulated DO events still show a time scale of about 1500 years (i.e. a spacing of typically 1100-1800 years) when each one of the two forcing periods is varied over a range of decades, while the second cycle is fixed. This shows that the periods of both forcing cycles can be modified over a large range without losing the about 1470-year quasi-period in the model output.

Moreover, the simulated 1470-year climate cycle in the output of CLIMBER-2 was found to be almost insensitive to changes in the ratio of the two forcing-amplitudes, provided that the sum of these amplitudes is fixed (chapter 8). When the sum of both amplitudes is varied, but their ratio is fixed, the simulated events exhibit a spacing that is typically 1470 years or integer multiples thereof, with possible deviations of about 500 years (figure 7.9). The tendency of the events to occur at multiples of 1470 years agrees well with the spacing of the observed DO events, as deduced from Greenland ice-cores[23, 31, 32].

For the validity of the hypothesis it is important that the simulated 1470-year climate cycle is robust with respect to changes of the forcing parameters: Proxies of solar activity suggest that the solar cycles have variable amplitudes, for example. If the glacial 1470-year climate cycle only occurred within a narrow range of forcing-amplitudes, the probable variability of the solar cycles would thus argue against the hypothesis. But since the 1470-year cycle in the model output occurs within a fairly large range of forcing parameters, a 1470-year quasi-cycle could still be present in the model response, even when realistic changes in the amplitudes, periods, and phases of the two solar cycles were considered in the forcing[1].

In chapter 8, it was also shown that noise, when incorporated in the forcing, acts as an amplifier: With noise, DO-like warming events in the North Atlantic region, which show a fairly regular time scale of 1470 years, can be triggered by a much smaller periodic forcing. This means that the existence of short-term natural climate variability in the "real" climate system does not argue against the hypothesis. Instead, noise could help to generate a 1470-year climate cycle in response to an even smaller forcing signal.

In the last part of the stability analysis that was performed in chapter 8, the response of CLIMBER-2 to two forcing types was investigated in which non-sinusoidal freshwater cycles were considered. It was shown that a glacial 1470-year climate cycle can also be simulated with CLIMBER-2 when non-sinusoidal profiles of the two freshwater cycles are used. This is important because the known solar cycles are not sinusoidal: In the Fourier spectrum of a sum of sinusoidal cycles, a single spectral peak occurs for each cycle. But in the case of non-sinusoidal cycles, a larger number of spectral peaks exists in the frequency domain (corresponding to harmonics and overtones). And since the Fourier spectra as calculated from proxies of solar activity indeed show sharp and pronounced peaks at frequencies close to harmonics and overtones of the roughly 210-year and 87-year solar cycles[49], it is very likely that the two solar cycles manifest themselves in a complex, non-sinusoidal way. It is therefore very important for the validity of the hypothesis that a glacial 1470-year climate cycle in CLIMBER-2 can still be obtained in response to non-sinusoidal forcing types. It was further demonstrated in chapter 8 that a glacial 1470-year climate cycle can also be simulated when the 86.5-year forcing cycle is considered to be the amplitude-modulation of an additional 11-year cycle. This is also essential for the hypothesis, since the 87-year Gleissberg cycle manifests itself in the solar data as an amplitude-modulation of the 11-year Schwabe cycle.

10.1.4 Plausibility of the simulated 1470-year climate cycle

The investigations with the CLIMBER-2 showed that in this model, DO-like abrupt warming events with a robust time scale of 1470 years can be obtained in response

[1] Up to now, a reconstruction of solar variability in the last glacial does not exist.

to a century-scale perturbation of the freshwater fluxes to the North Atlantic, with periods close to that observed in proxies of solar activity. Due to the complexity of this model, however, it is difficult to identify the reasons for the stability of the simulated climate cycle. In order to understand why the 1470-year climate cycle is so stable in the output of CLIMBER-2, it is more promising to construct a very simple conceptual model, which only accounts for the processes in the climate model that are thought to be responsible for the existence of this 1470-year cycle.

The conceptual model that was presented in chapter 9 is based on three assumptions:

- the existence of two different climate states, corresponding to the two states of the THC in CLIMBER-2.
- a high degree of non-linearity of the switches between these two climate states
- the existence of a characteristic time scale of the order of 1000 years (representing the relaxation time of the THC with respect to a large-scale anomaly in the density field of the North Atlantic)

Due to its simplicity, this model is more suitable for the interpretation of causal relationships between the forcing and the model response than the coupled climate model itself.

The conceptual model was validated against CLIMBER-2 by comparing the response of both models to the same forcing, for many variations in the forcing parameters. It was shown that in both models, a robust 1470-year climate cycle is triggered by the century-scale forcing. Both models agree very well in the stability properties of this 1470-year climate cycle with respect to changes of the forcing parameters. The good agreement between both models strongly suggests that the conceptual model successfully captures the main features in the dynamics of the DO events, as simulated by CLIMBER-2. The main limitation of the conceptual model is that it has an unrealistically large response for high-frequency spectral components in the forcing. Therefore, the conceptual model cannot reproduce the response of the climate model for some forcing types (for example for a "noisy" forcing profile).

On the basis of the conceptual model, the glacial 1470-year climate response of CLIMBER-2 to the century-scale forcing can be understood as a consequence of the high degree of non-linearity of the DO-oscillations and of the large characteristic time scale of the THC. From the pattern of the DO events, as documented in Greenland ice-cores, both of these properties appear to be plausible: First, the threshold character of the switch from the "cold" mode of the THC into the "warm" one is consistent with the almost sudden warming which occurs at the very beginning of most DO events (see figure 2.2). If the transitions between both modes were linear, a more gradual temperature rise would be expected. Second, the assumption of a large characteristic time scale of the THC agrees with the gradual cooling trend over several centuries as seen in the course of the DO events in Greenland. In any case, no dubious ad-hoc assumptions are necessary to explain the occurrence of the glacial 1470-year period in the response of the climate model to the forcing.

Based on the formulation of the conceptual model and on its phase space diagram (figure 9.3), the oscillations between both states of this model were interpreted in the context of a bifurcation (see chapter 9). For forcing-amplitudes smaller than some critical value, at least one of the two model states is stable, and repeated oscillations between both states consequently do not occur. For larger amplitudes, oscillations between both states are possible. A very similar pattern is found in the phase space diagram of CLIMBER-2 (figure 7.9). The similarities between both models strongly suggest that the DO events in CLIMBER-2 also result from the existence of a bifurcation, and that this bifurcation is due to the threshold behaviour of the switches between the two modes of the THC.

The similarities in the response of CLIMBER-2 and the conceptual model permit to anticipate what kind of output would occur in CLIMBER-2 if this model was not so close to the bifurcation point of the THC[2]: From the dynamics of the conceptual model it is clear that a scaling of the two thresholds, i.e. a multiplication of the four threshold parameters $\mathrm{T}_{W\to C}(t=0)$, $\mathrm{T}_{C\to W}(t=0)$, $\mathrm{T}_{W\to C}(t=\infty)$ and $\mathrm{T}_{C\to W}(t=\infty)$ (compare equations [9.1, 9.2]) by a factor λ, leads to exactly the same output, provided that the forcing is also scaled by this factor. If CLIMBER-2 were less close to the bifurcation point in the THC, it is therefore very likely that a robust 1470-year climate cycle would still result from the applied freshwater forcing. In this case, however, a stronger forcing would be required in order to excite the resonance in the THC that is inherent in the simulated DO events.

Although the conceptual model is highly simplified, it can reproduce many characteristic features in the response of the far more complex model CLIMBER-2 to the forcing. The conceptual model is therefore a very useful tool to interpret the output of CLIMBER-2 and to demonstrate the plausibility of the hypothesis that was proposed here.

10.2 Discussion of the new hypothesis

In this section, the main strengths and weaknesses of the new hypothesis to explain the glacial 1470-year climate cycle are discussed. The hypothesis is also compared with other hypotheses, which were already suggested in order to explain the occurrence or the time scale of the DO events.

[2]The precise location of a bifurcation point can be very different in different models and is not necessarily correct in any model.

10.2.1 Arguments in favour of the hypothesis

The hypothesis has a number of strengths compared with other possible explanations for the DO events:

1. **Successful testing of the hypothesis**

   One of the most important strengths of the hypothesis is that, unlike many other hypotheses, it has been successfully tested with a model which is most appropriate for the test: Most other hypotheses have either been tested only by more simplified models (by coupled energy balance models[19], for example, which do not explicitly account for the dynamics in the atmospheric circulation), by extremely simplified conceptual models[25], or they have not been tested at all[20, 22, 26]. The fact that it is possible to obtain a glacial 1470-year cycle of DO-like warming events in a test of this hypothesis, using an Earth system model of intermediate complexity, is thus an important support for the viability of the hypothesis, in particular because more complex models (general circulation models, for example) require far too much computation time for a test of the hypothesis with these models.

2. **Explanation of the regularity of the glacial 1470-year climate cycle**

   Another important strength of the hypothesis is that it can explain the existence of the 1470-year spectral peak in time series of Greenland paleotemperature[2]. Furthermore, it also provides an explanation for the tendency of the DO events to occur at multiples of 1470 years[31, 32]. The validity of the hypothesis therefore does not require that the apparent regularity of the DO events is only due to errors in the ice-core data (for example in the chronology) or in the spectral analysis methods. Many other hypotheses (for example the ones described in [18, 19, 20, 22, 26]) have difficulties in explaining the regularity of the 1470-year time scale of DO events, or they simply postulate the existence of a 1/1470-year^{-1} forcing frequency [21, 23, 24].

3. **Holocene response**

   For modern preindustrial boundary conditions, the ocean circulation in the climate model is more stable than the glacial one. Therefore, no shifts in the THC are triggered by the forcing. The hypothesis can thus explain why DO-like events do not occur in the Holocene. Moreover, since the hypothesis relates the glacial 1470-year climate cycle to forcing cycles of 210 years and about 87 years, it also explains why a 1470-year climate cycle is detected in the last ice-age, but not in the Holocene[2]. Were the events triggered by a forcing with a frequency of 1/1470 years^{-1}, as suggested in a couple of hypotheses[21, 23, 24], then at least a small signature of this cycle would also be expected to be present in the Holocene[3]. But according to the hypothesis that was presented here, climate archives from the Holocene would be expected to exhibit pronounced spectral components corresponding to periods of 210 years and about 87 years. Similar spectral peaks were indeed detected in a number of climatic time-series[2, 55, 56].

4. **Climate cycle related to pronounced and well-known forcing cycles**

   A couple of earlier hypotheses related the glacial 1470-year climate cycle to forcing cycles of secondary importance[22, 26]. The existence of forcing cycles with a potentially much higher relevance thus argues against these hypotheses: Were the DO events triggered by secondary cycles, it also needs to be explained why the dominant forcing cycles do not cause similar events. The hypothesis that was suggested here, however, relates the 1470-year climate cycle to the most pronounced[4] spectral components in time series of solar activity, corresponding to the best known solar cycles. And since solar variability is commonly considered to be the dominant external influence on the centennial-to-millennial scale, the considered solar cycles are probably the most important of all forcing cycles on the relevant time scale. This means that in the context of this hypothesis, the glacial 1470-year climate cycle is linked to the major driver of natural climate variability.

   Moreover, in the context of this hypothesis, only a small trigger is required in order to explain the occurrence of DO events. This is a consequence of the physical mechanism which is inherent in the events as simulated with CLIMBER-2: In this model, DO events represent switches between two modes of the glacial THC. The main difference between these two modes is a latitudinal shift in North Atlantic deep water formation, which can be triggered by a much smaller perturbation than a complete shutdown of the THC, for example. This means that a realistic (i.e. small) change in solar activity over the known solar cycles might indeed be sufficient to explain the occurrence of DO events.

[3] Note that the multi-centennial drift-ice cycle in the North Atlantic[28] has often been considered as a climatic signature of a yet unidentified 1470-year solar cycle. This drift-ice cycle, however, was shown to coincide with “rapid (100- to 200-year) conspicuously large-amplitude variations” in proxies of solar variability[28]. Moreover, higher resolution data suggest that the drift-ice oscillations occur mainly on the time scale of 300-500 years, but not on the millennial scale[29]. The drift-ice cycle is thus not the Holocene signature of a yet unidentified 1470-year solar cycle.

[4] In chapter 8 it was shown that the 11-year solar cycle can also be integrated in the hypothesis.

5. **High stability of the results**

   A further strength of the hypothesis is that the simulated 1470-year climate cycle is stable with respect to changes of the forcing parameters. Moreover, the cycle occurs for many profiles of the forcing and does not require "tuning" of the climate model. This robustness suggests that the hypothesis not only works for the idealised forcing types that were considered in this thesis, but also for realistic forcing profiles[5]. In contrast to that, many hypotheses which relate the glacial 1470-year climate cycle to internal oscillations (atmosphere-ocean oscillations[19], for example) are less robust: Internal oscillations of the THC as a possible mechanism for DO events only occur in models for certain boundary conditions and for very special choices of the model parameters[11]. This means that such hypotheses are less likely to be valid, because the "real" climate system was probably not in the specific part of its "phase space" at the relevant time.

10.2.2 Possible arguments against the hypothesis

In the following, two possible arguments against the hypothesis are discussed:

1. **A missing forcing cycle?**

   In the stability analysis performed in chapter 8, it was shown that DO-like warming events with a spacing of 1470 years can still be simulated with CLIMBER-2 when three different freshwater cycles, with periods of roughly 11, 87 and 210 years, are used in the forcing. These periods are close to the ones of three known solar cycles, the so-called Schwabe, Gleissberg and De-Vries cycles. But another spectral peak in the ^{14}C time series, corresponding to a quasi-period of roughly 2200 years, was suggested to represent a fourth solar cycle, the so-called Hallstatt cycle[50] (compare chapter 4). This cycle was not yet considered in the analysis. If such a cycle were also used in the forcing, the forcing would not show a period of 1470 years anymore. It is therefore not very surprising that it is more difficult to obtain a 1470-year cycle in the output of the climate model when a 2200-year cycle is also included in the freshwater forcing. This means that the possible existence of a 2200-year solar cycle might be considered as an argument against a solar origin of the DO events.

   How good is this argument? Of course, the existence of this peak in the ^{14}C time series only argues against the hypothesis if this peak is indeed of solar

[5] It is not yet possible to prescribe a realistic profile of the solar cycles in the last glacial, since a reconstruction of solar activity at that time is not yet available.

origin. The solar origin of the ^{14}C-peaks corresponding to periods of about 11 years and 87 years is evident, since these cycles also manifest themselves in the sunspot data (compare chapter 4). A solar origin of the 210-year peak is also very likely, for example because pronounced minima in the solar records coincide with this cycle (compare chapter 4). But because of the short length of the sunspot time series, it is not possible to relate the 2200-year cycle in the ^{14}C time series to any features in the sunspot data. This means that the solar origin of this cycle is by itself questionable. Moreover, the persistence of the 2200-year cycle in the ^{14}C time series is also more hypothetic, since the well-dated Holocene part of this time series covers only about five periods of the cycle. It is therefore possible that the relevant spectral peak in the time series only occurs by chance in the Holocene, and that a similar peak does not exist in ^{14}C time series from the last ice-age.

What else might be the reason for the existence of a 2200-year peak in the ^{14}C time series, if not solar variability? Changes in the geomagnetic dipole moment, which are commonly considered to be of the order of millennia, could in principle account for this peak, because the ^{14}C concentration in the atmosphere is also affected by such changes. Millennial-scale variations in the carbon cycle, caused by changes in the climate system, might be another potential cause for the 2200-year quasi-cycle. And even if this cycle was indeed of solar origin, the hypothesis would not necessarily break down: If the 2200-year cycle manifested itself mainly as a cycle in the magnetic flux of the Sun, but not in the luminosity[6], the existence of this cycle would not argue against the hypothesis (unless changes in the magnetic flux of the Sun were the dominant channel for solar influence on the Earth's climate).

Moreover, even if the 2200-year peak in the ^{14}C time series corresponded to a 2200-year solar forcing cycle of only small amplitude, the hypothesis would still not collapse: When a 2205-year cycle of small amplitude is included in the forcing, it is still possible to obtain regular DO-like warming events in the output of CLIMBER-2, with a mean spacing of 1470 years (figure 10.1). The existence of a roughly 2200-year peak in the ^{14}C time series of the Holocene is thus not a definite argument against the hypothesis, even if this cycle was indeed manifested as a quasi-periodic variation in solar forcing.

[6] The atmospheric ^{14}C-concentration changes with the magnetic flux of the Sun, and not necessarily with the luminosity.

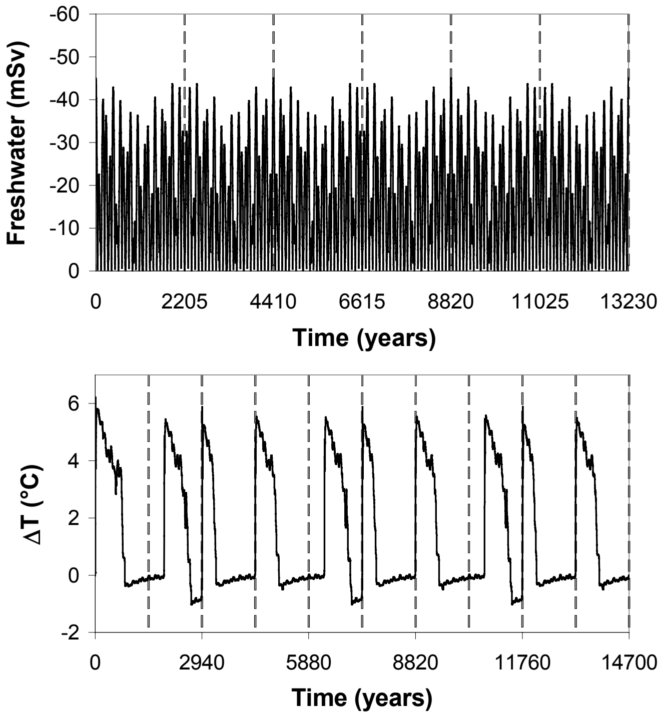

Figure 10.1: Forcing with an additional 2205-year freshwater cycle
The upper panel of the figure shows a forcing profile that contains three freshwater cycles: A 2205-year cycle, a 210-year cycle, and a 86.5-year cycle. The forcing is given by the following expression: F = $A_1 \cdot |\cos(\pi t/T_1) \cdot \cos(\pi t/T_2)| + A_2 \cdot |\cos(\pi t/T_2) \cdot \cos(\pi t/T_3)| + K$, with A_1 = -36 mSv, A_2 = -9 mSv, T_1 = 210 years, $T_2 \approx$ 86.5 years, T_3 = 2205 years and K = 10 mSv. The lower panel shows the model response. The dashed lines are spaced by 2205 years (upper panel) and 1470 years (lower panel), respectively.

2. **The missing link between freshwater anomalies and solar variability**

In the tests of the hypothesis, the 210-year and 87-year forcing cycles were considered as an anomaly in the freshwater flux to the North Atlantic (i.e. in the density field of the North Atlantic, because the density of water depends on its salinity). This means that the cycles were implemented in a climatic variable that is not directly related to changes in solar activity. This approach is highly simplified, since it assumes that the hydrological cycle responds to solar forcing in a way that it exhibits oscillations which are of the same frequency as the forcing. Although this is a rather plausible assumption, in particular because a couple of studies indeed suggest such a signature of the two solar cycles in the hydrological cycle[55, 56, 71], it would be more natural to implement the solar cycles as changes in solar irradiance, and to use a coupled model in order to simulate the response of the freshwater fluxes to these changes.

The main reason why solar variability was not directly included in the tests of the hypothesis is that the relevant processes are still very uncertain and/or by necessity not very well represented in climate models designed for millennial-scale simulations. In order to realistically simulate the solar imprint in the freshwater fluxes during the last ice-age, it is necessary to know the magnitude of the forcing, as well as the main channels for solar forcing upon climate. Until recently, changes in total solar irradiance were commonly regarded as the main channel for solar forcing, and these were considered to be of the order of 5 W/m^2 over the last centuries[61]. New studies, however, suggested that past variations in total solar irradiance might have been substantially smaller and other channels for solar influence on climate might thus be more important (see chapter 4). A more direct implementation of solar forcing in the model analysis is therefore very difficult and would also be highly speculative.

But even if the main channels for solar forcing upon climate were known, it would still be very unlikely that the response of the hydrological cycle to the forcing was realistically reproduced by the current version of the climate model CLIMBER-2: The main reason why the magnitude of the solar signature in the freshwater fluxes, as simulated with this version, is not correct is that the continental ice-sheets are fixed in the model. Therefore, no melting of continental ice can occur. Because of the large extent of the Northern hemisphere ice-sheets during the last glacial, however, it is likely that a solar-induced anomaly in the mass balance of these ice-sheets is one of the dominant channels for solar influence on the freshwater fluxes to that time. This means that a dynamical treatment of the continental ice-sheets is essential for more detailed tests of the hypothesis.

Preliminary simulations that were performed with the current version of the climate model CLIMBER-2 (with fixed ice-sheets) show that the occurrence of DO-like glacial warming events in the model does not require extremely large variations in total solar irradiance: DO events, with a fairly regular time scale of 1470 years, can already be triggered in the model by changes in total solar irradiance of the order of 7 W/m^2 (figure 10.2). In these simulations, changes in solar irradiance affect the freshwater fluxes to the North Atlantic by their influence on sea-ice: In times of higher irradiance (i.e. larger "solar constant"), the sea-ice extent in the model is somewhat reduced. Sea-ice, however, efficiently cools and insulates the ocean from the atmosphere. As a consequence, sea-ice strongly reduces local evaporation. The reduction in

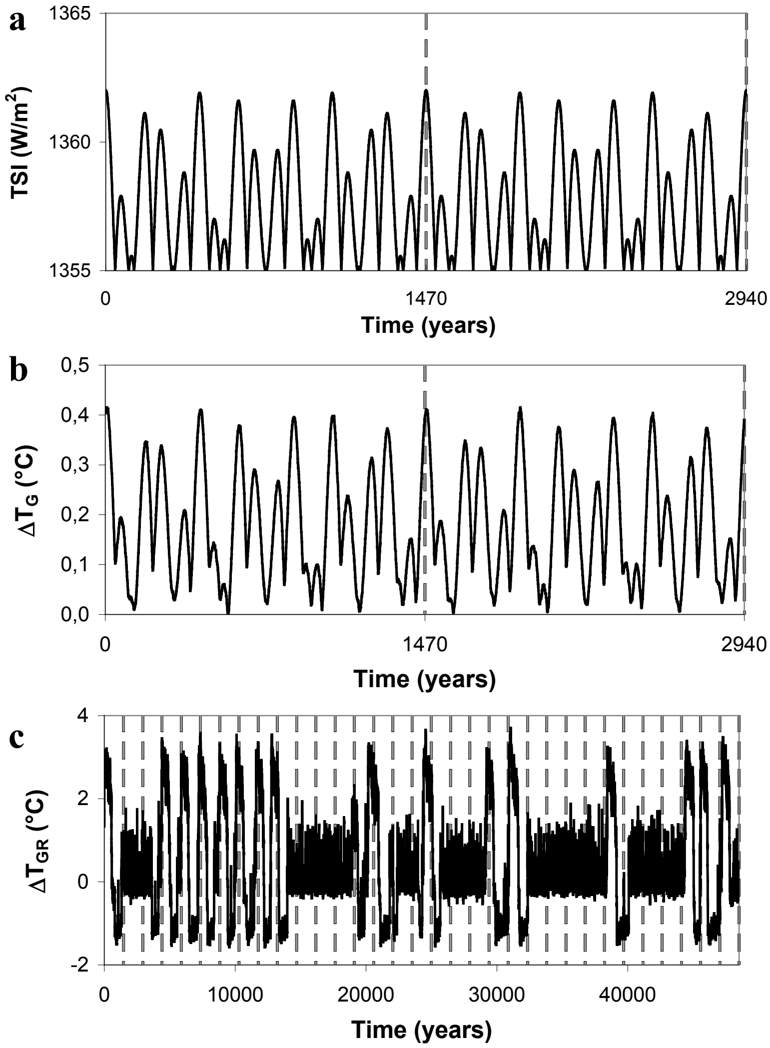

Figure 10.2: Model response to solar irradiance forcing

The upper panel shows a total solar irradiance (TSI) forcing profile, in which the 210-year cycle is the amplitude-modulation of a 86.5-year cycle. The forcing is given by the following expression for the "solar constant": $S_0 = A_1 \cdot |\cos(\pi t/T_1) \cdot \cos(\pi t/T_2)| + 1355\ W/m^2$, with $A_1 = 7\ W/m^2$, $T_1 = 210$ years, $T_2 \approx 86.5$ years (compare section 8.3). For the modern pre-industrial response (middle panel, shown is the anomaly ΔT_G in the global annual mean surface air temperature), no noise and no freshwater offset is used. For the LGM response (lower panel, shown is the anomaly ΔT_{GR} in Greenland annual mean surface air temperature), white noise with a standard deviation of 25 mSv is added to the freshwater fluxes to the North Atlantic, as well as an additional freshwater offset of -40 mSv. The dashed lines are spaced by 1470 years. The lower panel shows a continuous, about 50000-year segment of a longer (200000 years) model run.

the sea-ice extent in times of higher solar activity thus leads to a substantial increase in evaporation, as well as in the salinity and the density of the surface water in the North Atlantic. A sufficiently strong increase of the "solar constant" can thus trigger a switch from the "cold" mode to the "warm" mode of the THC. Similarly, a decrease of the "solar constant" can trigger a switch back into the "cold" mode of the THC.

As shown in figure 10.2, the spacing of the simulated DO events can again be close to integer multiples of 1470 years, although forcing cycles with periods of 210 years and 86.5 years are used. These results therefore suggest that fairly realistic DO events can also be simulated when instead of freshwater cycles, solar irradiance cycles are used in the model. It is interesting to note that the maximum amplitude of the solar signature in the pre-industrial model response (i.e. in the simulated global mean temperature) is only about 0.4 Kelvin. This value is not unrealistically large: It is well within the range of past temperature variations, as reconstructed on the basis of various paleo-climatic archives[72, 73]. Further tests of the hypothesis, however, should be performed with a coupled model that explicitly simulates the dynamics of the continental ice-sheets, as well as their interaction with the atmosphere and oceans. These tests will be performed in the near future, with a new version of CLIMBER-2.

To summarise, the new hypothesis passed all of the tests with CLIMBER-2, i.e. with a coupled climate system model of intermediate complexity. It was shown that the new hypothesis has a number of strengths compared with earlier hypotheses: Most of all, it can explain why a prominent 1470-year spectral peak is found in climatic time series from the last ice-age. The hypothesis can further explain the characteristic "waiting times" of the DO events. Moreover, it can also give a possible explanation for the lack of a 1470-year climate cycle in the Holocene. The model simulations showed that an accurate knowledge of the underlying dynamical processes is required in order to determine whether or not the glacial 1470-year climate cycle could have been caused by the Sun. In any case, the lack of a solar 1470-year cycle does not by itself argue against a solar origin of this climate cycle. Or, in the words of Sir Joseph Norman Lockyer, in order to discover the true nature of the connection between the Sun and the Earth, climatology must be regarded as a physical science and not as a mere collection of statistics. Accordingly, further tests are necessary in order to investigate by which process chains century-scale variations of solar activity can cause anomalies in the density field of the North Atlantic, which are sufficiently large to trigger DO events in the last glacial.

11 Bibliography

[1] Pantic, N. 1998. Kanon der Erdbestrahlungen und seine Anwendung auf das Eiszeitenproblem, New English Translation, Canon of Insolation and the Ice Age Problem. Alven Global.

[2] Grootes, P. M. and Stuiver, M. 1997. Oxygen 18/16 variability in Greenland snow and ice with 10^3 to 10^5-year time resolution. *Journal of Geophysical Research*, **102**, C12, 26455-26470.

[3] Johnsen, S., Dahl-Jensen, D., Dansgaard, W. and Gundestrup, N. 1995. Greenland palaeotemperatures derived from GRIP bore hole temperature and ice core isotope profiles. *Tellus*, **47B**, 624-629.

[4] Severinghaus, J. P. and Brook, E. 1999. Abrupt Climate Change at the End of the Last Glacial Period Inferred from Trapped Air in Polar Ice. *Science*, **286**, 930-934.

[5] Leuenberger, M., Schwander, J. and Johnsen, S. 1999. 16°C Rapid Temperature Variations in Central Greenland 70,000 Years Ago. Science, 286, 934-937.

[6] Voelker, A. H. L. and workshop participants. 2002. Global distribution of centennial-scale records for marine isotope state (MIS) 3:a database. *Quaternary Science Reviews*, **21**, 1185-1212.

[7] Bond, G., Broecker, W., Johnsen, S., McManus, J., Labeyrie, L., Jouzel, J. and Bonani, G. 1993. Correlations between climate records from North Atlantic sediments and Greenland ice. *Nature*, **365**, 143-147.

[8] Spötl, C. and Mangini, A. 2002. Stalagmite from the Austrian Alps reveals Dansgaard-Oeschger events during isotope stage 3: Implications for the absolute chronology of Greenland ice cores. *Earth and Planetary Science Letters*, **203**, 507-518.

[9] Blunier, T. and Brook, E. J. 2001. Timing of Millennial-Scale Climate Change in Antarctica and Greenland During the Last Glacial Period. *Science*, **291**, 109-112.

[10] Rahmstorf, S. 2000. The thermohaline ocean circulation - a system with dangerous thresholds? *Climatic Change*, **46**, 247-256.

[11] Stocker, T. F. 1998. The Seesaw Effect. *Science*, **282**, 61-62.

[12] Ganachaud, A. and Wunsch, C. 2000. Improved estimates of global ocean circulation, heat transport and mixing from hydrographic data. *Nature*, **408**, 453-457.

[13] Stommel, H. 1961. Thermohaline convection with two stable regimes of flow. *Tellus*, **13**, 224-230.

[14] Rahmstorf, S. 2002. Ocean circulation and climate during the past 120,000 years. *Nature*, **419**, 207-214.

[15] Sarnthein, M., Winn, K., Jung, S. J. A., Duplessy, J.C., Labeyrie, L., Erlenkeuser, H. and Ganssen, G. 1994. Changes in East Atlantic Deepwater Circulation over the Last 30,000 Years: Eight Time Slice Reconstructions. *Paleoceanography*, **9**, 209-267.

[16] Ganopolski, A. and Rahmstorf, S. 2001. Simulation of rapid glacial climate changes in a coupled climate model. *Nature*, **409**, 153-158.

[17] Yiou, P., Fuhrer, K., Meeker, L. D., Jouzel, J., Johnsen, S. and Mayewski, P. A. 1997. Paleoclimatic variability inferred from the spectral analysis of Greenland and Antarctic ice-core data. *Journal of Geophysical Research*, **102**, C12, 26441-26454.

[18] Broecker, W. S., Bond, G., Klas, M., Bonani, G. and Wolfli, W. 1990. A salt oscillator in the glacial Atlantic? 1. The concept. *Paleoceanography*, **5**, 469-477.

[19] Sakai, K. and Peltier, W. 1997. Dansgaard-Oeschger-Oscillations in a coupled atmosphere-ocean climate model. *Journal of Climate*, **10**, 949-970.

[20] van Kreveld, S. A., Sarnthein, M., Erlenkeuser, H., Grootes, P., Jung, S., Nadeau, M. J., Pflaumann, U., Voelker, A., 2000: Potential links between surging ice sheets, circulation changes and the Dansgaard-Oeschger cycles in the Irminger Sea, 60-18 kyr. *Paleoceanography*, **15**, 425-442.

[21] van Geel, B., Raspopov, O.M., Renssen, H., van der Plicht, J., Dergachev, V.A. and Meijer, H.A.J. 1999. The role of solar forcing upon climate change. *Quaternary Science Reviews*, **18**, 331-338.

[22] Keeling, C. D. and Whorf, T. P. 2000. The 1,800-year oceanic tidal cycle: A possible cause of rapid climate change. *Proceedings of the National Academy of Sciences of the United States of America*, **97**, 3814-3819.

[23] Alley, R. B., Anandakrishnan, S. and Jung, P. 2001. Stochastic resonance in the North Atlantic. *Paleoceanography*, **16**, 190-198.

[24] Ganopolski, A. and Rahmstorf, S. 2002. Abrupt glacial climate changes due to stochastic resonance. *Physical Review Letters* **88**(3), 038501.

[25] Rial, J. A. 2004. Abrupt Climate Change: Chaos and Order at Orbital and Millennial Scales. *Global and Planetary Change*, **41**, 95-109.

[26] Clemens, S. C. 2005. Millennial-band climate spectrum resolved and linked to centennial-scale solar cycles. *Quaternary Science Reviews*, **24**, 521-531.

[27] Alley, R. B. Icing the North Atlantic. *Nature*, **392**, 335-336.

[28] Bond, G., Kromer, B., Beer, J., Muscheler, R., Evans, M. N., Showers, W., Hoffmann, S., Lotti-Bond, R., Hajdas, I. and Bonani, G. 2001. Persistent solar influence on North Atlantic climate during the Holocene. *Science*, **294**, 2130-2136.

[29] Bond, G. 2003. Abstract submitted to the fall meeting 2003 of the American Geophysical Union (`http://lasp.colorado.edu/sorce/dec03_posters_presentations/Bond.htm`).

[30] Alley, R. B., Anandakrishnan, S., Jung, P. and Clough, A. 2001. Stochastic resonance in the North Atlantic: Further Insights. In: *The Oceans and Rapid Climate Change: Past, Present and Future.*, edited by D. Seidov, B. J. Haupt and M. Maslin. Geophysical Monograph 126, 57-68.

[31] Schulz, M. 2002. On the 1470-year pacing of Dansgaard-Oeschger warm events. *Paleoceanography*, **17**, 10.1029/2000PA000571.

[32] Rahmstorf, S. Timing of abrupt climate change: a precise clock. *Geophysical Research Letters*,**30**, 1510.

[33] Rahmstorf, S. and Alley, R. B. 2002. Stochastic resonance in glacial climate. *Eos*, **83** (12), 129-135.

[34] Wunsch, C. 2000. On sharp spectral lines in the climate record and the millennial peak. *Paleoceanography*, **15**(4), 417-424.

[35] Petoukhov, V., Ganopolski, A., Brovkin, V., Claussen, M., Eliseev, A., Kubatzki, C., Rahmstorf, S. 2000. CLIMBER-2: A climate system model of intermediate complexity. Part I: Model description and performance for present climate. *Climate Dynamics*, **16**, 1-17.

[36] Claussen, M., Mysak, L. A., Weaver, A. J., Crucifix, M., Fichefet, T., Loutre, M.-F., Weber, S. L., Alcamo, J., Alexeev, V. A., Berger, A., Calov, R., Ganopolski, A., Goosse, H., Lohman, G., Lunkeit, F., Mokhov, I. I.,

Petoukhov, V., Stone, P., Wang, Z. 2002. Earth system models of intermediate complexity: Closing the gap in the spectrum of climate system models. *Climate Dynamics*, **18**(7), 579-586.

[37] Peltier, W. R. 1994. Ice Age Paleotopography. *Science*, **265**, 195-201.

[38] Ganopolski, A., Rahmstorf, S., Petoukhov, V. and Claussen, M. 1998. Simulation of modern and glacial climates with a coupled global model of intermediate complexity. *Nature*, **391**, 351-356.

[39] Ganopolski, A., Kubatzki, C., Claussen, M., Brovkin, V., Petoukhov, V. 1998. The influence of vegetation-atmosphere-ocean interaction on climate during mid-Holocene. *Science*, **280**, 1916-1919.

[40] Ganopolski, A. and Rahmstorf, S. 2001. Stability and variability of the thermohaline circulation in the past and future: a study with a coupled model of intermediate complexity. In *The Oceans and Rapid Climate Change: Past, Present and Future*, edited by D. Seidov, M. Maslin and B. J. Haupt, AGU, Washington, 261-275.

[41] Claussen, M., Ganopolski, A., Brovkin, V, Gerstengarbe, F.-W. and Werner, P. 2003. Simulated global-scale response of the climate system to Dansgaard/Oeschger and Heinrich events. *Climate Dynamics*, **21**(5-6), 361-370.

[42] Fröhlich, C. and Lean, J. 1998. The Sun's total irradiance: Cycles and trends in the past two decades and associated climate change uncertainties. *Geophysical Research Letters*, **25**, 4377-4380.

[43] Willson, R. C. and Mordvinov, A. V. 2003. Secular Total Solar Irradiance trend during solar cycles 21-23. *Geophysical Research Letters*, **30**(5), 1199-1202.

[44] Ramanathan, V., Cess, R. D., Harrison, E. F., Minnis, P., Barkstrom, B. R., Ahmad, E. and Hartmann, D. 1989. Cloud-Radiative Forcing and Climate: Results from the Earth Radiation Budget Experiment. *Science*, **243**, 57-63.

[45] Lean J. 1991. Variations in the sun's radiative output. *Reviews of Geophysics*, **29**, 505-535.

[46] Gleissberg, W. 1958. The eighty-year sunspot cycle, *Journal of the British Astronomical Association*, **68**, 148-152.

[47] Feynman, J. and Fougere. P. F. 1984. Eighty-eight year periodicity in solar-terrestrial phenomena confirmed. *Journal of Geophysical Research*, **89**, 3023-3027.

[48] Stuiver, M., and Braziunas, T. F. 1993. Sun, ocean, climate and atmospheric CO2: An evaluation of causal and spectral relationships. *Holocene*, **3**, 289-305.

[49] Peristykh, A. N. and Damon, P. E. 2003. Persistence of the Gleissberg 88-yr solar cycle over the last 12,000 years: Evidence from cosmogenic isotopes. *Journal of Geophysical Research*, **108**, 1003, doi:10.1029/2002JA009390.

[50] Damon, P. E., and Sonett, C. P. Solar and terrestrial components of the atmospheric 14C variation spectrum. In: *The Sun in Time*, edited by C. P. Sonett, M. S. Giampapa and M. S. Matthews, The University of Arizona (Tucson), 360-388, 1991.

[51] Beer,J. Cosmogenic radionuclides in ice cores. In:*Advances in nuclear and radiochemistry*, edited by S. M. Qaim and H. H. Coenen (Aachen), 489-92, 2004.

[52] Wagner, G., Beer, J., Masarik, J., Muscheler, R., Kubik, P. W., Mende, W., Laj, C., Raisbeck, G. M., Yiou, F. 2001. Presence of the solar de Vries cycle (≈205 years) during the last ice age. *Geophysical Research Letters*, **28** (2), 303-306.

[53] de Vries, H. L. 1958. Variation in Concentration of Radiocarbon with Time and Location on Earth. *Proceedings Koninlijke Nederlandse Akademie Wetenschappen B*, **61**, 94-102.

[54] Suess, H. E. 1980. The radiocarbon record in tree rings of the last 8000 years. *Radiocarbon*, **22**, 200-209.

[55] Neff, U., Burns, S. J., Mangini, A., Mudelsee, M., Fleitmann, D., Matter, A. 2001. Strong coherence between solar variability and the Monsoon in Oman between 9 and 6 kyr ago. *Nature*, **411**, 290-292.

[56] Hodell, D. A., Brenner, M., Curtis, J. H., Guilderson, T. 2001. Solar forcing of drought frequency in the Maya Lowlands. *Science*, **292**, 1367-1370.

[57] Stocker, T. F. and Wright, D. G. 1998. The Effect of a succession of ocean ventilation changes on 14C. *Radiocarbon*, **40**, 359-366.

[58] Rind, D. 2002. The Sun's role in climate variations. *Science*, **296**, 673-678.

[59] Mangini, A., Spötl, C. and Verdes, P. 2005. Reconstruction of temperature in the Central Alps during the past 2000 yr from a $\delta^{18}O$ stalagmite record. *Earth and Planetary Science Letters*, **235**, 741-751.

[60] Lean, J., Beer, J. and Bradley, R. 1995. Reconstruction of solar irradiance since 1610: Implications for climate change. *Geophysical Research Letters*, **22**, 3195-3198.

[61] Bard, E., Raisbeck, G., Yiou, F. and Jouzel, J. 2000. Solar irradiance during the last 1200 yr based on cosmogenic nuclides. *Tellus B*, **52**(3), 985-992.

[62] Foukal, P., North, G. and Wigley, T. 2004: A stellar view on solar variations and climate. *Science*, **306**, 68-69.

[63] Balachandran, N. K. and Rind, D. 1995. Modeling the effects of UV variability and the QBO on the troposphere/stratosphere system. Part I: The middle atmosphere. *Journal of Climate*, **8**, 2058-2079.

[64] Shindell, D., Rind, D., Balachandran, N., Lean, J. and Lonergan, P. 1999. Solar cycle variability, ozone, and climate. *Science*, **284**, 305-308.

[65] Kodera, K. and Kuroda, Y. 2002. Dynamical response to the solar cycle. *Journal of Geophysical Research*, **107**(D24), 4749, doi:10.1029/2002JD002224.

[66] Dickinson, R. E. 1975. Solar variability and the lower atmosphere. *Bulletin American Meteorological Society*, **56**, 1240-1248.

[67] Carslaw, K. S., Harrison, R. G., Kirkby, J. 2002. Cosmic rays, clouds and climate. *Science*, **298**, 1732-1737.

[68] Dai, A. and Trenberth, K. E. 2002. Estimates of Freshwater Discharge from Continents: Latitudinal and Seasonal Variations. *Journal of Hydrometeorology*, **3**, 660-687.

[69] Braun, H., Christl, M., Rahmstorf, S., Ganopolski, A., Mangini, A., Kubatzki, C., Roth, K. and Kromer, B. 2005. Possible solar origin of the 1,470-year glacial climate cycle demonstrated in a coupled model. *Nature*, **438**, 208-211.

[70] Braun, H., Christl, M., Rahmstorf, S., Ganopolski, A., Mangini, A., Kubatzki, C., Roth, K. and Kromer, B. 2005. Possible solar origin of the 1,470-year glacial climate cycle demonstrated in a coupled model (Supplementary information). *Nature*, **438**, 208-211 (`http://www.nature.com/nature/journal/v438/n7065/suppinfo/nature04121.html`).

[71] Weber, S. L., Cowley, T. J. and van der Schrier, G. 2004. Solar irradiance forcing of centennial climate variability during the Holocene. *Climate Dynamics*, **22**, 539-553.

[72] Mann, M. E. and Jones, P. D. 2003. Global surface temperatures over the past two millennia. *Geophysical Research Letters*, **30**, 10.1029/2003GL017814.

[73] Moberg, A., Sonechkin, D. M., Holmgren, K., Datsenko, N. M. and Karlen, W. 2005. Highly variable Northern Hemisphere temperatures reconstructed from low- and high-resolution proxy data. *Nature*, **433**, 613-617.

12 Acknowledgement

This thesis would not have been possible without the support of my supervisors, my colleagues and my family. Thank you very much to all of you! I very much enjoyed my project, and I definitely learned a lot. I am sure that I will always have pleasant memories of my time at the IUP in Heidelberg and of the collaboration with the PIK in Potsdam.

In particular I would like to thank:

- My supervisors, Prof. Kurt Roth and Prof. Augusto Mangini. Without their scientific and personal support, and without their trust in me, my PhD project would not have been realised. I very much appreciated the independence and flexibility that they gave me, since with my two children this flexibility was a great help to conduct the project successfully.

- Dr. Marcus Christl, Dr. Andrey Ganopolski, Dr. Bernd Kromer, Dr. Claudia Kubatzki, Prof. Augusto Mangini, Prof. Stefan Rahmstorf and Prof. Kurt Roth for their help with my publication. Especially I want to thank Prof. Stefan Rahmstorf and Dr. Marcus Christl for their considerable support on writing and improving the manuscript. Without their valuable help the paper would not have been published in Nature.

- My present and former colleagues in my working group in Heidelberg for help and for the friendly atmosphere at the IUP, namely Frank Bernsdorff, Evelyn Böhm, Dr. Marcus Christl, Rene Eichstädter, Jens Fohlmeister, Dr. Bernd Kromer, Nicolas Latuske, Jörg Lippold, Ricardo März, Christian Mühlinghaus, Daniela Polag, Daniel Schimpf, Dr. Denis Scholz, Dr. Andrea Schröder-Ritzrau, Boris Schulze, Karoline Thomas, Ingmar Unkel, Dr. Pablo Verdes, Nicole Vollweiler, and Patrick Wenderoth. In particular, I want to thank Dr. Denis Scholz, Dr. Bernd Kromer, Dr. Pablo Verdes, Jens Fohlmeister and Jörg Lippold (and of course Prof. Kurt Roth) for helpful comments on my thesis.

- My present and former colleagues in Potsdam, namely Dr. Eva Bauer, Dr. Reinhard Calov, Prof. Martin Claussen, Dr. Andrey Ganopolski, Dr. Claudia Kubatzki and Prof. Stefan Rahmstorf for aid and support throughout the project.

- The late Prof. Gerard Bond for the invitation to the AGU Fall Meeting 2004, and for the subsequent discussion and feedback on my model results.